DESIGN - BASED OPTIMIZATION STRATEGIES OF URBAN PUBLIC MICROCLIMATE IN MEDITERRANEAN CONTEXT. THE CASE OF TIRANA, ALBANIA.

A THESIS SUBMITTED TO
THE FACULTY OF ARCHITECTURE AND ENGINEERING
OF
EPOKA UNIVERSITY

BY

KLEA MECAJ

IN PARTIAL FULFILLMENT OF THE REQUIREMENTS
FOR
THE DEGREE OF MASTER OF SCIENCE
IN
ARCHITECTURE

JULY, 2023

Approval sheet of the Thesis

This is to certify that we have read this thesis entitled **"Design-based optimization strategies of urban public microclimate in Mediterranean context. The case of Tirana, Albania."** and that in our opinion it is fully adequate, in scope and quality, as a thesis for the degree of Master of Science.

_____

Assoc. Prof. Dr. Edmond Manahasa
Head of Department
Date: July , 4 , 2023

Examining Committee Members:

Prof. Dr. Sokol Dervishi (Architecture) _____

Dr. Ina Dervishi (Architecture) _____

Dr. Paolo Camilletti (Architecture) _____

I hereby declare that all information in this document has been obtained and presented in accordance with academic rules and ethical conduct. I also declare that, as required by these rules and conduct, I have fully cited and referenced all material and results that are not original to this work.

Name Surname: Klea Mecaj

Signature: _____

ABSTRACT

DESIGN - BASED OPTIMIZATION STRATEGIES OF URBAN PUBLIC MICROCLIMATE IN MEDITERRANEAN CONTEXT. THE CASE OF TIRANA, ALBANIA.

Mecaj, Klea

M.Sc., Department of Architecture

Supervisor: Prof. Dr. Sokol Dervishi

Co supervisor: Dr. Ina Dervishi

The quality of life in urban areas is greatly affected by the comfort and health of the environment there. As a result, the issue facing urban design and planning studies that attempt to improve the outdoor thermal comfort and microclimate conditions of urban areas is expanding. Comparing urban thermal comfort analysis to indoor thermal comfort study is more complicated since outside surroundings have a greater variety of dynamic analysis. While several studies have suggested, assessed, and analyzed residential blocks, high rise buildings, neighborhood patterns, or the performance of inner courtyards with regard to various elements, there is a gap in the literature addressing public squares and how they are connected to the thermal comfort of their users. In order to evaluate whether or not morphology significantly affects outdoor thermal comfort, this study will analyze those public squares and their surroundings through literary examination, followed by data analysis utilizing simulation tools. The purpose of this paper is to provide urban planners in Tirana and other municipalities with comparable climatic conditions with guidelines to help them make the most effective decisions possible when creating open spaces that are crucial to the city. This study will additionally provide design-based strategies for the optimization of these open places following evaluation, conveying improved microclimate but also alternative user experiences.

Keywords: *morphology, thermal comfort, open spaces, public squares optimization, sustainability, design, ideas, urban planning, simulation*

ABSTRAKT

STRATEGJITE E OPTIMIZIMIT TE MIKROKLIMES SE ZONAVE PUBLIKE URBANE TE BAZUARA NE DIZENJIM. KONTEKSTI I KLIMES MESDHETARE NE QYTETIN E TIRANES.

Meçaj, Klea

Master Shkencor, Departamenti i Arkitektures

Udhëheqësi: Prof. Dr. Sokol Dervishi

Bashkë udhëheqës: Dr. Ina Dervishi

Cilësia e jetës në zonat urbane ka një ndikim të konsiderueshëm nga rehatia dhe shëndeti rreth mjedisit perkatës. Si rezultat, çështja me të cilën përballen studimet e projektimit dhe planifikimit urban që përpiqen të përmirësojnë komfortin termik të jashtëm dhe kushtet mikroklimatike të zonave urbane po zgjerohet. Krahasimi i analizës së komfortit termik urban me studimin e komoditetit termik të brendshëm është më i ndërlikuar pasi mjediset e jashtme kanë një larmi më të madhe analizash dinamike. Megjithëse disa studime kanë sugjeruar, vlerësuar dhe analizuar blloqet e banimit, ndërtesat e larta, modelet e lagjeve ose performancën e oborreve të brendshme në lidhje me elementë të ndryshëm, ka një boshllëk në literaturën që trajton sheshet publike dhe mënyrën se si ato lidhen me komfortin termik. komoditetin e përdoruesve të tyre. Për të vlerësuar nëse morfologjia ndikon ndjeshëm ose jo në komoditetin termik të jashtëm, ky studim do të analizojë ato sheshe publike dhe rrethinat e tyre përmes ekzaminimit letrar, e ndjekur nga analiza e të dhënave duke përdorur mjete simulimi. Qëllimi i këtij punimi është t'u sigurojë planifikuesve urbanë në Tiranë dhe bashki të tjera udhëzime në kushte të krahasueshme klimatike për t'i ndihmuar ata të marrin vendimet më efektive të mundshme kur krijojnë hapësira të hapura që janë vendimtare për qytetin. Ky studim do të ofrojë gjithashtu strategji të bazuara në dizajn për optimizimin e këtyre shesheve publike pas vlerësimit, duke përcjellë mikroklimë të përmirësuar, por edhe përvoja alternative të përdoruesëve.

Fjalët kyçe *morfologji, komfort termik,hapesira te hapura, sheshe publike optimizim, qendrueshmëri, projektim, ide, planifikim urban, simulim*

ACKNOWLEDGEMENTS

I would like to express my heartfelt gratitude to my supervisor Prof.Dr Sokol Dervishi and my Co Supervisor Dr. Ina Dervishi for their unwavering support, guidance, and mentorship throughout this journey. Their expertise and encouragement have been instrumental in shaping the outcome of my work. I am also deeply indebted to my parents and my brother Leo, whose love, sacrifices, and constant belief in me have been the driving force behind my success. Their unwavering support and encouragement have been a constant source of inspiration, motivating me to strive for excellence. Without their support, this success would not have been possible. I would like to take a moment to thank myself for the effort and determination that I invested those years, which has resulted in a sense of accomplishment and personal growth. Finally, I offer my sincere gratitude to God for providing me with strength, guidance, and blessings throughout this journey, making the achievement possible.

TABLE OF CONTENTS

LIST OF TABLES

TABLE OF FIGURES

CHAPTER 1

INTRODUCTION

1.1 Overview

The country's and society's advancements have also greatly raised people’s life quality. Increasing numbers of people are moving from rural regions to cities, especially when urban building is rising. The above provides an enough labor force for urban development and construction. (Chen, 2021) The continual population increase of cities is also a factor, though. The city is now experiencing several issues due to the expansion and quick urban development. From the standpoint of urban space architectural design, rational and scientific space planning and construction of the city may not only meet people's need for a better living environment but also take a broad view of urban environmental protection and environmental pollution. An organizational structure and direction are provided by the improvement. In order for a city to realize the goals of joint development of economic construction and ecological environmental conservation, a smart city must organically integrate a decent ecological environment with people's healthy lives. (Haarstad & Wathne, 2019)

1.2 Motivation

Albania's capital, Tirana, will have 850 530 residents in 2020. Currently, there are 768 people living in the city per square kilometer. The population of Tirana has quickly increased since the early 1990s, when communism was overthrown. About 250,000 people lived there in 1990; by 2021, that number had risen to almost 900,000. This significant rise in population may be linked to a number of variables, particularly rural-to-urban migration, economic possibilities, and enhanced city services and infrastructure. One of the city's mainly arteries is the Boulevard of Tirana, which has an extensive past. The boulevard, Tirana's most significant axis, has contributed to the city's urban expansion and is a key component of the city's identity because it is where

the majority of the city's significant structures are located. Thousands of people utilize this axis every day since it is home to parks, open spaces, and crucial routes that link various locations in the city.

1.3 Thesis objective

Numerous studies on internal thermal comfort have been completed over the past years for a wide range of building types in climatically diverse locations; however, little research has been done on occupant thermal comfort in urban settings. There hasn’t been any previous study that have considered and evaluated areas that comprise public buildings like governmental, educational, and commercial ones. As a result, the main objective of this study is to analyze the boulevard’s two main squares, which are currently Tirana's most important public areas.

1.4 Organization of the thesis

The structure of this thesis is organized into 6 chapters. The introduction and objective of the thesis are presented in the first chapter. In the second chapter, the literature review and studies related to this paper are presented. On the chapter 3 it is shown a historical overview of Tirana. Chapter 4 presents the method used to conduct the study. In the fifth chapter, the results are illustrated and then discussed in the following chapter. The conclusions and research recommendations are presented in the final chapter.

CHAPTER 2

LITERATURE REVIEW

2.1 Introduction

The city in which a person resides is accountable for ensuring that person's happiness in life. The country's and society's advancements have also greatly raised peoples' living standards. Increasing numbers of people are moving from rural regions to cities, especially when urban building is rising. This supplies enough workforce for urban expansion and building. Yet, it is also a result of cities' ongoing population growth. (Chen, 2021) The considerable changes in the microclimate of contemporary cities and the frequency of higher air temperatures in urban districts contrasted to the nearby rural regions are closely connected to the expanded process of urbanization of the twentieth and twenty-first centuries. (Tsoka et al., 2020) Urban density, land use, and land cover all alter dramatically as a result of intense urbanization in built-up regions. These modifications have led to exceptionally high temperatures being seen in metropolitan areas. These high temperatures are a result of both regulated (like urban planning) and uncontrollable forces (such as meteorological parameters and environmental conditions). (Kouklis & Yiannakou, 2021)

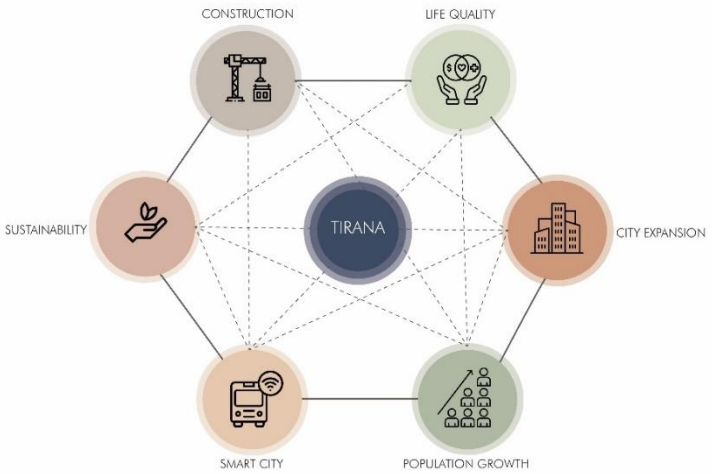

Figure 1.Relationship of the main concepts.

Many studies on indoor thermal comfort have indeed been completed over the past 40 years for a variety of building types in climatic zones with a wide range of climates; however, little research has been done on human thermal contentment in urban environment. (Dang & Pitts, 2020) The link between air temperature and urban form must be better understood in order to enhance environmental comfort and urban design. (Yang et al., 2023) Urban regions are renowned for creating distinctive microclimates that tend to get hotter than for the microclimates of surrounding rural areas or of other locations inside cities. (Aleksandrowicz et al., 2020) The outdoor microclimate characteristics are significantly impacted by a variety of urban geometry elements. (Shareef & Abu-Hijleh, 2020) To create a sustainable urban design with the necessary outdoor thermal performance, several urban design variables and components can be changed. The urban heat island (UHI) impact causes the air temperatures to be greater, and wind shielding causes the average wind speeds to be lower. (Allegrini et al., 2015)

In adding to the aforementioned, a network of highways that are typically covering more than a 25% of dense urban areas have a substantial impact on the urban climate. (Kouklis & Yiannakou, 2021) Green and tree-planted regions that influence the urban climate, which primarily affects the built environment, typically have a good effect on thermal comfort. Urban vegetation especially influences the microclimate by capturing a significant amount of solar radiation, lowering heat transfer through transpiration, lowering air speed near the ground, and other mechanisms. (Yan et al., 2019) Wind speeds of wind, which are experienced as abrupt surges in speed, are caused by the significant variations in wind speed that occur in cities over relatively small distances and during relatively short time periods. The highest buildings stop the passage of strong winds and frequently direct them to the axis of the roadways, resulting in their ventilation, in modern dense urban areas whose form is composed of stacked buildings of varied heights. (Kouklis & Yiannakou, 2021)

The current study studies the microclimatic conditions inside a typical urban compact form, concentrating on a region within the city of Tirana public, cultural and commercial district. Moreover, it assesses how open spaces vegetation and other factors affect such urban forms and how urban morphology's unique characteristics affect the development of certain microclimatic conditions.

2.2 Theoretical background

2.2.1 Smart and sustainable cities

The idea of smart and sustainable cities has arisen as a potent remedy to solve the issues faced by our more congested and linked globe in an era of rapid urbanization. (Sugandha et al., 2022) The need of developing new strategies to manage resources, improve quality of life, and reduce the ecological imprint has increased as cities become the hubs of economic, social, and environmental activity. The subject of urban sustainable development has attracted increasing attention. (Macke et al., 2019)

The exponential increase in the world's population, however, presents a significant obstacle to the creation of smart, sustainable cities. Urban populations throughout the world are growing quickly. The percentage of people who reside in urban areas is expected to increase to approximately 68 percent by 2050 from the current level of more than 55% in 2021. (Kim & Kim, 2022) The supply of services, infrastructure, and resources, as well as sustainable urban development, are significantly hampered by this urban population expansion. (Niemets et al., 2021) Cities must implement cutting-edge plans to deal with this inflow that not only handle population increase but also guarantee a good standard of living for all citizens.

Effective urban planning and design is a crucial component of urban renewal in the face of population growth. Urban planners may lessen the ecological impact of expansive urban expansion by carefully planning cities with an emphasis on compactness, varied land use, and well-connected transit networks. (Niemets et al., 2021) Compact cities permit the supply of key services closer together, encourage walkability, and allow for a more effective use of land, decreasing the need for lengthy drives and consuming less energy.(Haarstad & Wathne, 2019) (Chen, 2021)

2.2.2 Urban microclimate

It has long been recognized that the diverse microclimates that exist inside the various urban open spaces provide cities with a number of challenges. The characteristics of both the urban climate are generally the consequence of human activity, with cities' planning, development, and construction as well as the events they host being the most significant examples. (Yang et al., 2020) An understanding of the peculiarities of the urban microclimate is the foundation of the environmentally, or important consideration in the design, approach to urban planning. Microclimate refers to the climatic conditions prevalent in cities, mainly due to the configuration of the urban fabric. (Allegrini et al., 2015) Specific forms of urban fabric are determined by land use and urban design, and of course, by human activities in this form of physical urban development. The microclimate is thus affected by human intervention in the built environment, which often results in unintentional climatic conditions, concentrated in small areas of the urban fabric. (Allen-Dumas et al., 2020)

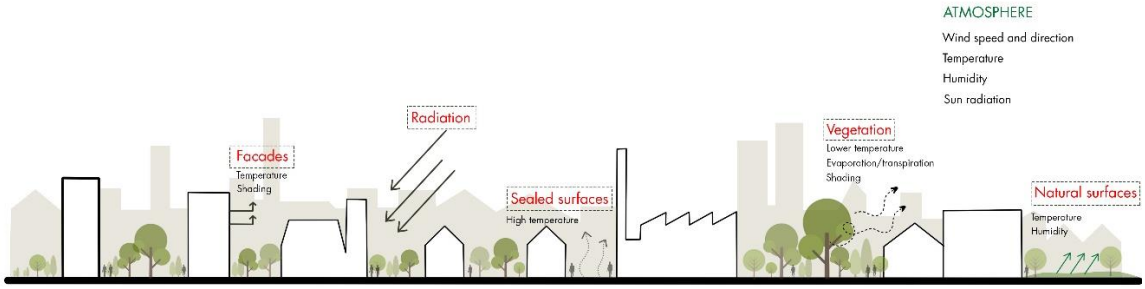

Figure 2. Illustrated scheme of urban microclimate.

2.2.3 Urban density

Two fundamental indicators of the built-up area's spatial distribution are the ratios of "envelope surface-to-volume" (S/V) and "building height-to-width outdoor space" (H/W), both of which have a significant impact on the microclimate. The building volume's degree of coherence is expressed by the S/V factor. The SVF is a significant element impacting the microclimate, air pollution, surface temperature distribution, and microscale air circulation of the urban environment. (Miao et al., 2020) Contrarily, the sky view factor in H/W reflects the degree of "openness," or the ratio

between the size of the structure and the nearby outdoor places (SVF). SVF is a measurement of the solid angle of sky view from a populated area. A big S/V and small H/W ratio, less land covered by buildings, greater open spaces, and a lower building volume density, on the other hand, are characteristics of flexible urban forms. (Kouklis & Yiannakou, 2021)

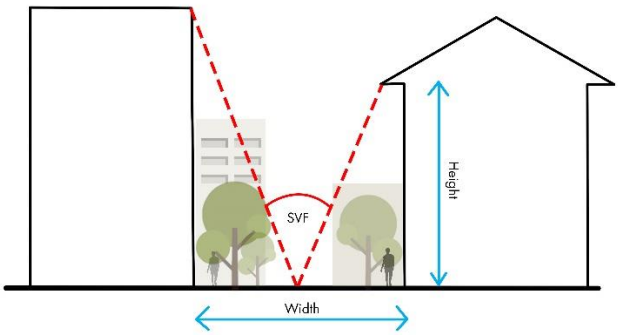

Figure 3.Illustration of sky view factor between two buildings.

2.2.4 Urban heat islands

The establishment of the urban microclimate is substantially influenced by the climate present in urban areas, which has a direct bearing on the phenomena of UHI. (Synnefa et al., 2006) The microclimatic alterations brought on by anthropogenic interventions in the urban environment represent this phenomenon. Numerous causes, including urban morphology, wasted heat, the characteristics of construction materials, and a lack of open space, green areas, and water surfaces, might be blamed for these changes. Regarding the link between urban geometry and the phenomena of UHI, the intensity of the UHI phenomenon rises as the H/W ratio increases. (Kouklis & Yiannakou, 2021) The urban environment is significantly influenced by the above listed factors as well as a network of highways that generally covers more than a 25% of compact urban areas. Urban roads are defined by their height/width and length/width ratios, which set them apart from other types of roadways geometrically. These variables, which directly affect solar radiation absorbed and emitted as well as urban environment ventilation, result in significant temperature fluctuations.

Various meteorological conditions may be seen on roadways with different orientations (such as North-South or East-West). The E-W roads have the least pleasant temperatures

since they receive winters shade and summertime "sunbathing." (Kouklis & Yiannakou, 2021)

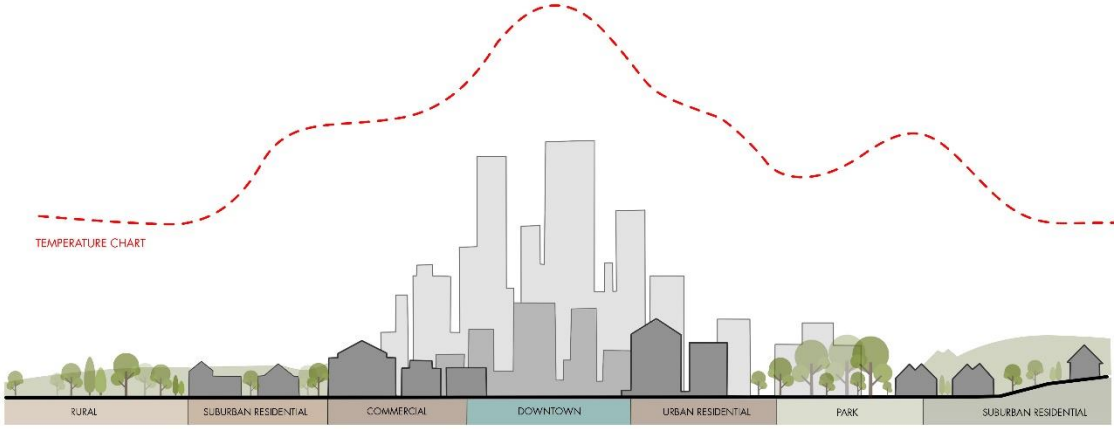

Figure 4.Illustration of an urban heat island.

2.2.5 Universal Thermal Climate Index (UTCI)

It is now commonly acknowledged that environmentally responsible urban design and development must take city residents' outdoor thermal comfort into account. The physiological stress that results when the environment temperature approaches or surpasses the physiological threshold of 37 °C can be harmful to human health. (Speak & Salbitano, 2022) A network of pedestrian walkways are part of a healthy and environmentally friendly urban environment that may be used for recreation, exercise, or transportation. The linear walking routes' ambient thermal state, which impacts a person's comfort conditions, will inevitably have an impact on how likely people are to use them. Both the human body's physiological reaction and the ambient temperature play significant roles in determining thermal comfort during walking. (Hwang et al., 2022) One of the often-used thermal indices for assessing outdoor thermal comfort is the Universal Thermal Climate Index (UTCI). UTCI was tested with the Physiological Equivalent Temperature (PET) and outside air temperature (Ta) concurrently to investigate its usefulness in all types of climates. (Nie et al., 2022)

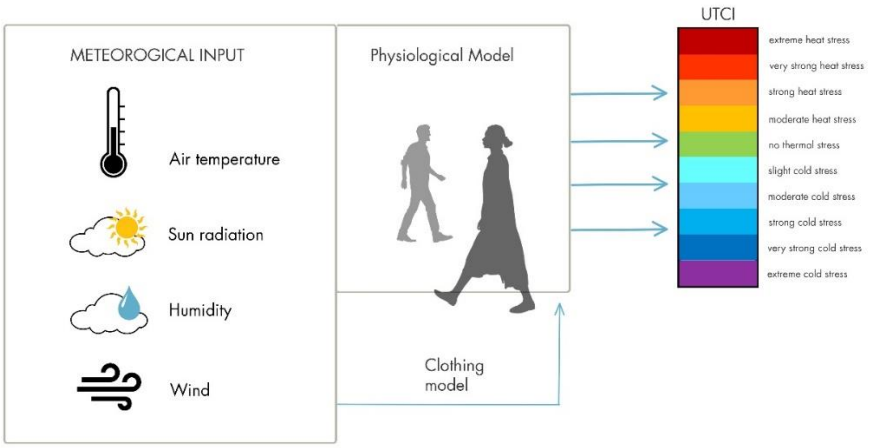

Figure 5.Illustration of UTCI.

2.2.6 Vegetation

Beyond a fact, including vegetation when developing urban spaces is one of the aspects that has the most influence and affects the microclimate of urban places. (Yahia & Johansson, 2014). Urban vegetation is a crucial component in the solution to the problem of rising urban temperatures brought on by the expansion of the built environment. From solar energy absorbed during the day, plants generate thermal heat flux and latent heat flux at night. This is because the region around the flora is cooler than the area near the built-up areas and concrete surfaces. (Zaki et al., 2020) This necessitates changing the urban shape and adding vegetation to create and sustain thermally suitable outdoor urban habitats. Additionally, it has been discovered that, on average, tree shade contributes to around 80% of the overall cooling impact. The most popular strategy for reducing the detrimental effects of the UHI is vegetation. (Dissanayake et al., 2021) When scattered greenery is placed within the city borders, the temperature drops by up to 1.20 C. It is discovered that the street alignment scenario is the most effective design for lowering the city's temperature because it covers more ground with trees that can withstand heat and drought. The area-average change in temperature as a baseline for comparison. Although not as much as the street alignment scenario, the expansion of an existing urban forestry and the development of a park both lower temperatures. (Bachir et al., 2021)

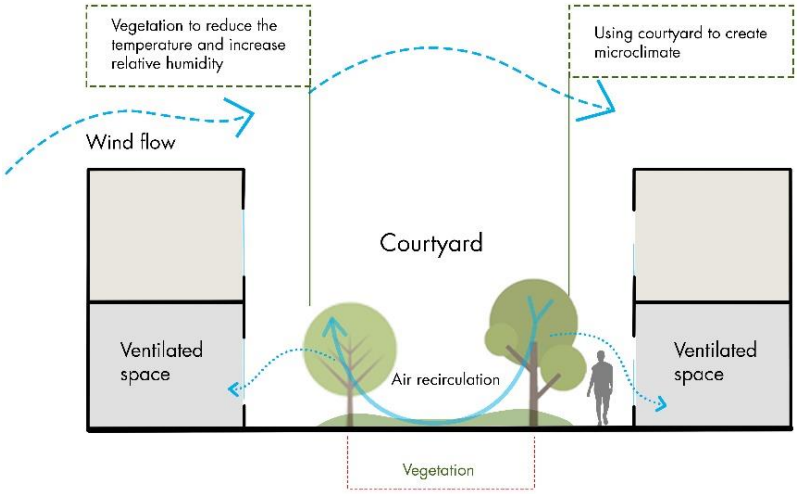

Figure 6. Impact of courtyards and vegetation.

2.2.7 Air Pollution

Air pollution, which is increasingly the major issue in high-density places, is affected by wind flow as well. The area's air pollution may considerably increase as the fast-turning bend wraps around tall structures. The degree of air pollution in the city is caused by variations in urban winds, which are caused by building morphology. While some assert that there is no connection between air pollution and the urban shape of the city, it is feasible to take specific measures to improve pollution dispersion. (Hultgren, 2014), (Yang, et al., 2019) Pollution cannot be controlled or eliminated by urban morphology. On a smaller scale, such in communities, the relevance of street direction and diverse building and street proportions is stressed. Ventilation corridors have proved to have a beneficial influence on lowering pollutants. On a smaller scale yet, the key determinants of air pollution are building elevation, direction, form, and volume. (Yang, et al., 2019)

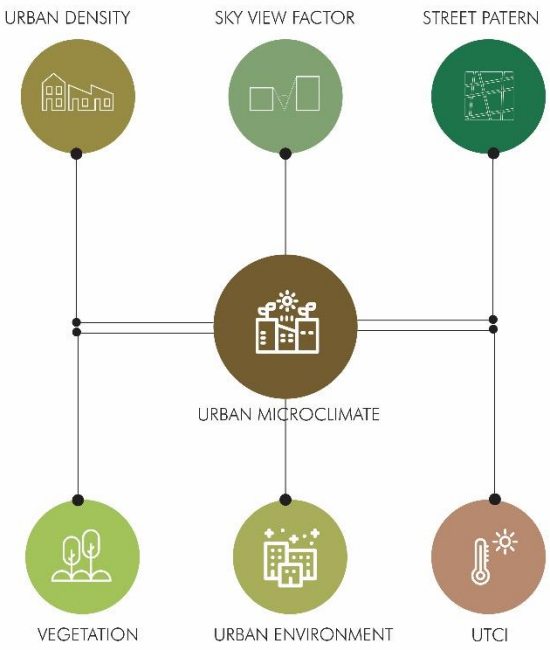

Figure 7. Urban microclimate cluster.

2.3 Previously related studies

A literature study of earlier research connected to urban morphology studies is undertaken to have a better understanding of how to create and analyze city patterns.

On Neighborhood scale (residential blocks):

(Wang 2021) analysis that the plot's thermal micro-environment is greatly affected by the block form characteristics of plot ratio, greening rate, and aspect ratio. Blocks with higher plot ratios, higher rates of greening, and higher ratios of aspects have better thermal microclimates.

(Allegrini et al., 2015) says that the air temperatures can nevertheless significantly vary for urban topologies with comparable surface temperatures because varied wind flow patterns result in variable rates of heat extraction by wind.

(Heris et al., 2020) explains that designers and planners may improve the site design, including building shape, street layouts, and landscaping standards, to reduce urban heat using more analytical techniques.

In (Gusson & Duarte, 2016) given the low-rise periphery neighborhood with low building density and greater open sky view, the air temperature values are lower at night and higher during the day.

(Shareef & Abu-Hijleh, 2020) studies that the air temperature decreased in a NW-SE direction as a result of the large variance in building heights being oriented along the urban block's short axis.

Based on prior studies that highlighted the crucial importance of shade in minimizing daytime heat stress under Israeli climatic conditions, (Aleksandrowicz et al., 2020) the usage of a Shade Index (SI) at street and neighborhood levels for assessing summer microclimatic features of urban environments.

In (Loeffler et al., 2021) is shown that the need for dense structures to reduce the demand for heating energy is less important when thermal comfort of the facades is improved.

(Yahia et al., 2017) talks about giving the current heat and wind circumstances, providing shade is a far more effective strategy to lower PET than increasing wind speed.

In (Li, 2021) the results show that those with higher incomes typically reside in areas that are warmer.

(Zhang et al., 2022) indicates that the number of floors in a building has a major impact on the daily average temperature; however, when a building does have more over 20 stores, the temperature is not greatly impacted by the height of the structure.

Studies based on city centers including public buildings:

In (Kouklis & Yiannakou, 2021) the results show that both the production of the microclimate and the effect of the bioclimatic parameters are significantly influenced by the urban structure, the urban canyon, and the accessible green areas in a compact urban form.

(Zaki et al., 2020) demonstrated how urban morphological characteristics including a higher percentage of green space, a low H/W ratio, and a high SVF might give a cooling impact to the surrounding region.

(He et al., 2021) analyzes that the lower the total wind speed, the more buildings there were in the study area. Moreover, the wind route surrounding the school was important for maximizing the school's wind environment, as were street direction, thick tree cover, and land height.

Around officially planned housing complexes in (Dang & Pitts, 2020), occupant thermal contentment was seen, whereas packed neighborhoods were characterized by lower temperatures but limited ventilation and lighting.

Studies related to pedestrian comfort:

(Speak & Salbitano, 2022) shows that between streets and land types with trees or a high height to width ratio (tight alleyways), as well as between treeless piazzas and those with trees, there were significant changes in the Universal Thermal Comfort Index (UTCI). The building of multivariate models was made possible by the different levels of SVF and tree coverage in the locations. These models showed that, under typical summer afternoon conditions, SVF drops of 12.5% or increases in tree cover of 25% can reduce the UTCI by 1.

(Pantavou et al., 2013) results show that people generally preferred warmer thermal conditions, which led to a higher tolerance for heat and a propensity to underestimate the hazards of heat exposure.

In (Park et al.,2014) midday was when there was the most heat stress. 28–38 C UTCI, moderate to severe heat discomfort in sunny places. Shaded regions experienced mild heat stress (20–27 C UTCI) but no thermal stress. In both places, narrow alleys showed lower UTCIs than wide areas.

(Nie et al., 2022) indicates that the average skin temperature and subjective thermal perception are not considerably impacted by the decline in UTCI in the incorrect interval.

(Hwang et al., 2022) Due to the context of urban morphology, the conventional evaluation of air temperature is based on the heat balance of the body under constant environmental circumstances, which is seldom true in the continuously changing outside situations.

In (Fahed et al., 2020) the district's use of fountains and spray nozzles both during the day and at night produces a distinct feeling of freshness. The largest temperature drop in the vicinity of water sources is 7 °C, and the freshness effect is noticeably spatially extended in the direction of the wind.

(Zhang et al., 2022) shows that when the typology changed, such as through changes in building form, building layout, and enclosure, the microclimate shifted obviously. A low UTCI caused by MRT and shade conditions might arise from a considerable increase in FAR (by roughly 1.0).

Studies related to vegetation and its impact in urban microclimate:

(Liu et al., 2020) results indicate that in order to satisfy the demands of the local population for recreation, the urban park system must have accessible, well-maintained, compact green areas.

By employing trees, green roofs, and vertical greening systems effectively in (Priya & Senthil, 2021), tropical towns may dramatically enhance their microclimate by lowering air temperatures by up to 4°C, 9°C, and 12°C. Urban greeneries must be implemented if cities and communities are to become sustainable through an ideal fusion of green landscape components.

(Teshnehdel et al., 2020) studies how PET reaches 26.16, which is nearer to the comfort zone, since the daily average ambient temperature and Tmrt in the summer decline by 0.29 C and 20.04 C, respectively (slightly warm sensation). The best-case scenario entails increasing the number of trees on the property by more than threefold and choosing a deciduous tree type to prevent severe winter solar shade.

According to (Bachir et al., 2021), tree alignments can reduce the city's temperature by about 1.2 C. Yet, it has the potential to cool the surface by up to 4 C. The addition of vegetation to the area often resulted in a decrease in air temperature, which comparatively increased the degree of comfort.

(Yan et al., 2019) analyzes that urban cooling is primarily influenced by tree cover, although tree and grass arrangements also have a significant impact, with impacts typically reaching 40% of those of tree cover. Increased edge density and the complexity of a vegetation patch's form warm some areas of vegetation while cooling the landscape. On the other hand, a hotter landscape may result from enlarging individual plant patches and lowering form complexity.

(Zaki et al., 2020) The air temperature may be lowered by up to 1% with about 25% greenery coverage, low H/W, and high SVF. In other words, having greater green space coverage, a lesser H/W ratio with crowded construction conditions, and more tree shade coverage will all contribute to the best cooling impact. Moreover, vegetation and bushes should be planted in open places to lower the ground surface heat in the lack of tree

planting. Due to evaporative cooling, a concrete and grass surface mix can provide a stronger cooling impact.

2.4 Aim and Originality

The research mentioned above demonstrate a relationship between local microclimate conditions and the morphology of urban communities. A study of the evolution of the city's urban patterns over time hasn't been completed, though. Additionally, the majority of research have focused on residential buildings, whereas in this case we are analyzing public structures that are crucial for the city. Below is a list of the literature gaps this topic addresses.

The best and worst morphologies for air temperature, radiant temperature, relative humidity, and wind speed have never previously been determined by developing and simulating city layouts development under multiple political regimes in a society.

No previous research has looked at a boulevard axis that contains significant public structures that are largely used by city residents. Other studies, including (Kouklis & Yiannakou, 2021), have looked at and assessed the city center's current residential blocks, which are largely made up of different densities, built-to-unbuilt surface areas, building heights, and other factors.

There is very little research, both in terms of morphology and on a large scale, comparing different city layouts across different political regions as well as examining city boulevard axes. Since boulevards are a major artery across the city and have a far higher influence on all levels of architecture than larger scale constructions like low- and high-rise buildings, this article intends to launch a comprehensive study of Tirana's urban morphology. It is important for Tirana to undertake this research since this axis is still developing and will play a significant role in the expansion of the city as a whole. For Albania's capital, the boulevard is also significant from an economical, touristic, and historical standpoint.

CHAPTER 3

HISTORICAL BACKGROUND

3.1 HISTORICAL OVERVIEW OF TIRANA

3.1.1 Overview of the chapter.

As it entered several eras—from the Ottoman Empire to the democratic nation that is modern-day Albania—Tirana has gone through many phases of altering urban architecture. As a result of the collapse of the state organizational framework that was in place until 1990 and for primarily economic reasons, the function of the state does indeed marginalize the phenomena of internal and external migration. In this view, Tirana develops into a significant draw for residents of lesser towns and cities.

Both structurally and functionally, Tirana still has the characteristics of a concentric-radial metropolis, with the majority of institutional, cultural, financial, and recreational activities taking place in the city's core. A decentralization trend has occurred with time and the settling of populated areas in previously undeveloped regions surrounding the inhabited center in 1990.

Numerous studies and territorial analyses on various stairways conducted in the past, both on Tirana and on suburbs and the informal, where reality frequently does not correspond more to the card, are made irrelevant by the ongoing changes of shapes and types urban developments and territorial expansion. But most importantly, they change the boundary conditions as the quantitative increase in population has led to a qualitative change in the structure of the city. After a decade during which the administrations were mostly immobile, urban interventions now primarily—if not exclusively—focus on the city center. The development approach used is consistent with many significant European cities and regions, where architecture plays a crucial role.

Tirana is still in a transition process started in 1990 that it was thought it should have end at a certain point and instead persists. Transition is not just a characteristic of Tirana or Albania; it is a broad feature of modern civilization that affects all facets, not just urban ones, and where change and uncertainty are realities. This chapter provides details on every government Tirana has had, along with the effects each political choice had on the city's development. Additionally, it will examine all the characteristics of each urban planning effort, demonstrating how the morphology of Tirana has evolved and identifying the components and their impacts on the city.

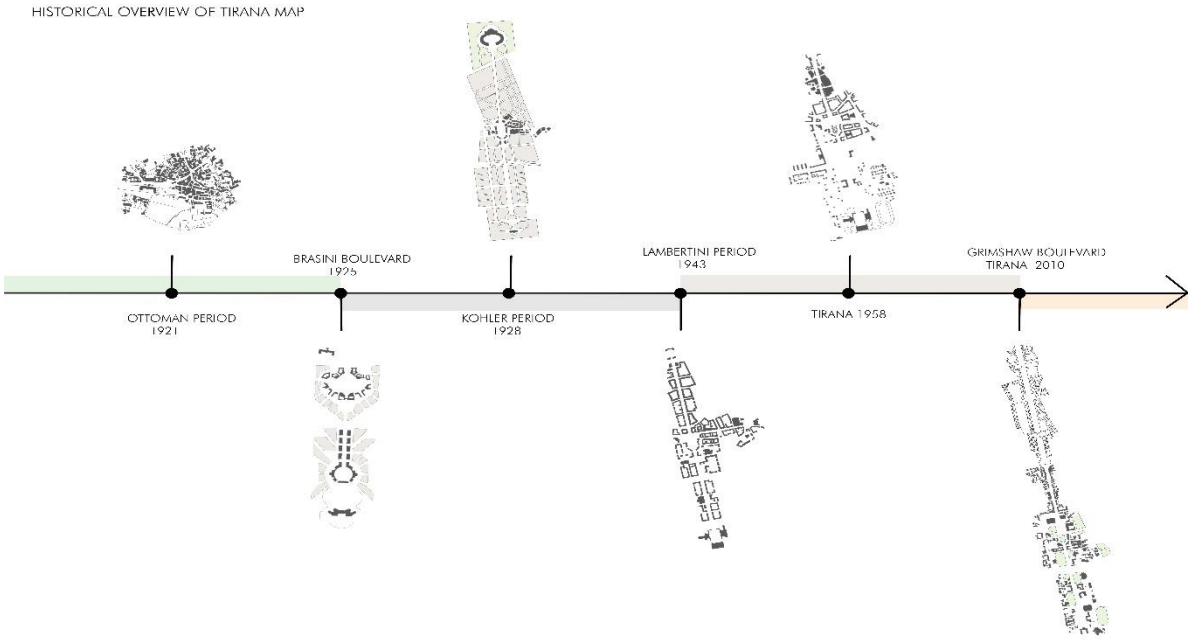

Figure 8. Tirana timeline map showing the morphology and development of the boulevard axis.

3.1.2 Tirana under ottoman period 1921

Like all of the Balkans, Albania was a part of the Ottoman Empire from the thirteenth century until its prolonged independence in 1912. The construction of a mosque, a hammam, a bakery, and an inn from Sulejman Pashe Bargjini[1]'s land signifies the start of the city, though the settlement is difficult to date ,which gradually led to the establishment of the bazaar. Since the 16th century, interregional trade networks have

been consolidated at Tirana's foundation. They led to the country from Durres and Vlora, the two port cities.

The city during this time frame expands in a similar manner to a spinning, expanding from these centers and others successively until these do not meet. Tirana witnessed spontaneous non-geometric morphological development during the medieval era. In this feudal society, extended families live in single-family homes and never part ways, but fences function as a buffer between them. As the centers expand, the streets and pathways evolve at random.

And hence, there is clear break with the Ottoman era, which has direct consequences from an urban perspective. Tirana suddenly finds itself hosting the entire state apparatus, and they will focus all of their efforts on providing the new capital with the institutions it must operate and plan for future growth. A variety of concepts are created in the following ten years for planning.

Figure 9.Map of Tirana in Ottoman period 1921

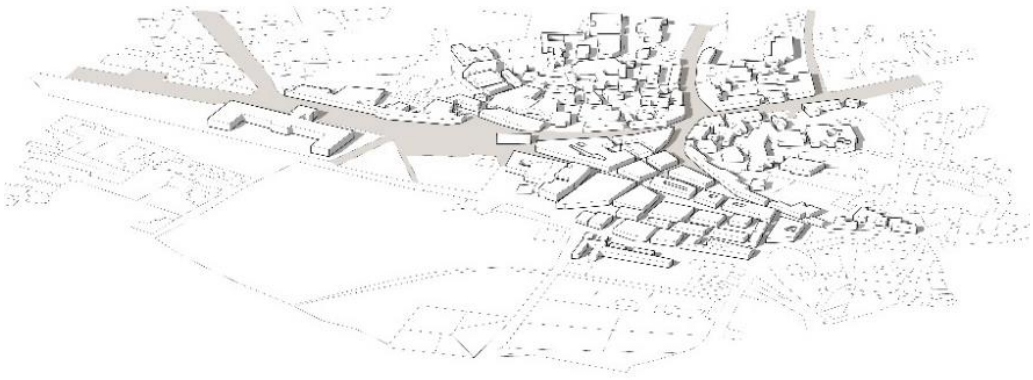

Figure 10. 3D Modelling of the center of Tirana in Ottoman Period

Figure 11.Sections of neighborhoods in Tirana 1921

3.1.3 Brasini boulevard proposal 1925

Tirana is officially declared the capital in 1925. Ahmet Zogu becomes prime minister and engages the Italian architect Armando Brasini to design a concept for Tirana for a quick but accurate explanation of the historical events of the time. In order to organize the operations of the capital, Brasini proposes the installation of a monumental axis. The proposal that Brasini offered was not followed out at time, but the principle of the axis was preserved in the city's layout (and in projects up until 1931) and would be re-proposed in the future.

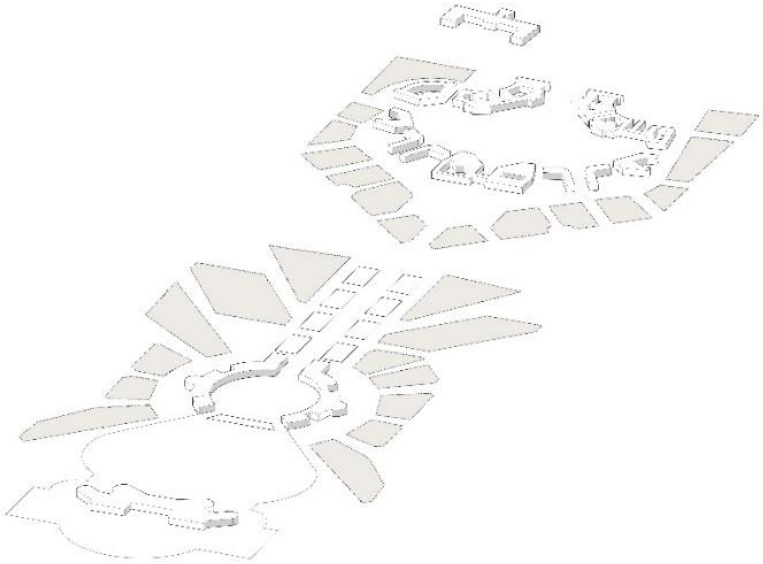

Figure 12. 3D Modelling of Brasini boulevard axis proposal 1925

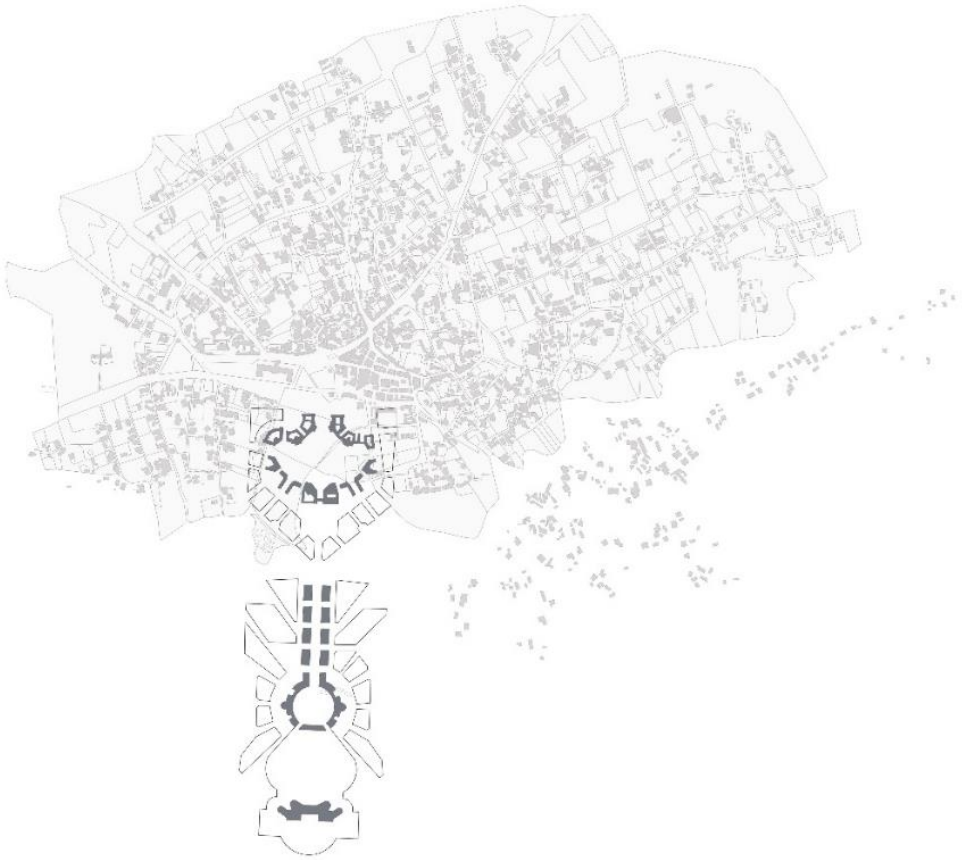

Figure 13.Brasini boulevard proposal put in Tirana's 1921 map

3.1.4 Kohler geometric grid on tirana 1929

Ahmet Zogu declared himself king of Albania in 1928 and offered the Austrian Kohler and the Albanian Frasheri directions to enlarge the area in order to amend the 1926 plan. In 1929, an additional land use plan by the Italian Di Fausto[2] was added to these.

Di Fausto is in charge of planning the Tirana center, whereas Kohler[3] is in charge of the growth of the city south beyond the Lana stream. Later, in 1930 and 1931, two additional, improved, and more detailed proposals have been prepared territorially based on the 1929 plan. In 1931, six buildings are implemented, still trying to define the southern portion of the city's city center, designed by Di Fausto and designed as ministries of Zog I's reign, and the northern portion, which will be demolished in 1982.

From an urban perspective, throughout this turbulent decade, the main common components—or tools, if we prefer—of nineteenth-century town planning may be seen in the urban design interventions of the period: Boulevard, gr[1]id, and geometric garden.From the earliest expansion interventions of the main arteries of the building of the city, such as in the concept of the central axis of Brasini, it is possible to see how the boulevard idea, which was widely employed by Haussmann onward, was applied. (Besnik et al., 2004) The grid, which has been employed in military contexts since the Roman era, fell out of favor throughout the Middle Ages for several centuries until making a comeback in the 19th century.

[2] Florestano Di Fausto- Italian architect who worked during the Fascist age in Italy and around the Mediterranean territories.
[3] Köhler - Austrian architect who worked on the regulatory plan of Tirana, proposing geometrical grid approach.

Figure 14. On the upper part is shown Kohler circulation proposal, below is shown city planning proposal, map of land plots, buildings and green areas 1929.

3.1.5 Ivo lambertini planning the city 1939

According to the time's territorial expansion objectives, Italy invades Albania in 1939. Since Italy came to power, King Zog I had economic and cultural exchanges with it. Large investments, particularly in Tirana, will be undertaken under the Italian rule in an effort to integrate in and begin the colonization process. A new regulation plan for Tirana is said to have been developed a few months after the invasion, and Gherardo Bosio, a Florentine architect, was given the task. The strategy will be finished in 1943. Bosio died in 1941, and Ivo Lambertini[4] and Ferdinando Poggi will take his post.

Private property was given a lot of consideration, as well as how to construct the city without endangering the previously established economic hubs and, consequently, the investments of the people. .(Capolino, 2011) As a result of the population growth, the core programming in the plan was considered necessary for accommodating the population for the 60 years that would follow.[2]

Zoning and class divisions, two constantly innovative ideas that first appeared in Tirana planning, are featured in the plan. One of Mussolini's key goals was to industrialize the nation, and Tirana was laying the groundwork for this to happen in Albania. (Besnik et al., 2004) The adoption of the garden city settlement type, thus, with a central populated population and outlying sites made up of industrial regions or huge equipment, will serve as the preparation to the industrialization that would occur starting in 1947.

In terms of structure, the plane maintains the current radial routes, to which extensions were made in past years, and connects them with a very wide infrastructure ring that has a diameter of about 3 km. The Brasini[5] axis continues to serve as the fascist movement's graphical backbone, and the floor's design is similar of the type system used in newly formed fascist cities like Latina.Bosio[6] will personally supervise the precise planning of the structures that face many of those that will be constructed, as they still stand as a significant cultural heritage today.

[4] Ivo Lambertini-Italian Architect who worked on Tirana's urban planning during King Zog I region.
[5]Armando Brasini- Italian architect and urban designer of the twentieth century who first designed the axis the boulevard of Tirana.
[6]Gherardo Bosio-Italian architect working on the planning of the center of Tirana.

Bosio favours the lictorian style, which is a combination of monumentality and formal simplicity of the materials. In contrary to Brasini, who took a neoclassical approach to the project, his style is much more formal and less ornamental.

Figure 8. Unbuilt areas and circulation of Tirana under Lambertini planning on the upper part, buildings, plots and green areas on the bottom.

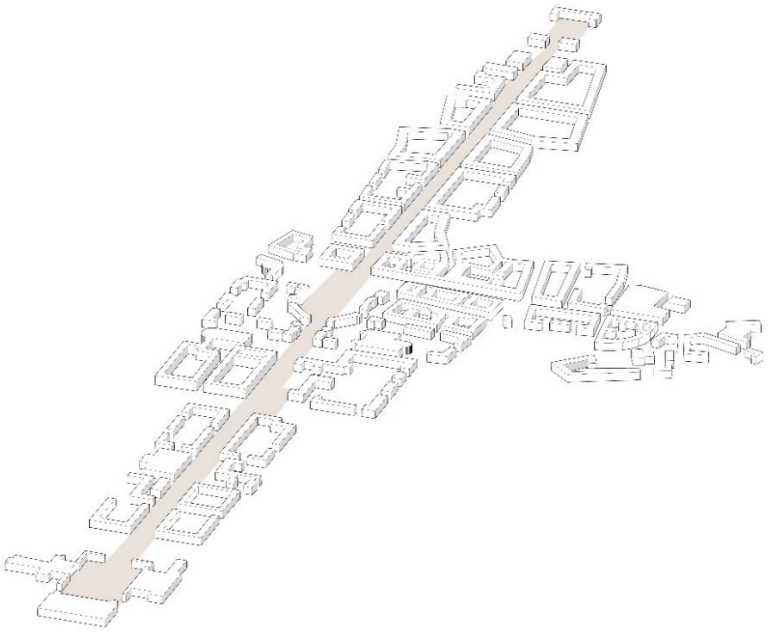

Figure 9.3D Modelling of Tirana boulevard proposal of Lambertini 1939

Figure 10. Sections of buildings in Lambertini city planning proposal 1939

3.1.6 Tirana under communism period 1958

Ideological appearance over the duration of the regime has also been seen in urban settings. Through purposeful urban manipulations, the desire to disobey was demonstrated in the case of Tirana. An example is the 1950s destruction of the historic market in the heart of Tirana to generate place for the Palace of Culture. Another is the adaptation of the initial parliament's seat into the Puppet Theater. Another example of

the intended symbolic appropriation of the city via architecture is the 1982 destruction of the previous town hall building constructed in the 1930s and replacement with the National Historical Museum.

The Soviet influence is evident not only because Soviet experts and Bulgarians directly contributed to the creation of these plans, but also because the majority of the Albanian architects whom collaborated on them received their education in the nations of the Soviet block.

Components of the Bosio plan's structural implementation are maintained by the 1958 plan. On the same foundation as the preceding level, the ring was created in the years that followed, with an additional inner ring.

The proposal for the sizable park, now known as Lake park, was realized south of Tirana. Instead of the courtyard structures and villas that were the principal construction types in the 1943 design, the buildings will now be placed more in line with contemporary Soviet urban planning. .(Capolino, 2011) The communist ideology, which promotes equality and collectivization and will be represented in both the distribution and the urban typologies, is incompatible with the partition of society into classes as outlined in the plan di Bosio. (Besnik et al., 2004) The villas will make way for communal structures, and the arrangement will be equitable for all inhabitants, at least in theory. The goals of this strategy may be summed up as follows:

- increase in urban density

- the reassignment of functions

- enhancing and expanding the plant road

- maintenance of the city's historic areas

- sensible land use

The redevelopment of Tirana will be based on the 1957–1958 plan, from which further, more specific plans were also produced until 1990. Tirana's urban growth was significantly influenced by economic and technological reasons. The outer of the two rings was manufactured almost totally, whilst the inner one was only made up of a few small pieces. They practically seldom build homes with more than five levels.

Figure 11. Map of Tirana under communism period 1957

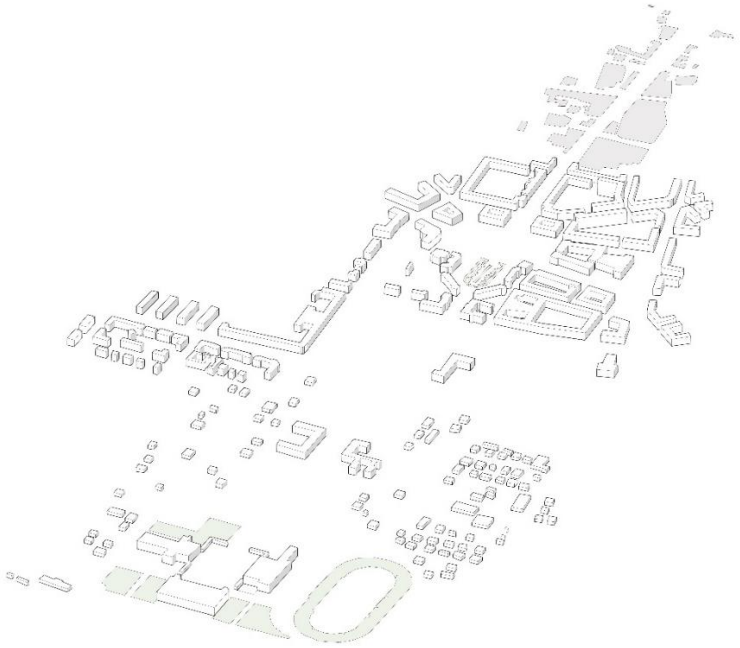

Figure 12.3D Modelling of boulevard in 1957

Figure 13. Sections of Tirana buildings located in boulevard 1957

3.1.7 Tirana planning and boulevard extension Grimshaw 2012-present

The interventions during communism overlapped the pre-existing tissues morphologically. However, once communism fell, the propensity for irregular textiles resurfaced. The Hotel Tirana, with fifteen high plans, was the tallest structure up until 1990. Currently being constructed behind it on the display is a 25-story slab building, and just next to it is an even larger structure. Hold trace of all the buildings that are being constructed—and are presently being built—that are more than 15 stories tall. There are countless examples that might be given, but none of them would serve our needs. In contrast to the Tirana that it was at the time, the apartment complexes also come from a different dimension.

The enlargement of the boulevard and the restoration of the Tirana River are the two most significant elements of recent Tirana development. Given the crowded nature of the consolidated metropolis, a special focus is placed on the ecological system, environmental protection, and recreational areas. The river and the boulevard are

categorized as ecological corridors in the competition brief. The expectations and objectives are clearly stated in a simple manner. Sustainability is a key factor in both the requests made and the vision for urban development.

The point-like form of the suggested interventions is a recurrent feature throughout Grimshaw's[7] proposed design for the Tirana. This may be inferred from the basic masterplan, which has several shapes depending on the region it covers. Everything in the consolidated city except for the boulevard and the riverbanks is designed using an urban acupuncture approach, which involves inserting needles at strategic locations throughout the constructed environment to revitalize the natural habitat.

Regarding the central office instead, it should be highlighted that the boulevard and river axes are, respectively, marked by high density, the predominance of the constructed one, and the predominance of the environmental system, respectively. In the second measure, even if the river's axis and the expansion of the boulevard maintain some degree of unity, the explanation for the urban planners' planning mostly relies on quick interventions.

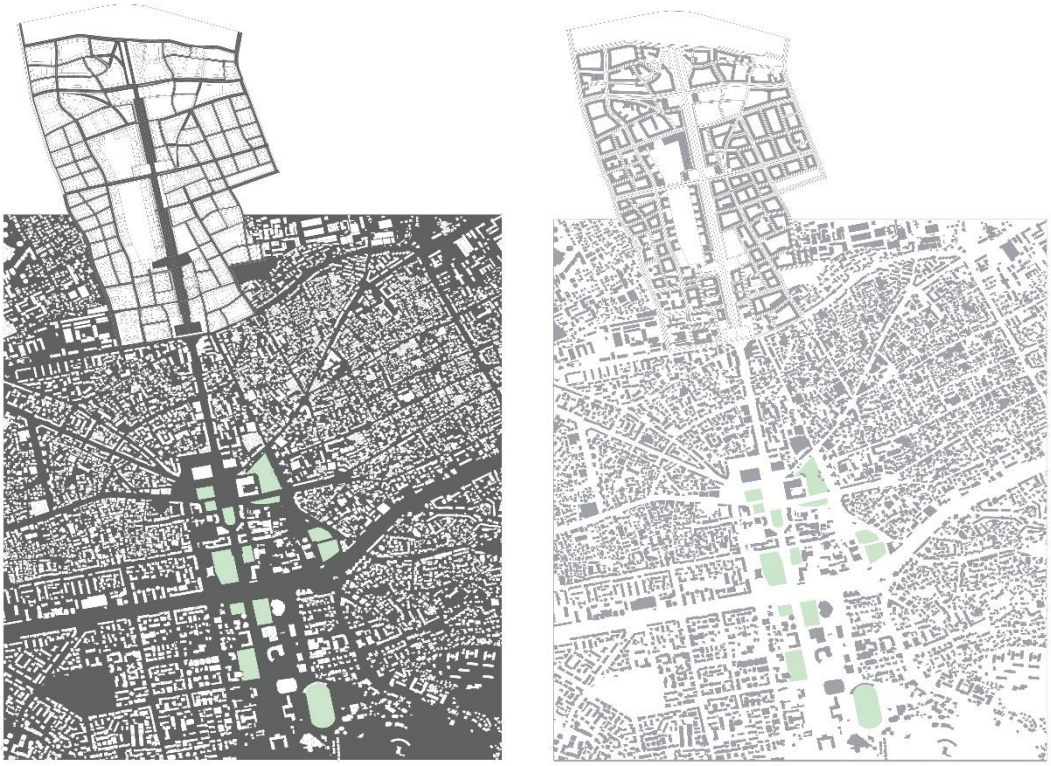

Figure 14. On the right the unbuilt areas map of Tirana, on the left map of built areas.

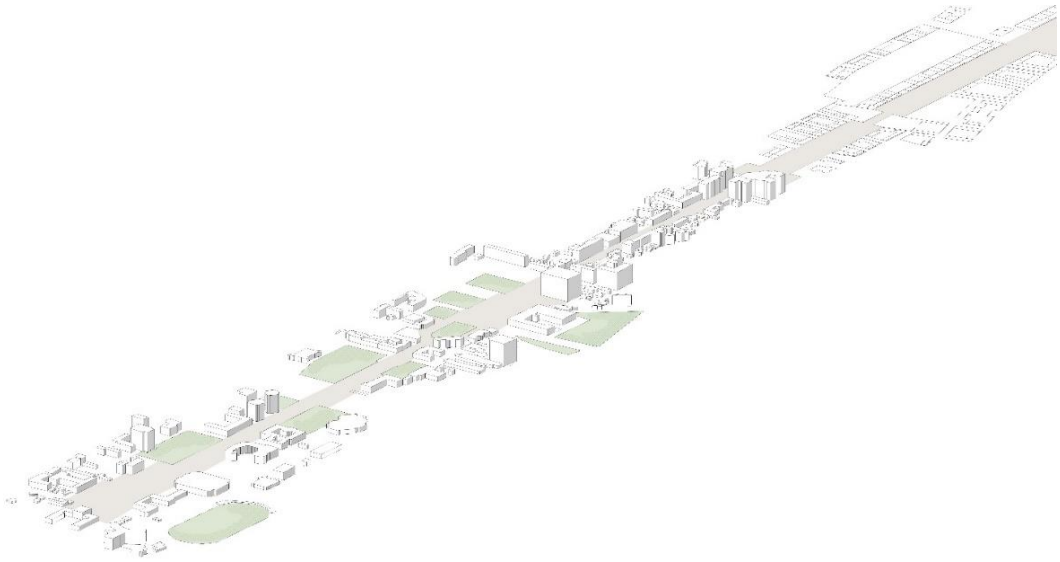

Figure 15.3D Modelling of Tirana boulevard from "Mother Teresa "Square to the end of Grimshaw boulevard.

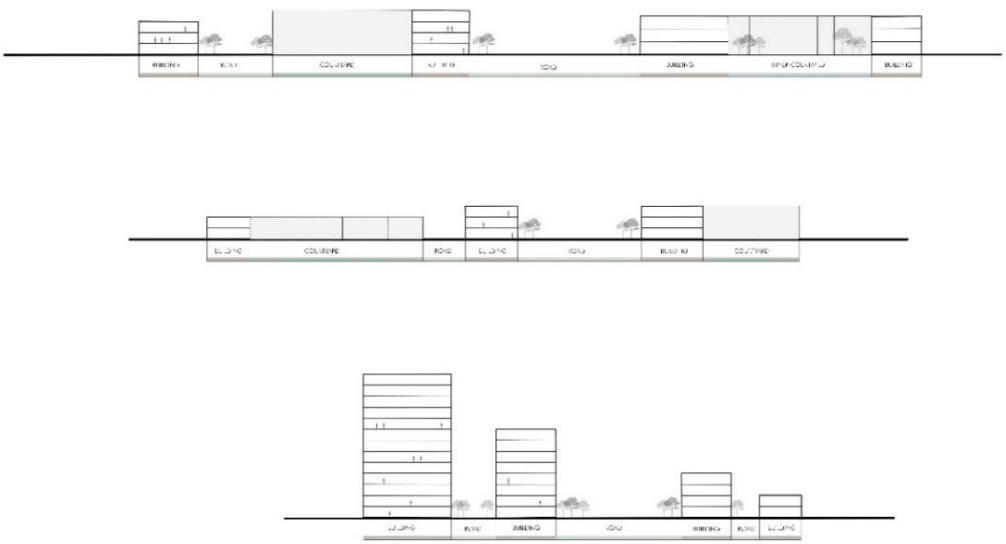

Figure 16. Sections of Tirana buildings located along the boulevard.

Figure 15.Boulevard of Tirana project idea proposals (Park of Faith,SdARCH Trivelli&Associati 2015)

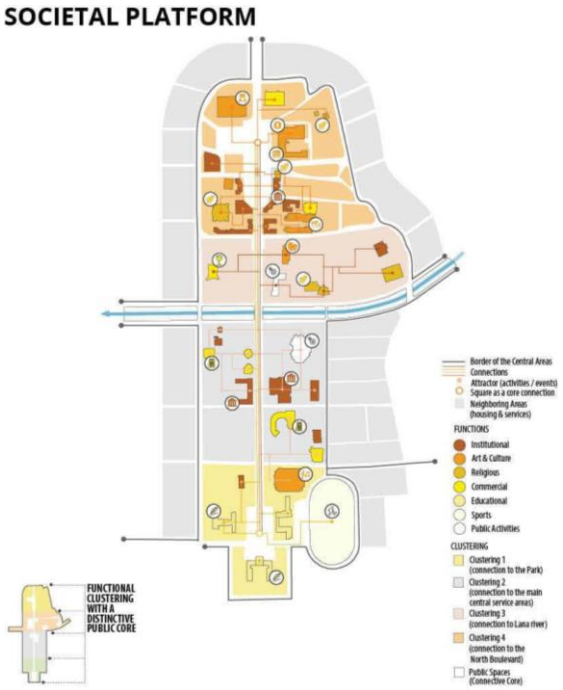

Figure 16.Societal platform analysis of the todays boulevard of Tirana (Park of Faith, Metropolis studio 2015).

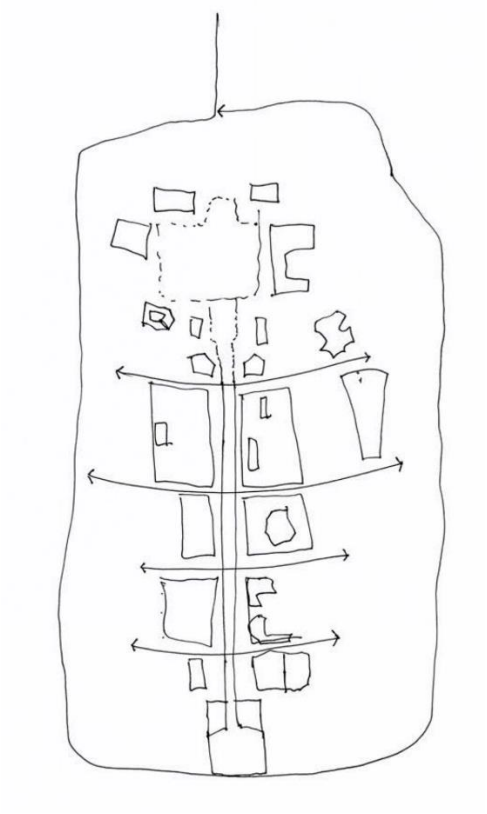

Figure 17. Boulevard of Tirana (Park of Faith, SdARCH Trivelli&Associati 2015)

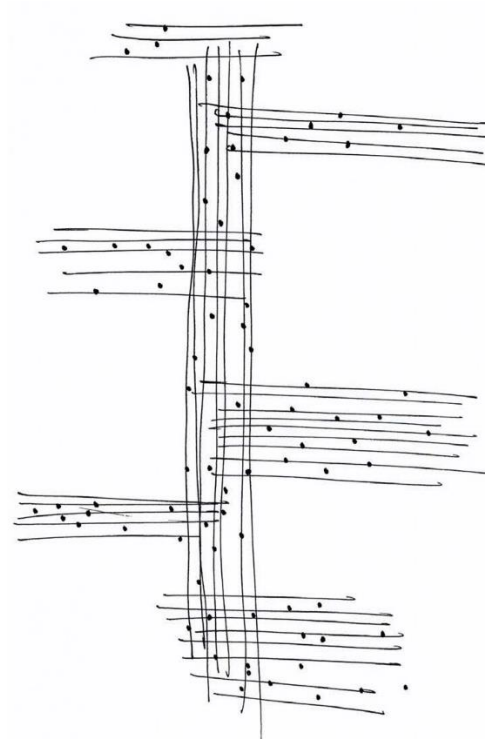

Figure 18.Boulevard of Tirana (Park of Faith, SdARCH Trivelli&Associati 2015

3.1.8 Comparison between periods of urban planning in Tirana

Ottoman period 1921	Brasini 1925	Kohler 1929	Lambertini 1939	Communism period 1958	Grimshaw-present 2012
Low rise dwellins			Buildings arise to 3-4 floors high	Dwellings are up to 5 floors and higher (Example of international hotel of Tirana 15 floors high)	Larger structures
Single family homes	Public buildings design		Family homes integrated with public buildings along the axis	Reassignment of the functions Maintenance of city's historic areas	Different functions of the buildings, public, private, semi private etc.
Inner courtyards		Geometric courtyards	Inner courtyards are mostly used in public, government buildings	Proposal of lake park, green areas	TR030 by Stefano Boeri
Narrow paths	Distance between buildings becomes wider		New plazas and wider roads along the axis of boulevard		Plazas, wider roads, parks sidewalks etc. depending on the context
Not an actual urban plan	Proposal of axis or boulevard	Grid planning layout	Zoning and class divisions Garden city settlement type	Inner and outer ring play and important role	The enlargement of Boulevard and restoration of Tirana river Ecological corridors
City extending in various directions	City extending depending on the boulevard axis proposal	Extensions in the most important arteries of the city	Radial routes, the outer ring of Tirana around 3 km	Addition of inner ring of Tirana Enhancing and expanding the plant road	Sustainable city

Table 1. Comparison of historical periods of Tirana from the urban planning perspective.

CHAPTER 4

METHODOLOGY

4.1 Climate

Tirana, which serves as Albania's capital, is situated in the country's geographic center, some 25 kilometers (15 miles) inland from Durres. Tirana has a Mediterranean climate with hot, sunny summers and warm, wet winters. The wettest month is November and the driest is July. On average, there are 9.9 days per year with more than a millimeter of precipitation. When considering all forms of precipitation, Tirana is ranked as the third-wettest city in Europe. In Tirana, the yearly average temperature is 14.8 °C (58.6 °F).

December (73.3%) has the greatest relative humidity of any month. August has the least relative humidity of any month (62.69 percent). December is the season with the most days with rain (12.7 days). July is the month with the least amount of rainy days (5.10 days) Tirana has a total of 2500 hours of sunshine each year, making it one of the sunniest cities in Europe while being one of the wettest. It receives 198,6 hours of sunlight in January, but 394,56 hours in July.

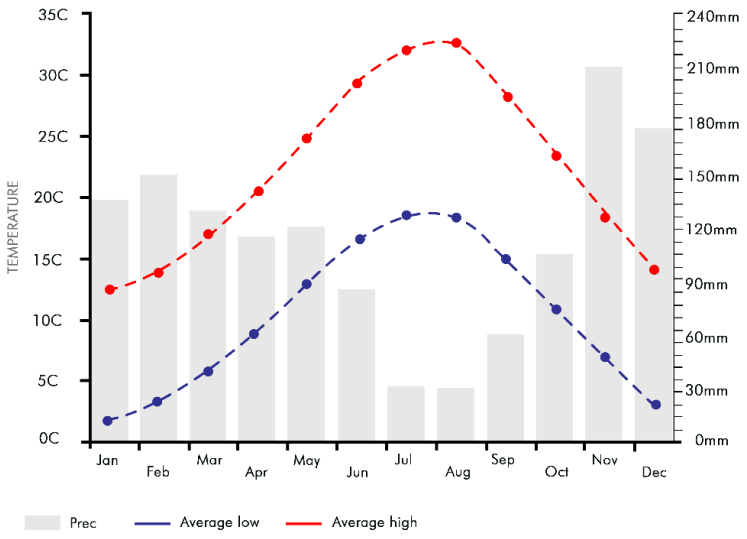

Figure 19.Average temperatures and precipitation in Tirana.

4.1.1 Case study selection

Since it links some of the most useful and walkable parts of the city, the Boulevard of Tirana will serve as our case study. It additionally functions as an important axis in terms of history and culture. One of the case study venues will be Skanderbeg Square in Tirana, which is bordered by a large number of noteworthy public and private structures. It is also one of the city's most walkable squares. The second zone to be examined is the Nene Tereza plaza, which is located at the end of the boulevard. It is a highly significant square that is surrounded primarily by educational buildings, which stimulate pedestrian movement.

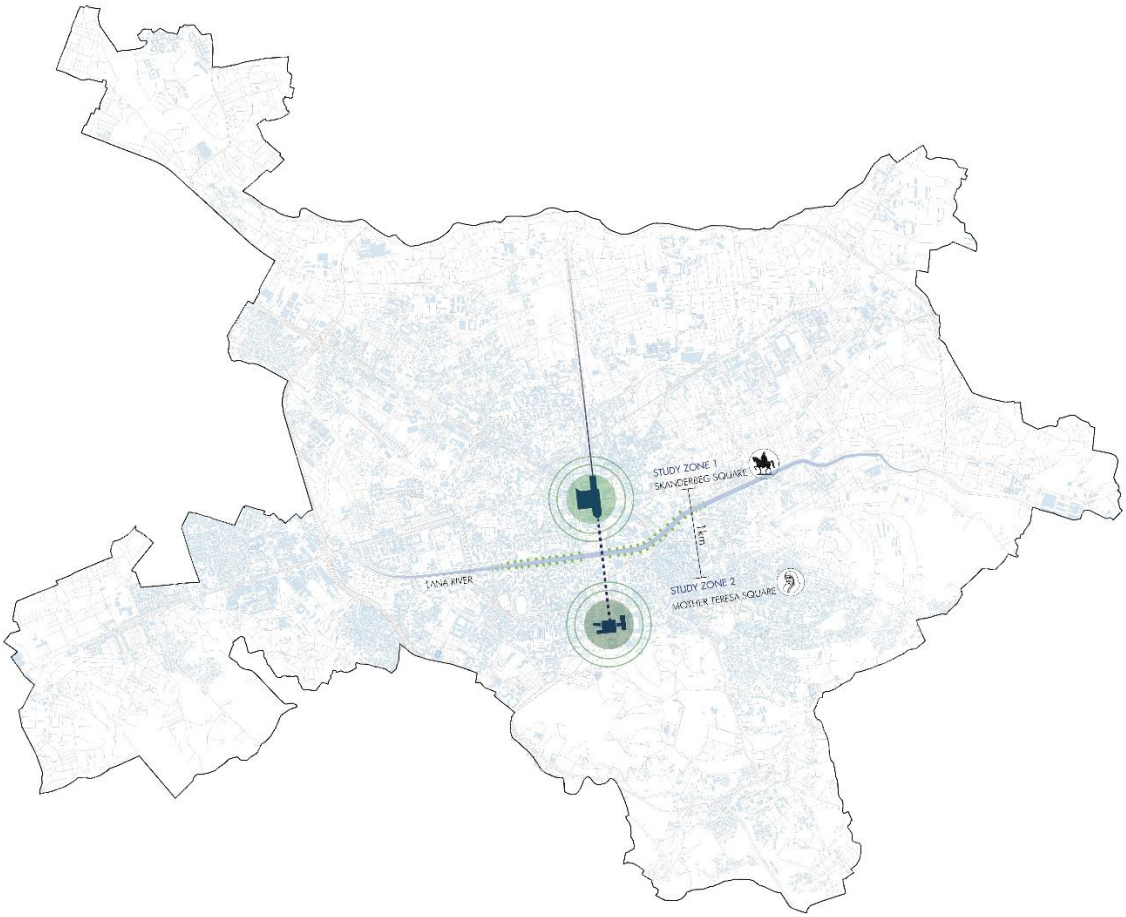

4.2 Zone 01 [Skanderbeg square S.S]

The main square of Tirana, Albania, is called Skanderbeg Square. There are around 97,344 square meters in all. The square is home to a number of structures, such as the Tirana International Hotel, the Palace of Culture, the National Opera, the National

Library, the National Bank, the Ethem Bey Mosque, the Clock Tower, the National Historical Museum etc.

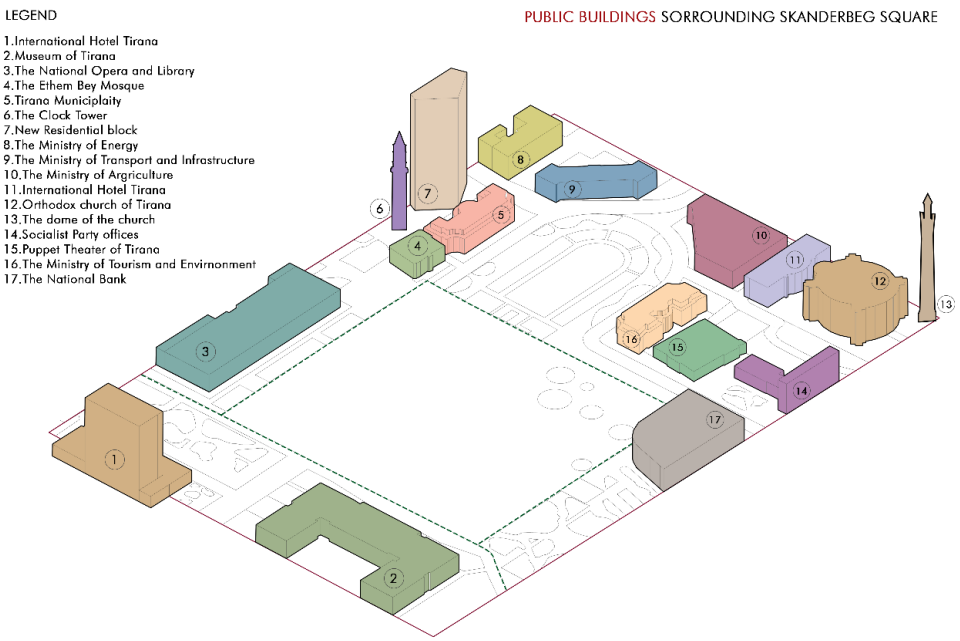

Figure 20. Illustration of public buildings surrounding the Skanderbeg square.

Several political eras have seen some alterations to the plaza. The concept to turn the square into a pedestrian-only and public transportation-only area first emerged in March 2010. The square would be balanced with a 2.5% inclination and a two-meter high spire would be constructed. The new fountain would be using rainwater as its source of water. The following mayor stated that the 2010 design will instead be reintroduced with minor adjustments such as greener space surrounding the plaza, underground parking, and the use of stone material from all regions of Albania and Albanian-inhabited territories. The grounds around the area would showcase Albania's diverse plant life, while Europe Park, once the garden behind Skanderbeg's monument, would be restored to its pre-2010 appearance.

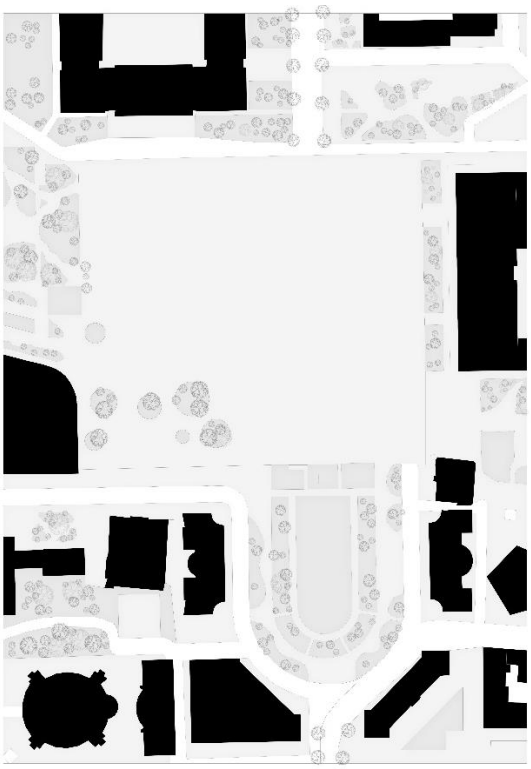

Figure 21.Nolli map and building height analysis of Skanderbeg square area.

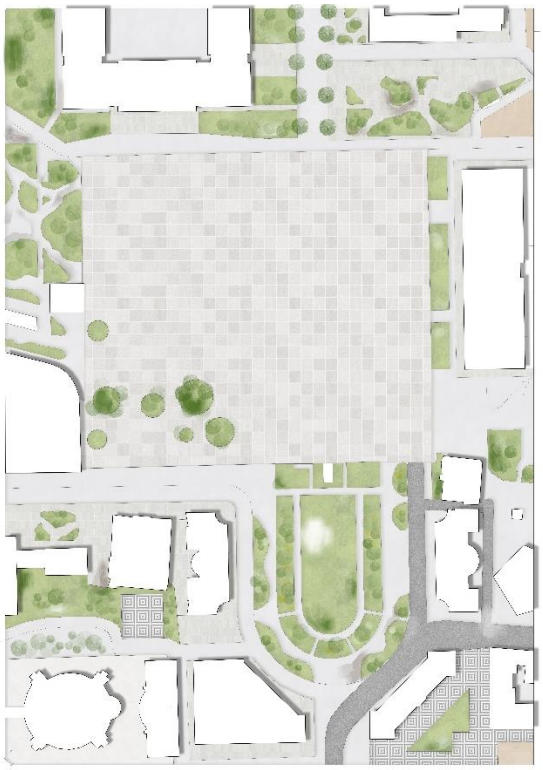

Figure 22.Site plan of the Skanderbeg square area.

Twelve gardens make up the square's green belt, and each one is connected with a particular one of the either private or public organizations that line the area.

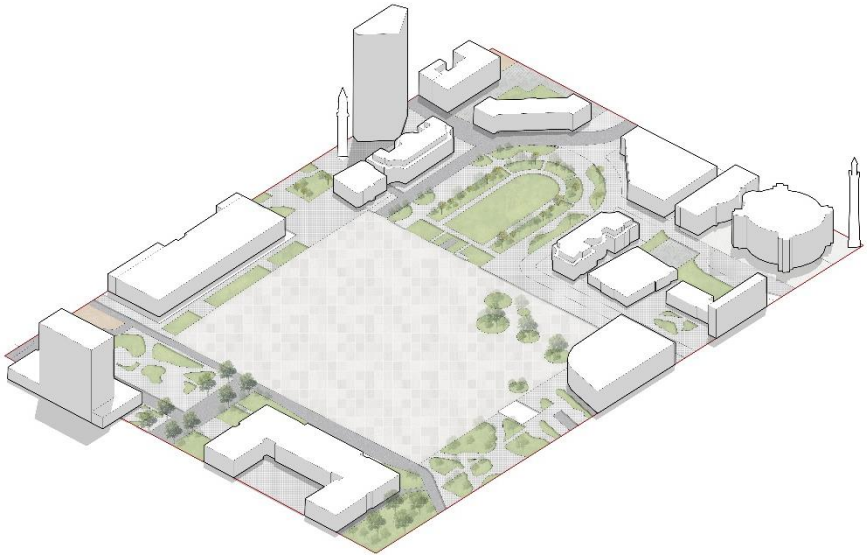

Figure 23.3D illustration of Skanderbeg square area.

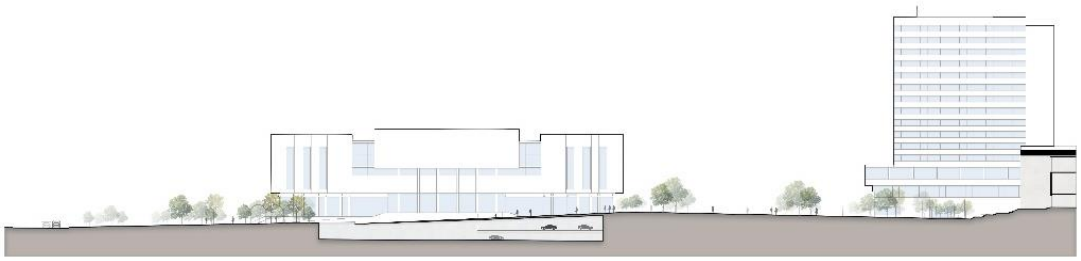

Figure 24.Section of the Skanderbeg square area.

Skanderbeg square vegetation analysis

Surveys on the plaza show that most people prefer to hang out in the shade of the urban forest beyond the museum garden throughout the day. It now has the most greenery in the square. The vegetation that surrounds the plaza is made up of about 1973 trees, 7382 high and low shrubs, and 75881 perennials that bloom all year long. There is also a 5335 m2 section of lawn that is spread out across the plaza. The museum garden, which is located behind the national history museum, and the book garden, which is located in front of the national library, appear to be the most opulently large and intense gardens.

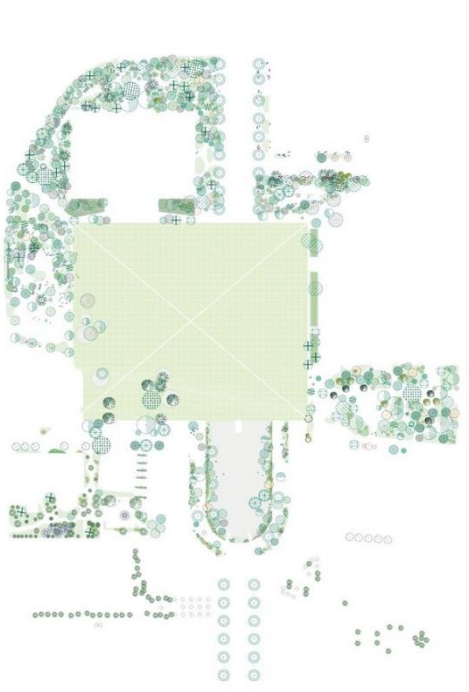

Figure 25.Skanderbeg square vegetation plan (51N4E,2016)

Figure 26.View from the urban forest near the National Museum of Tirana.

Figure 27. Pictures of vegetation on the site.

Water presence

At Skanderbeg Square, water is handled more as a component to be organized, as a complex model that interacts with the other eco-systems while yet actively interacting with the everyday users. There are three various types of water present on the site, including drinking fountains, spray fountains, and leaky fountains.

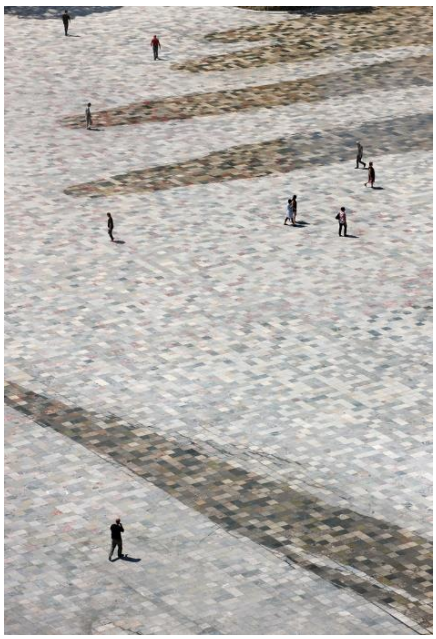

Figure 28.View from the square fountains in the summer (51N4E, 2016)

They like it as a stand-alone activity on the plaza even if it is a really pleasant aspect of nature that has been incorporated into a public place. During the sweltering summer

days, they use it as a game element, drinking water, and anti-heat refreshment. The center project of Tirana, which imports and exports a significant volume of water in a continuous circle, is the city's greatest import and export. The water is pumped from the mechanical room, is pushed up and dispersed through the group's leading pipes to further reach the leaky fountains and softly flow over the pyramidal square's topography.

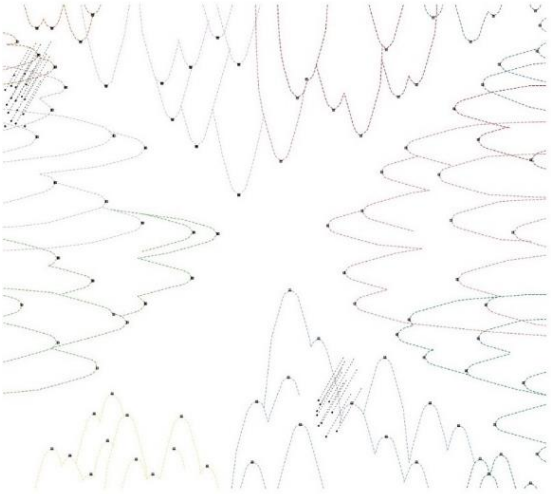

Figure 29.Scheme of the fountains. (51N4E, 2016)

In total, the water system has about 100 leaky fountain points that leak water to cover the entire solid pyramid. It is also enhanced with 30 jet water features that are divided into two groups and placed close to the Skanderbeg statue and the national bank, respectively. Additionally, it has 7 drinkable water fountains hidden among the trees next to the puppet theater garden.

Square and pedestrians.

We met 279 individuals that were either permanently residing in the area around the square, employed nearby, or merely traveling to and from their places of employment. Interestingly, the majority of these individuals frequently use the square. As seen in the chart below, only 7.1% of them rarely used the square, and 2.8% of them used it on weekdays. Those who used to live in the capital but no longer call Albania home and only visit for vacations account for the majority of the few times each year. On the other side 14.5% of them used the square at least three times a week and 21.4 % of them

used it everyday, to pass by while going to work or just staying there. According to the report, 72.2% of the questioned individuals use the facility on a weekly basis.

Figure 30. View from the square, people sitting in front of the Opera.

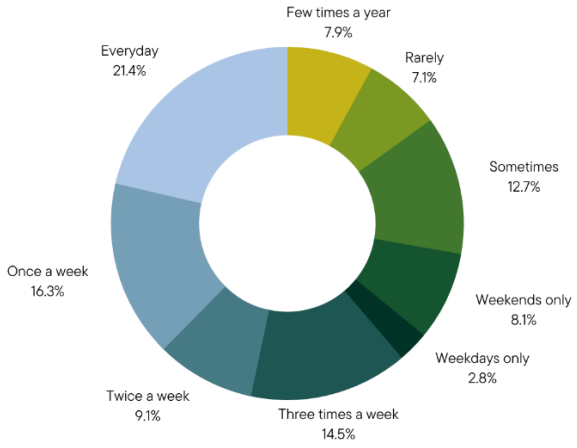

Figure 31 . Chart illustrating the frequency of participants in the survey.

Microclimate of the zone.

People primarily cross the plaza and pass by throughout the day since it receives exposure to the sun. Few individuals choose to remain in the square. But then, it is easy to 64 observe people trying to find shaded corners, on the main square, under the trees, under the monumental entrances of the premises around or even under the Skanderbeg statue. The moving of the sun, though very quickly after sunset allows for the plaza to

get filled with people. Seems that solar radiation and lack of shading on the main square pushes the people to use more the surrounding garden during the day, where they find shadow, freshness under the trees and cooler temperatures.

In the garden nearby, they are more shielded from the elements such as wind and rain in the winter. Passengers often traverse the plaza rapidly during the day, but in the evening it becomes a pleasant unhurried walk. As the sun sets, all of the evening walkers, cyclists, and all-wheel vehicle users congregate in the open space in the middle.

4.2.1 Microzones of [Skanderbeg square]

To understand how orientation influences temperature, radiation, wind, and relative humidity, zones with different patterns of the same square are compared to one another at the microscale.

4.2.2 Microzone 1 [MS.01]

The real square, a paved area that has been renovated and made mostly pedestrian-friendly, is located in Microzone 1 [M1.S]. Numerous sculptures and monuments are there, along with broad promenades, fountains, and green spaces. It serves as a connection between multiple locations in the heart of Tirana, which is makes it essential.

Figure 32.Microzone 1 [M1.S] located in Skanderbeg square.

The real square, a paved area that has been renovated and made mostly pedestrian-friendly, is located in Microzone 1 [M1.S]. Numerous sculptures and monuments are there, along with broad promenades, fountains, and green spaces. It serves as a connection between multiple locations in the heart of Tirana, which is makes it essential.

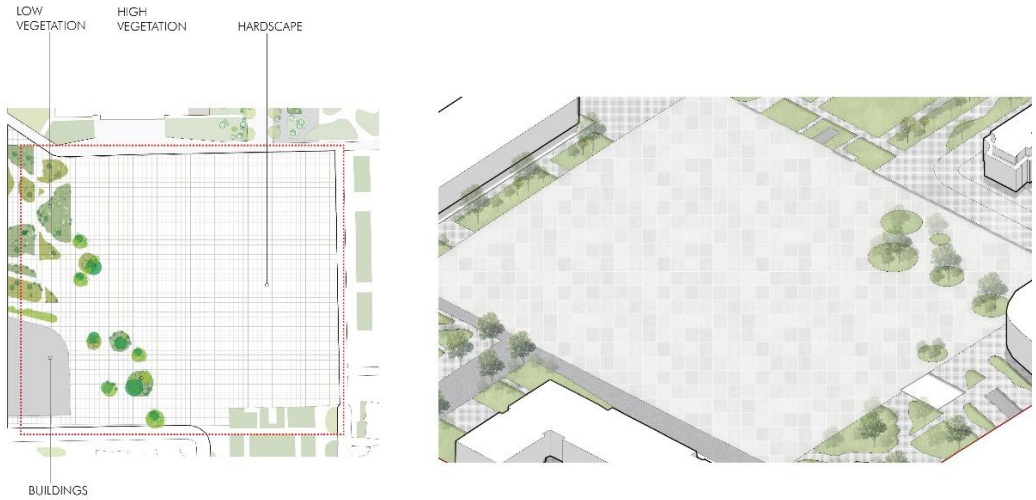

Figure 33. Closer site plan and 3d illustration of the microzone [MS.01].

Different materials are included into the square's design, which improves both its aesthetic value and symbolic significance. The pavement, which is primarily composed

of premium granite and marble, gives the square's opulence an attractive and sturdy base. Visitors may wander and take in the surrounding sites in comfort and safety thanks to the smooth, textured tiles that line the pedestrian routes. The Skanderbeg Statue, which serves as the centerpiece of the plaza and is elevated on a solid bronze pedestal, represents the fortitude and tenacity of the nation's hero. Architectural buildings that surround the area have a tasteful fusion of glass, steel, and concrete, expressing the city's contemporary urban growth while paying homage to its ancient heritage.

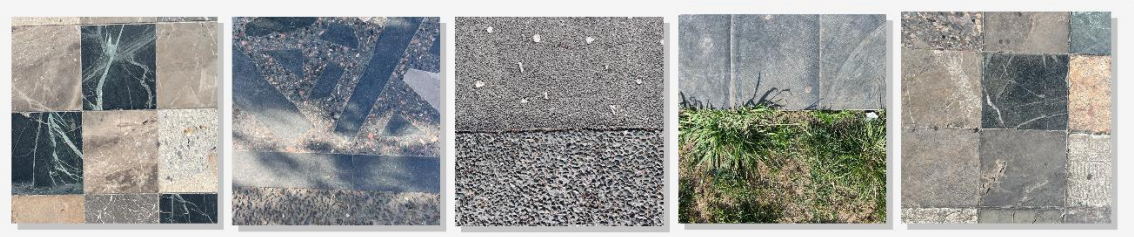

Figure 34. Material palette of the microzone.

Figure 35.Photos from the site.

4.2.3 Microzone 2 [MS.02]

Microzone [M2.B] named as Europa park is located at the beginning of the boulevard “Deshmoret e Kombit”, at the southern part of the Skanderbeg square. It has a considerable green park where people may sit or pass by. There is evidently vegetation there, including trees and shrubs that cast shadows along the region. It is a useful site that serves as a recreational space for all ages.

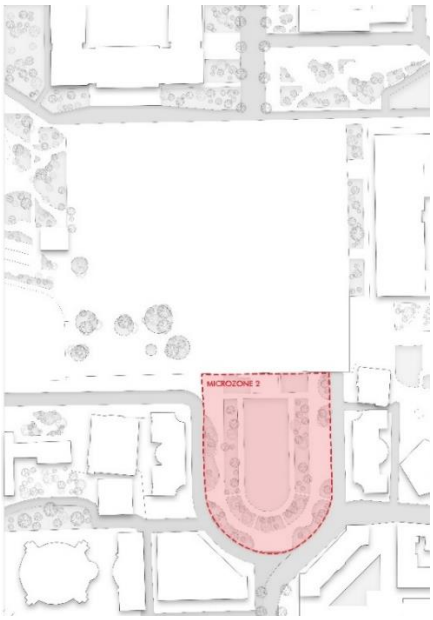

Figure 36.Microzone 2 [M2.B] located in Skanderbeg square.

It is a captivating retreat that mixes the beauty of the natural world with carefully chosen materials, drawing tourists both near and far. The park's walkways were created utilizing stone and brick that was found locally, fitting in perfectly with the verdant surrounds.

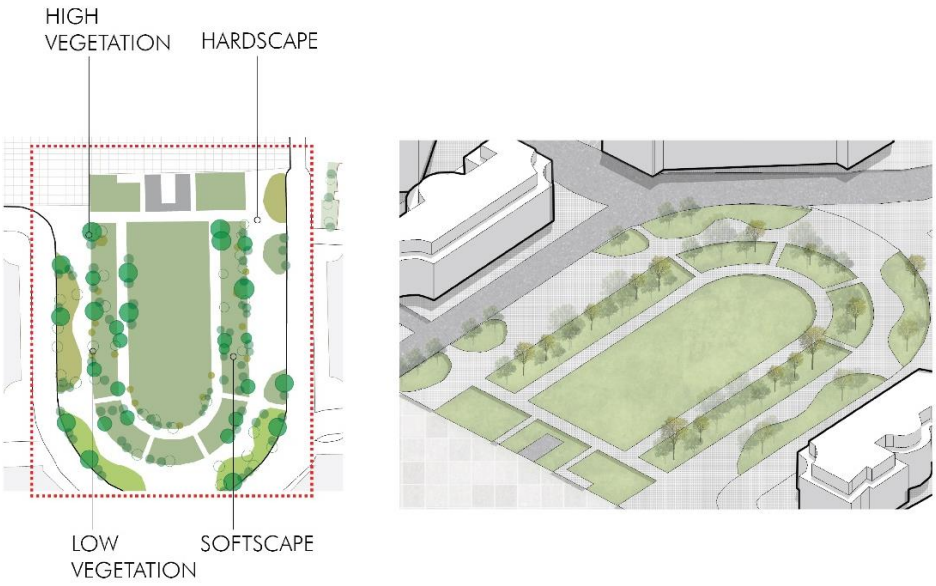

Figure 37 .Closer map and 3d illustration of the microzone [MS.02].

The infrastructure of the park is skillfully built using a combination of tough materials like stone, concrete, and other hard and softscape surfaces to ensure both aesthetically pleasing and long-lasting areas. High-quality stone and brick were used for the paths

and pavements, giving visitors a beautiful and stable base from which to explore the park.

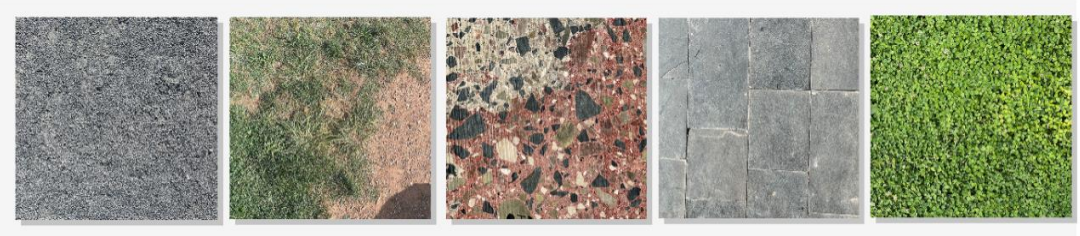

Figure 38. Material palette of the microzone.

Figure 39. Photos from the site.

4.2.4 Microzone 3 [MS.03]

Microzone 3 [M3.Z] is located at the northen part of Skanderbeg square, at the end of the boulevard “Zogu I Pare”. The area serves as a corridor for persons passing from the boulevard to the Skanderbeg Square and is located between the National Museum of Tirana and the International Hotel of Tirana.

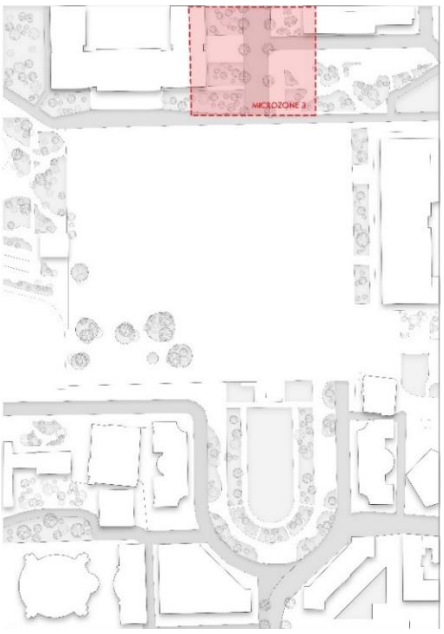

Figure 40.Microzone 3 located in Skanderbeg square.

Microzone 3 [M3.Z] is located at the northen part of Skanderbeg square, at the end of the boulevard “Zogu I Pare”. The area serves as a corridor for persons passing from the boulevard to the Skanderbeg Square and is located between the National Museum of Tirana and the International Hotel of Tirana.

Figure 41. Closer map and 3d illustration of the microzone [MS.03].

Concrete and granite, two long-lasting and aesthetically pleasing building materials, were used to construct the boulevard's foundation, resulting in a strong structure that can handle significant foot traffic. It becomes clear that the boulevard draws a diverse crowd of tourists as they wander down it. Both locals and visitors congregate here because of the area's lively ambiance and welcoming cafés beside the International hotel of Tirana.

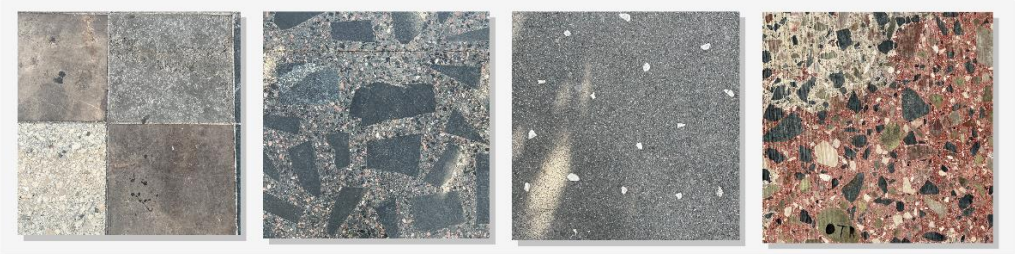

Figure 42. Material palette of the microzone.

Figure 43. Figure 35. Photos from the site.

4.3 Zone 02 [Mother Tereza Square N.S]

This square is located at the end of “Deshmoret e Kombit Boulevard”. The Presidency, the Academy of Arts, the Corps of the University of Tirana, the Bust of Mother Teresa, the Sheraton Hotel, the Rectorate of the University of Tirana, the Archaeological Museum, and the Palace of Congresses are just a few of the significant public structures that surround the area.

The square was firstly designed by Italian architect Gherardo Bosio and constructed in a rationalist style between 1939 and 1941, while Italy was occupying Albania. In honor of Mother Teresa, an Albanian Catholic nun, missionary, and recipient of the Nobel Peace Prize, the area is known as Mother Teresa area.

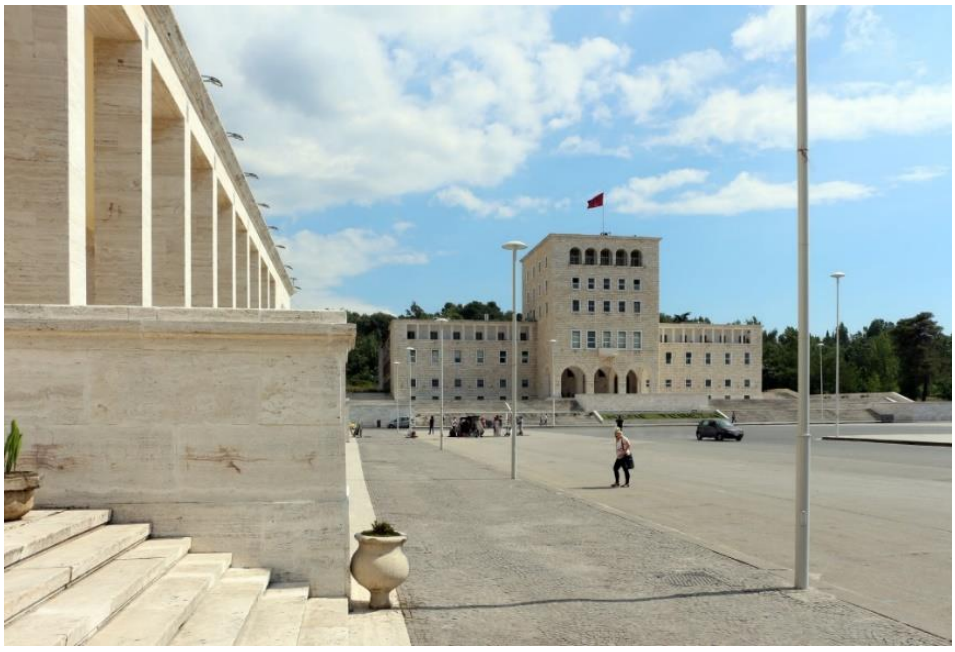

Figure 44.Mother Teresa square (Source: Wikipedia)

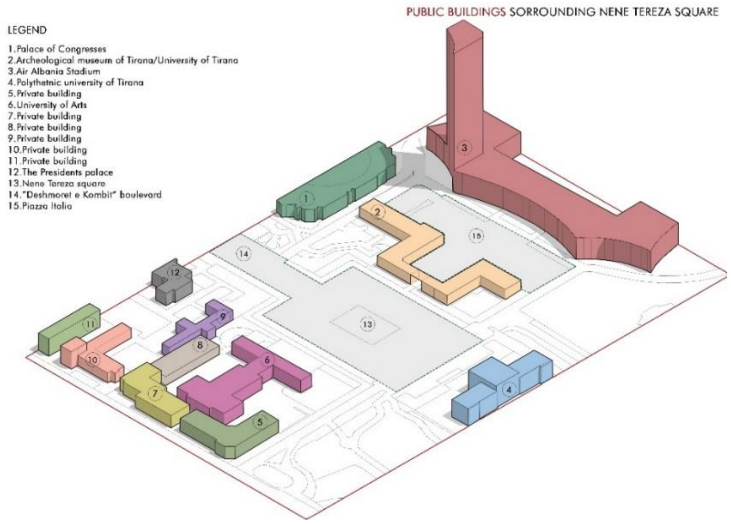

Figure 45.Illustration of public buildings surrounding the Mother Teresa Square.

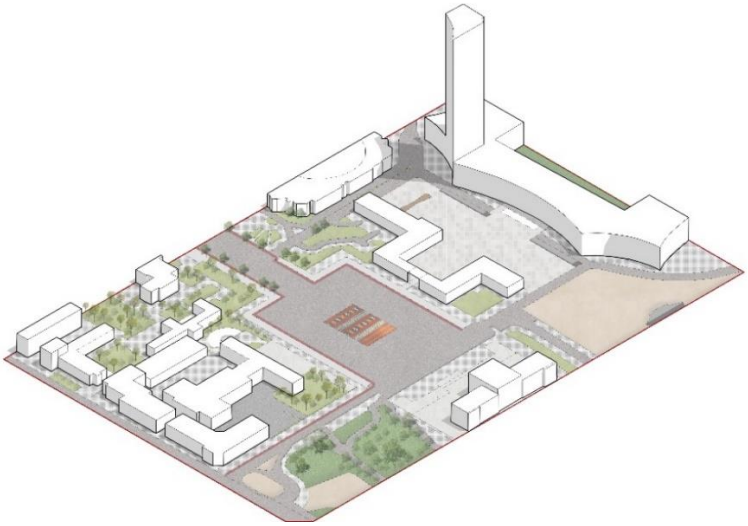

Figure 46. 3D Illustration of Mother Teresa Square.

During regular hours, the area is frequently buzzing with activity. Residents and visitors frequently congregate there, and several activities and festivities take place there. The square is well-known for its spaciousness, fountains, and greenery, which make it a desirable location for unwinding, mingling, and engaging in outdoor activities.

Figure 47.Nolli map and building height analysis of Mother Teresa square area.

Figure 48. *Building height analysis of Mother Teresa Square.*

A range of materials are used in the square's design to create a stunning setting. The pavement provides a sturdy and beautiful basis since it is made from marble and granite of the highest grade. Polished bronze was used to create the main Mother Teresa monument, representing her eternal influence and altruistic spirit. The neighboring buildings combine current architectural aspects and express the development and modern identity of the city by employing materials like glass, steel, and concrete. Recently, the square's center was covered with a massive rug painting in celebration of the Mediterranean 18 Young Artists Biennale, which incorporated traditional patterns from the nearby county of Saint Gjergj.

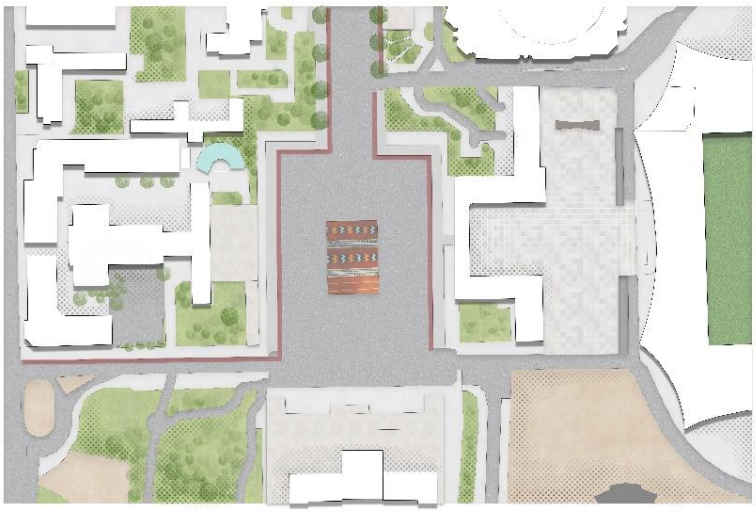

Figure 49. Site plan of Mother Teresa Square.

SECTIONS.

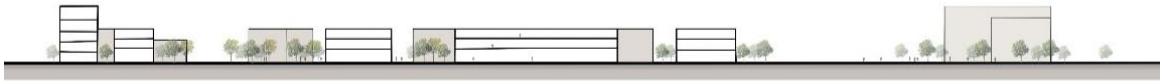

Figure 50. Section A-A of Mother Teresa Square.

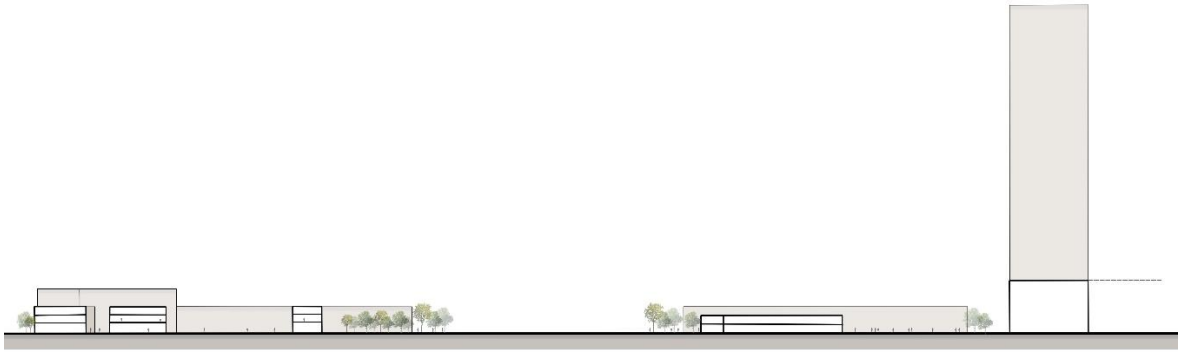

Figure 51. Section B-B of Mother Teresa Square.

4.3.1 Microzones of [Mother Teresa Square N.S]

Four smaller study areas that are going to be named "microzones" have been chosen, and simulation techniques are going to be used to generate the microclimate conditions in these areas while taking into consideration their layout, materials, vegetation, and structures.

4.3.2 Microzone 1 [MN.01]

Plaza Italia is the first microzone.The square is located between the Air albania stadium and the archaeological museum. After the stadium was completed, it gained a lot of popularity, especially among young people who may use it for a variety of sports including cycling and skating. Mostly populated on weekends, but also throughout the day. Being surrounded by commercial space increases the likelihood that many people will pass by and notice the area.

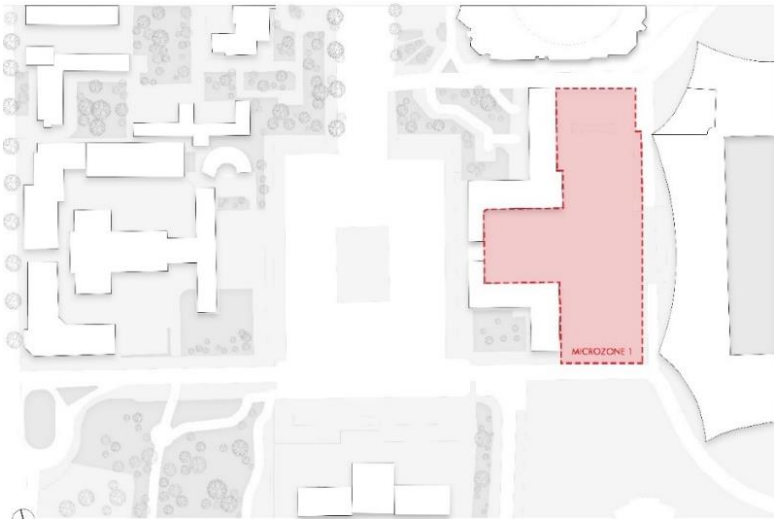

Figure 52. Microzone 1 located in Mother Teresa Square.

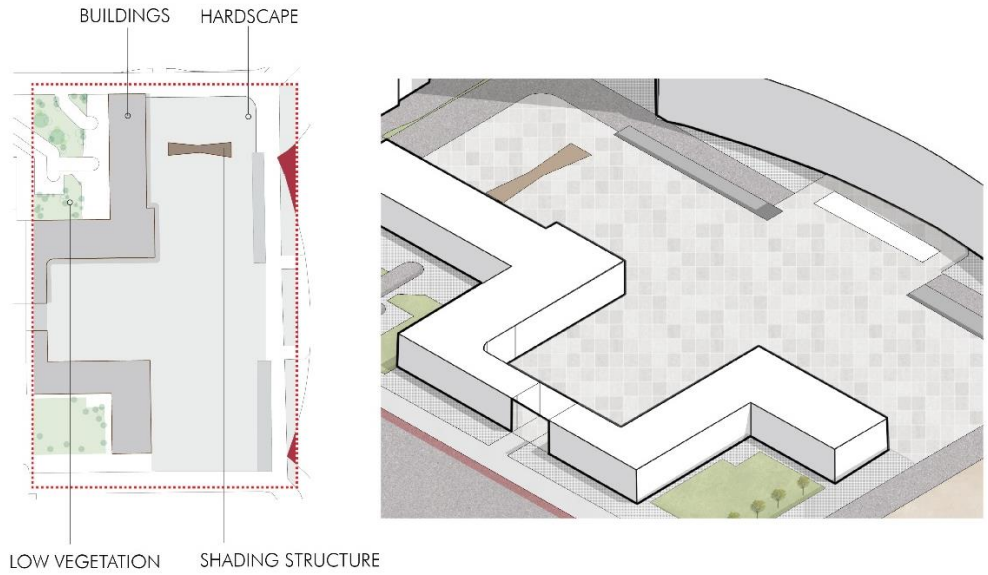

Figure 53. Closer map and 3d illustration of the microzone 1 [MN.01].

Different kinds of materials are used in the square's design, which adds to its visual appeal. High-quality stones such as marble and granite are used to decorate the pavement, producing an eye-catching base. The monument or sculpture that serves as Plaza Italia's focal point may be made of bronze or stone to represent the relationship among Albania and Italy. Steel, glass, or concrete may be used in the construction of nearby buildings, such as seats or architectural details, adding an urban flair to the square's design as a whole. Plaza Italia's carefully chosen materials produce a compelling area that honors the cultural interchange connecting Albania and Italy despite fitting in with the surrounding urban environment.

Figure 54. Material palette of the microzone.

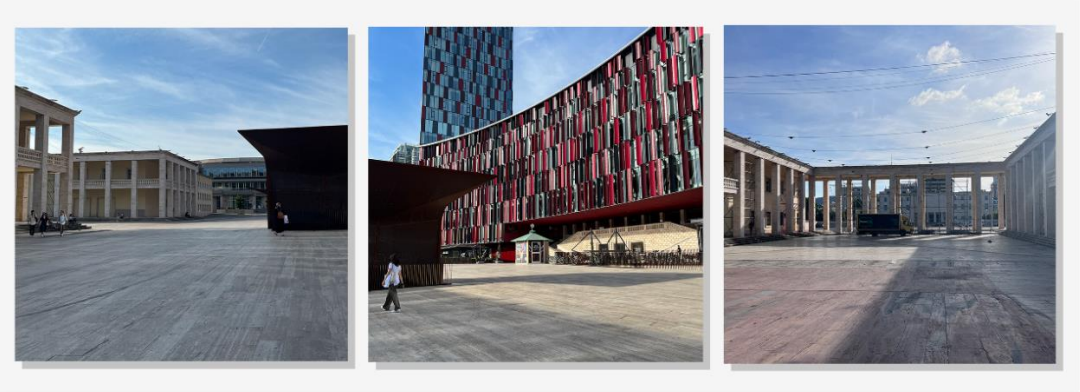

Figure 55. Photos from the site.

4.3.3 Microzone 2 [MN.02]

Located between the university of the arts and a private structure, Microzone 2 is a little inner courtyard. For those who reside or work nearby, it resembles a corridor. In this microzone, there are either quite few or no vegetation prints.

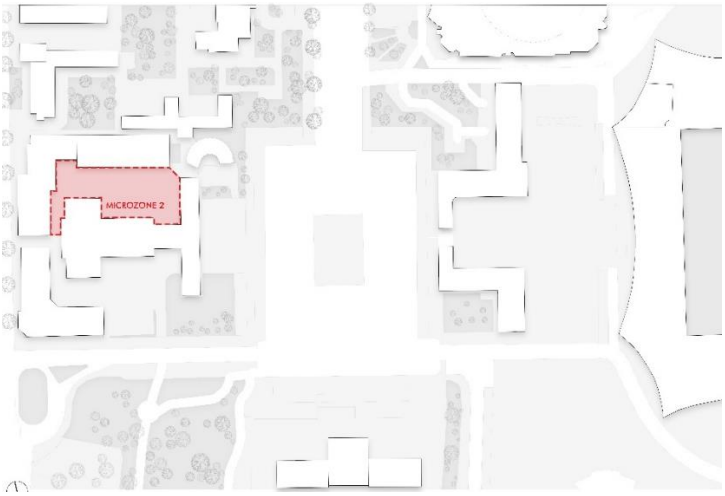

Figure 56.Microzone 2 located in Mother Teresa Square.

Microzone 3 [M3.Z] is located at the northen part of Skanderbeg square, at the end of the boulevard “Zogu I Pare”. The area serves as a corridor for persons passing from the boulevard to the Skanderbeg Square and is located between the National Museum of Tirana and the International Hotel of Tirana.

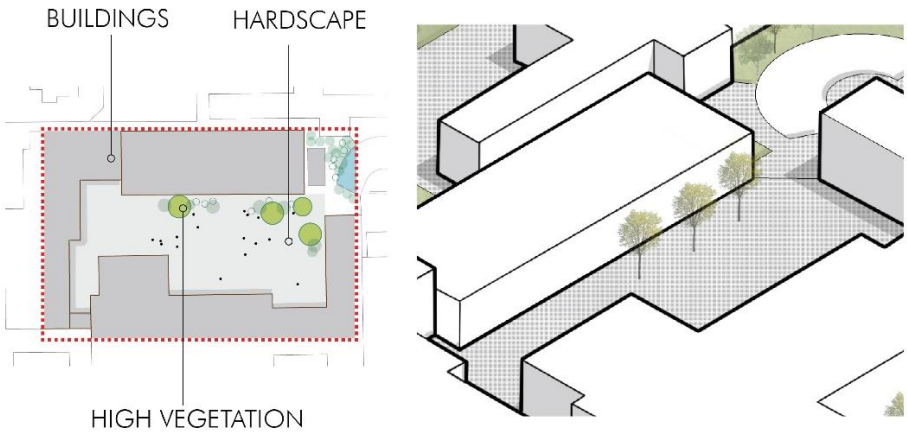

Figure 57. Closer map and 3D illustration of the microzone [MN.02].

The courtyard is an attractive spot where staff members and students may relax and get ideas from their surroundings. The courtyard's visual appeal is enhanced by low vegetation, a few modest planted gardens, and creative sculptures, which together create a perfect fusion of the natural world and creativity. In addition to providing chances for socializing and casual gatherings, these outdoor spaces also encourage community building and cooperation within the university's creative community. The University of Arts' inner courtyard offers a warm and revitalizing area where creative ideas may grow, whether it's a solitary moment of contemplation or an animated dialogue among peers.

Figure 58. Photos from the site.

4.3.4 Microzone 3 [MN.03]

The third microzone lies in front of the university of the arts and is surrounded on the north and east sides by the square and a small Amphitheatre. Due to the presence of educational institutions in the region, it is particularly popular with young people. However, it is also quite popular with those passing through on their way to the Tirana Lake or other nearby neighborhoods.

Figure 59. Microzone 3 located in Mother Teresa Square.

The third microzone lies in front of the university of the arts and is surrounded on the north and east sides by the square and a small amphitheater. Due to the presence of educational institutions in the region, it is particularly popular with young people. However, it is also quite popular with those passing through on their way to the Tirana Lake or other nearby neighborhoods.

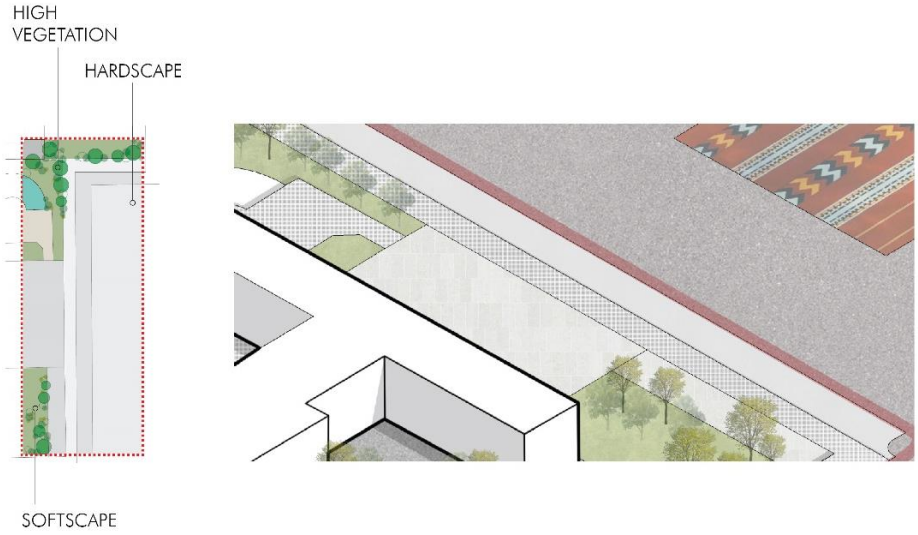

Figure 60. Closer map and 3D illustration of the microzone [MN.03].

Figure 61.Material palette of the microzone.

Figure 62. Photos from the site.

4.2.3.4 Microzone 4 [MN.04]

The third microzone lies in front of the university of the arts and is surrounded on the north and east sides by the square and a small amphitheater. Due to the presence of educational institutions in the region, it is particularly popular with young people.

However, it is also quite popular with those passing through on their way to the Tirana Lake or other nearby neighborhoods.

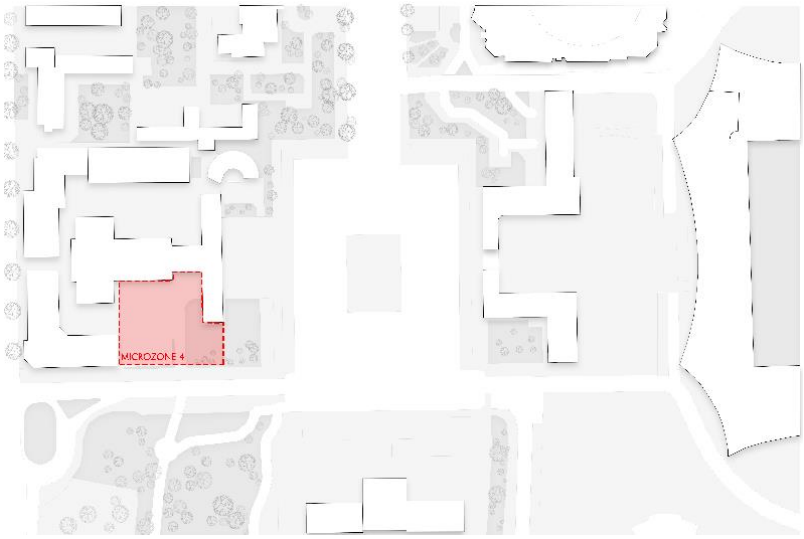

Figure 63. Microzone 4 located in Mother Teresa Square.

The third microzone lies in front of the university of the arts and is surrounded on the north and east sides by the square and a small amphitheater. Due to the presence of educational institutions in the region, it is particularly popular with young people. However, it is also quite popular with those passing through on their way to the Tirana Lake or other nearby neighborhoods.

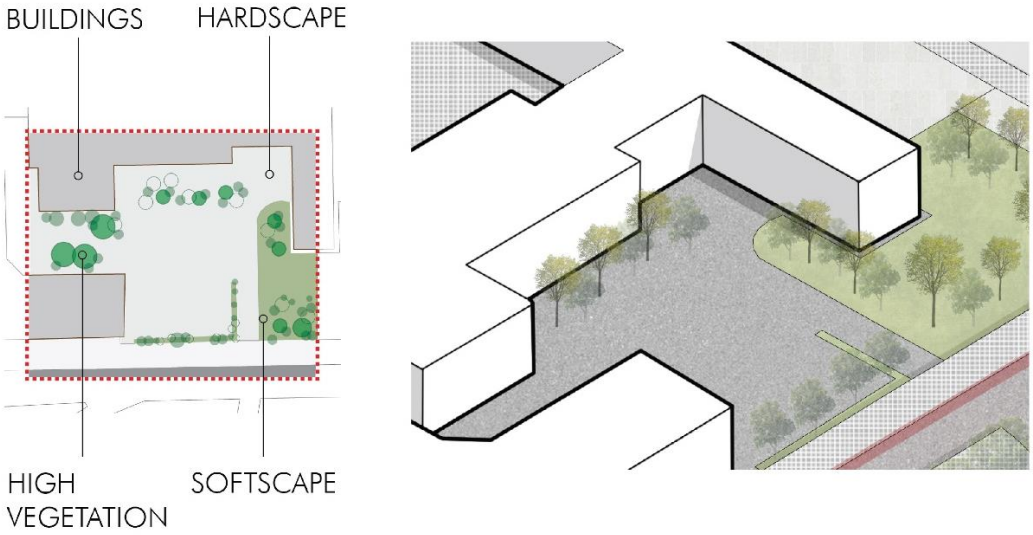

Figure 64. Closer map and 3D illustration of the microzone [MN.04].

Figure 65. Photos from the site.

4.4 Computation

Software introduction.

ENVI-met is the application that will be used for the microclimate analysis in my thesis. The software is used to model and study metropolitan settings and microclimates. By simulating various urban environments, ENVI-met can analyze how various design choices will impact energy consumption, thermal comfort, and air quality.

In our scenario, environment will be employed to mimic the thermal comfort of pedestrians passing through the above-described microzones. More specifically, it will

be able to employ it to produce the UTCI, which considers humidity, wind speed, radiant temperatures, and air temps. The simulation will last for 24 hours on the warmest day of 2022.

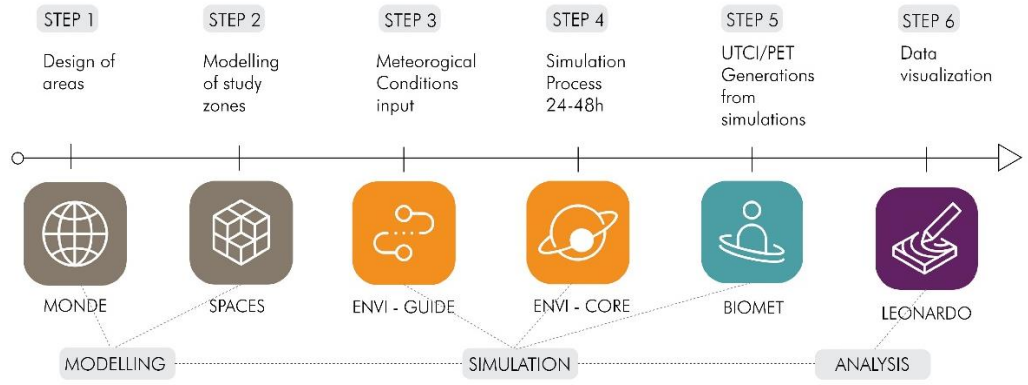

Figure 66. Steps into analyzing in Envimet.-

Using a grid approach, we built the two models of Skanderbeg Square and Mother Teresa Square in environmental settings. The systems are made up of cells, each of which contains a real-world area. Skanderbeg Square area is measured as 250 x 350 meters and has a grid of 50 x 70 x30 meters and a maximum height of 120 meters. Mother Teresa Square area is measured as 260 x 390 meters and has a grid of 78 x 50 x50 meters and a maximum height of 250 meters, which is greater than the previous model because to the tower near the Air Albania stadium. The envimet database, which offers many models of trees, shrubs, and species of grass, developed the model's vegetation.

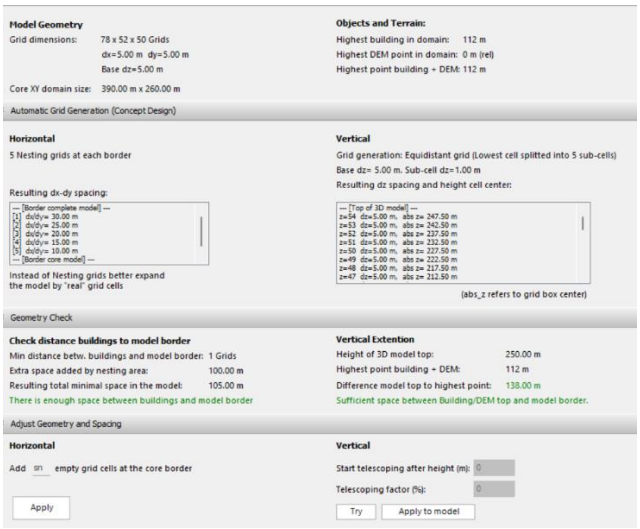

Figure 67.Mother Teresa square Envimet model analyzer.

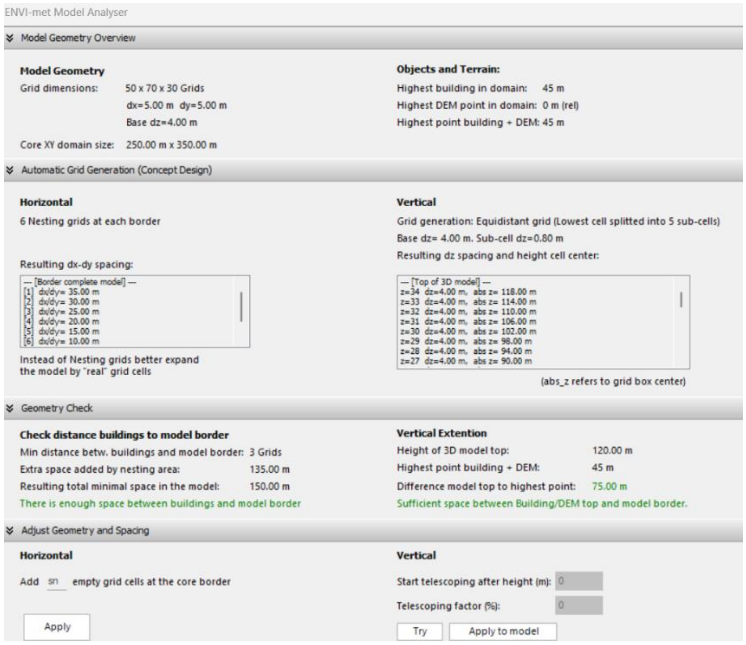

Figure 68. Skanderbeg square Envimet model analyzer.

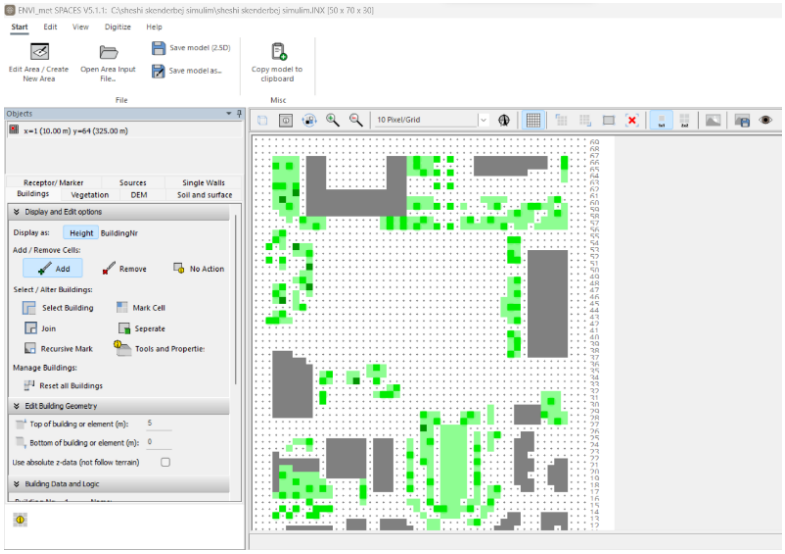

Figure 69. Envimet Spaces workspace showing the modelling of Skanderbeg square.

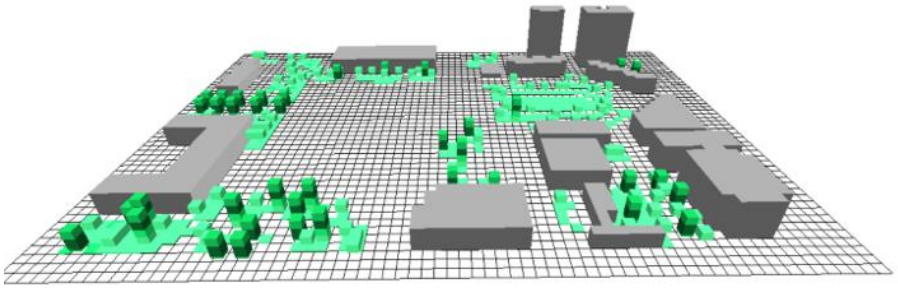

Figure 70. 3D modelling of Skanderbeg square in Envimet software highlighting the grid and vegetation.

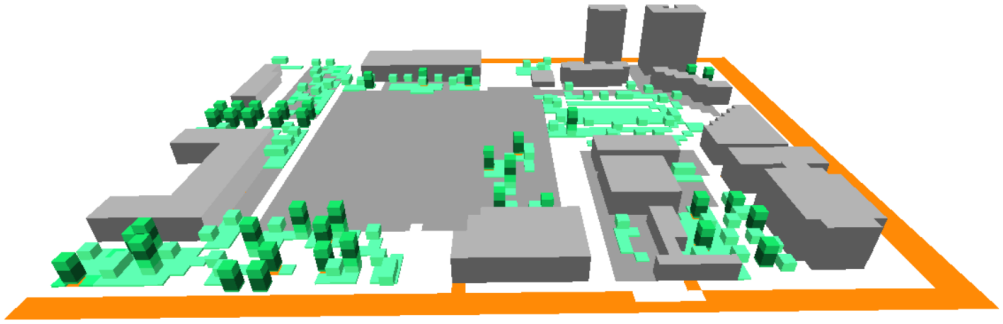

Figure 71. 3D modelling of Skanderbeg square in Envimet software highlighting the materials with different colors.

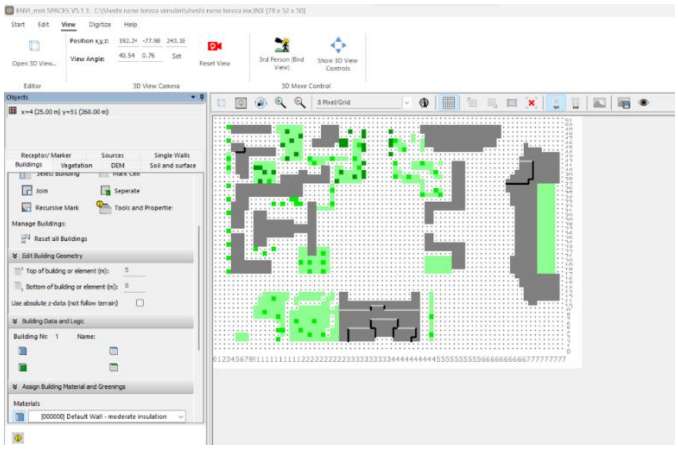

Figure 72. Envimet Spaces workspace showing the modelling of Mother Teresa square.

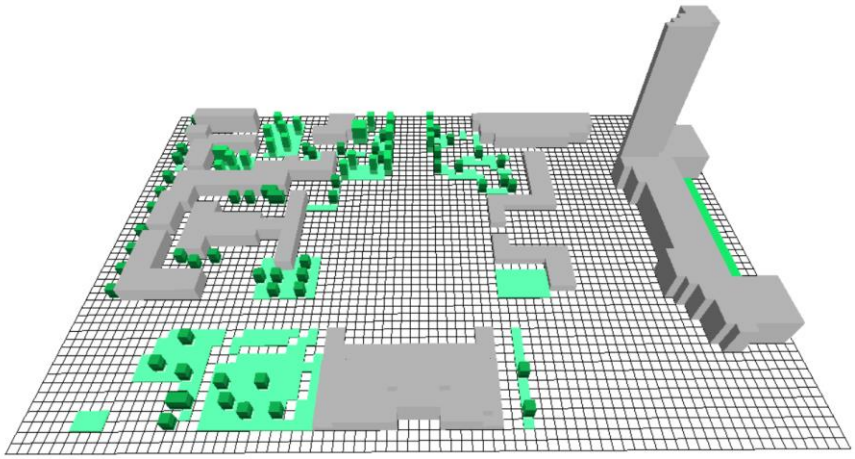

Figure 73. 3D modelling of Mother Teresa square in Envimet software highlighting the grid and vegetation.

The materialization of the site was another crucial envimet phase because it will later greatly affect the simulation's outcomes. The material gallery was also found on Envimet; it can be altered based on the specifications that are required. On the two square models, paving materials for open areas, plaster for the walls, grass, soil, and other hardscape materials are used along with grey and darker pavement for vehicle paths. Envimet enables the creation of models in two dimensions as well as three dimensions, which may be seen in layers that include vegetation and the grid, the materials, or just the structures themselves.

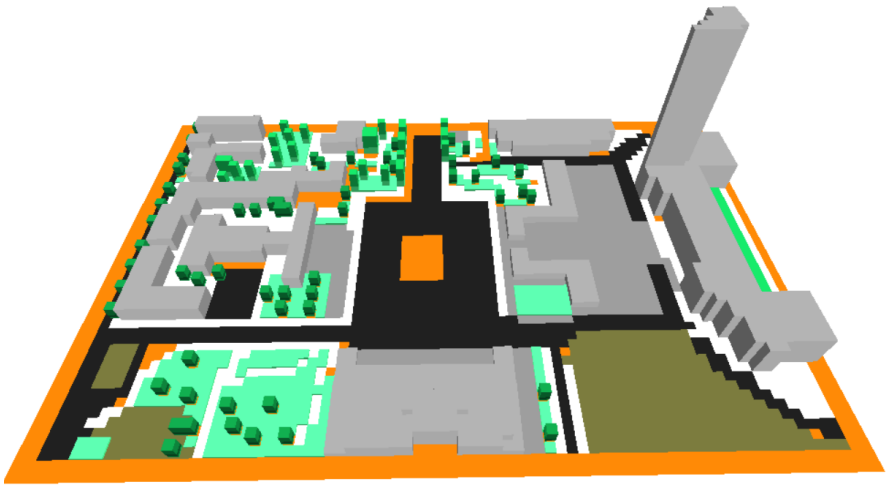

Figure 74. 3D modelling of Skanderbeg square in Envimet software highlighting the materials with different colors.

The stimulation step follows the modeling of the two research zones. An epw file with the country's meteorological conditions, in this case Tirana, is necessary to stimulate the models. Our simulation took place over the course of 24 hours on August 1, 2022, from 05 am to 4 am the following morning. Since the simulation ran for 45 to 60 minutes for every hour, it lasted around 24 hours. The simulation considered variables such as air temperature, mean radiant temperature (the temperature that buildings' facades transferred), wind speed, humidity, and UTCI.

4.4.1 Python integration

We utilized python code to determine the average temperature in a certain location after obtaining the utci, air temperature, mean radiant temperature, wind speed, and humidity the simulation's output was presented as values for each grid cell for the aforementioned elements in a CVS format. Our goal was to determine the typical temperature, wind speed, or humidity for each of our closed polygon microzones. The next stage was using the envimet program to determine the coordinates of the vertexes of these polygons. These were discovered using the environment grid, which has the x and y values that are really distances between the provided places.

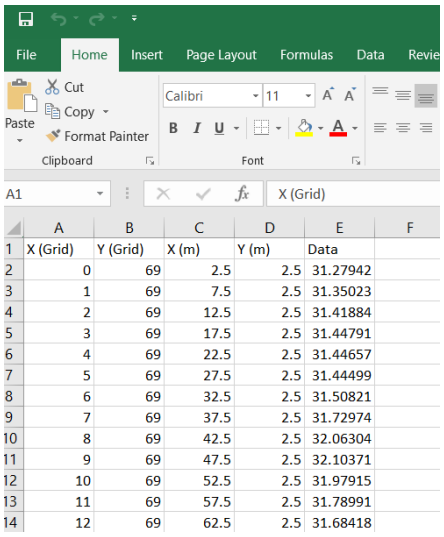

	A	B	C	D	E	F
1	X (Grid)	Y (Grid)	X (m)	Y (m)	Data	
2	0	69	2.5	2.5	31.27942	
3	1	69	7.5	2.5	31.35023	
4	2	69	12.5	2.5	31.41884	
5	3	69	17.5	2.5	31.44791	
6	4	69	22.5	2.5	31.44657	
7	5	69	27.5	2.5	31.44499	
8	6	69	32.5	2.5	31.50821	
9	7	69	37.5	2.5	31.72974	
10	8	69	42.5	2.5	32.06304	
11	9	69	47.5	2.5	32.10371	
12	10	69	52.5	2.5	31.97915	
13	11	69	57.5	2.5	31.78991	
14	12	69	62.5	2.5	31.68418	

Figure 75. CVS file output from Leonardo ENVI-met

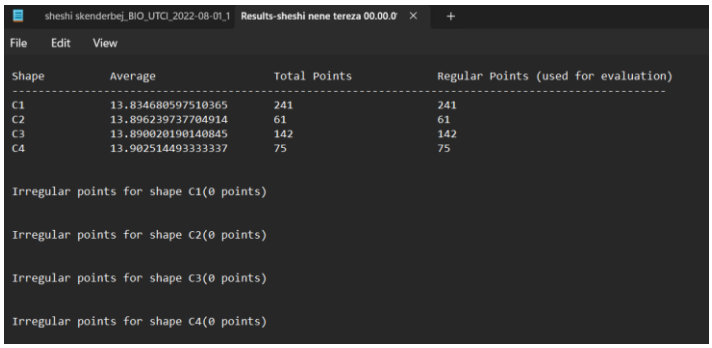

Figure 76.Python complier output showing the average temperatures of the microzones.

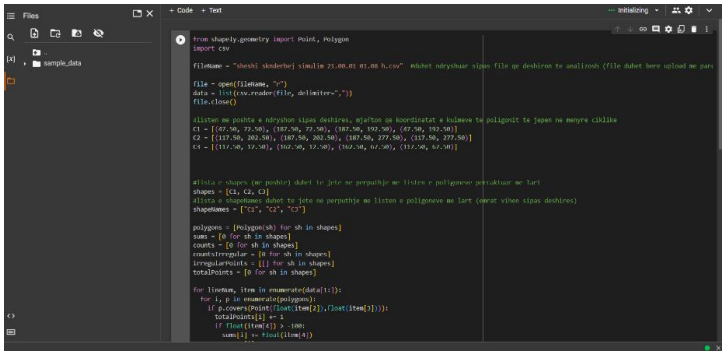

Figure 77.Phython coding used to measure the average input from the Envimet outputs in excel format.

The highlighted microzones on the coordinate system and the vertices required for the python code are displayed below. In order to get the average value for the whole region, the coding was used to add the values of the temperatures or wind speeds of each cell inside the polygon and divide them by the number of cells. Every hour, this process was repeated, and the results were then utilized to make graphs and tables.

Figure 78. Skanderbeg square microzone coordinates used for python coding.

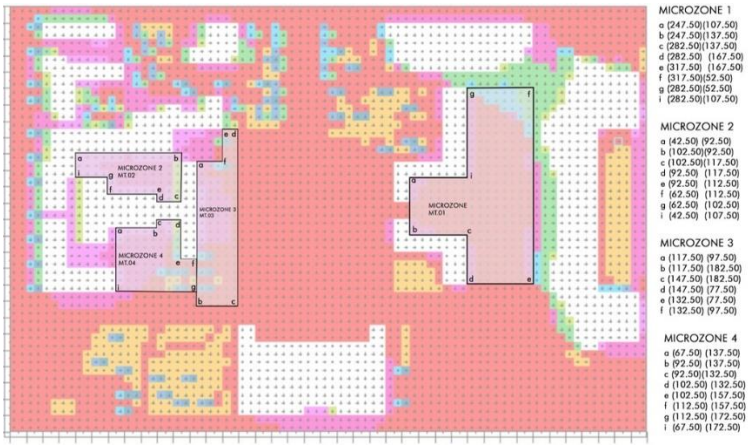

Figure 79. Mother Teresa square microzone coordinates used for python coding.

CHAPTER 5

RESULTS AND DISCUSSION

5.1 Results and discussion of [Mother Teresa square]

The simulation findings for the four microzones that we will study in the Mother Teresa Square are displayed below in graphs of UTCI, air temperature, mean radiant temperature, wind speed, and humidity.

5.1.1 Microzone 1 [MN.01]

The graph of UTCI (C) for microzone 1 [MN.01] is shown below. The greatest temperature, 38.4 degrees Celsius, was recorded at 14:00. Early in the morning, at 04:00 by 18.25, the temperature is the lowest. The graph indicates that nighttime is when temperatures are lowest and that they gradually rise during the day.

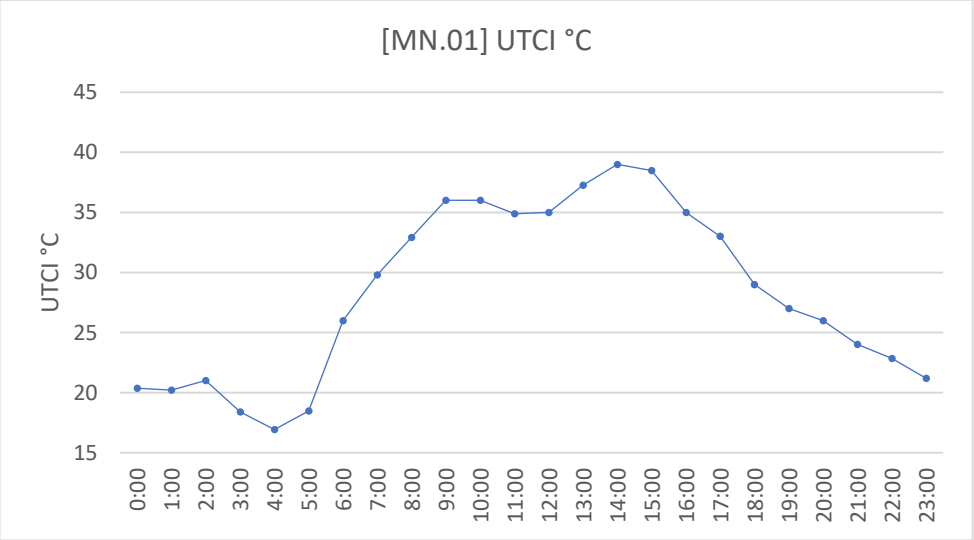

Figure 80. Microzone 1 [MN.01] UTCI values.

The air temperature data for the Microzone 1 [MN.01] are displayed on the graph below. The temperature reaches its peak at 31.8 degrees Celsius at 14:00, and it reaches its lowest point at 19.08 degrees Celsius at 04:00.

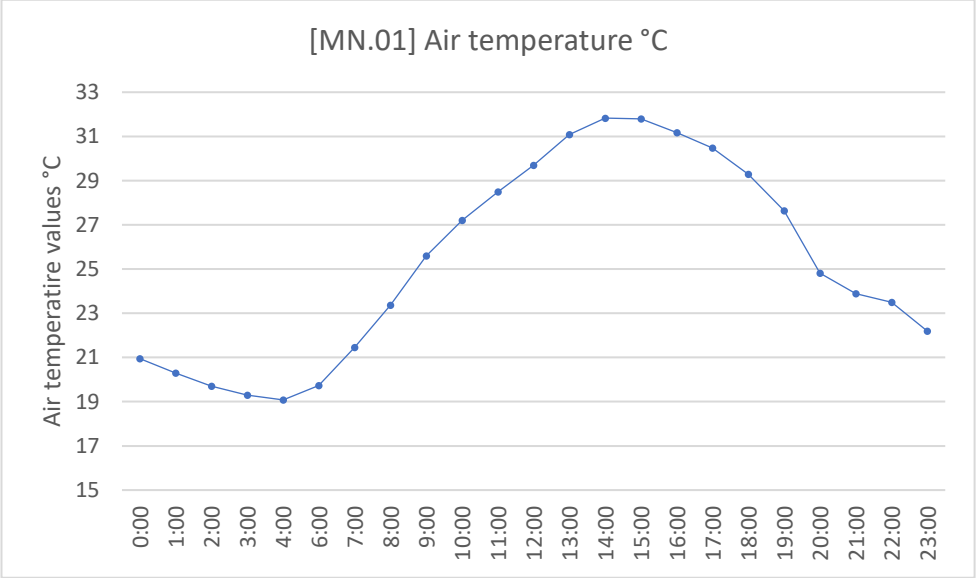

Figure 81.Microzone 1 [MN.01] air temperature values.

The mean radiant temperature data for Microzone 1 [MN.01] are displayed on the graph below. The temperature reaches its peak at 14:00 and reaches its lowest point at 05:00, both measured in degrees Celsius.

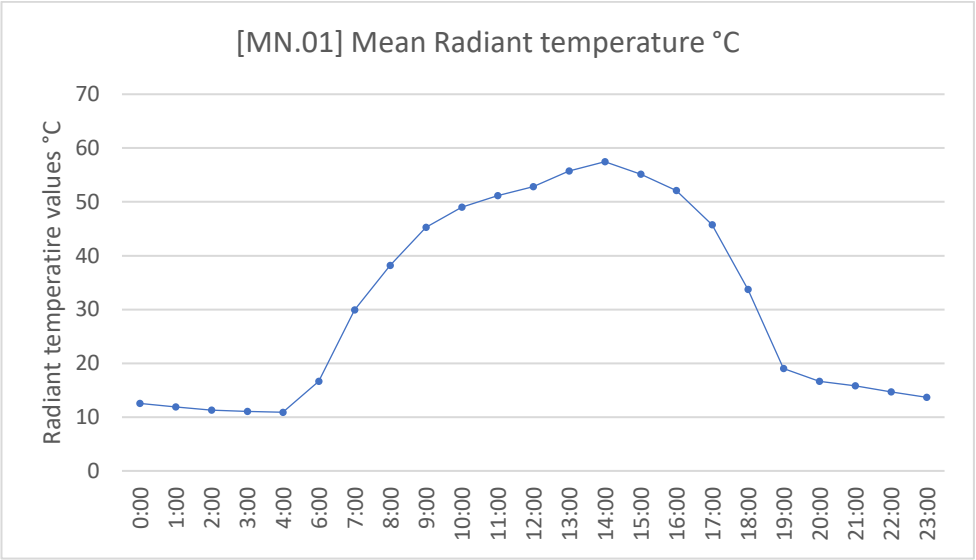

Figure 82. Microzone 1 [MN.01] mean radiant temperature values.

The values for the wind speed for Microzone 1 [MN.01] are displayed on the graph below. The lowest value is at 9:00 a.m. by 0.15 m/s, while the highest value is at 18:00 a.m. at 1.75 m/s.

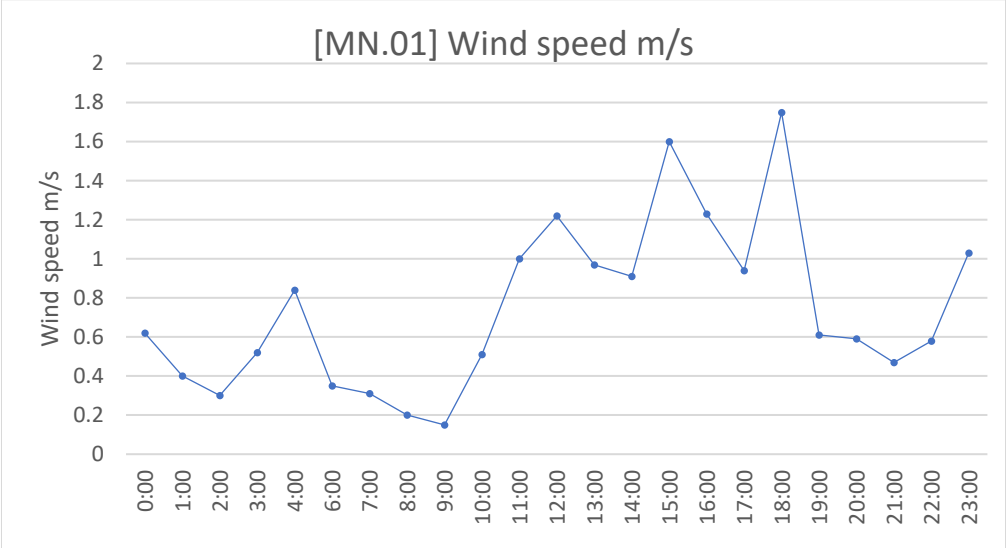

Figure 83. Microzone 1 [MN.01] wind speed values.

The Microzone 1 [MN.01] humidity levels are displayed on the graph below. The greatest value is 15.3 g/kg at 20:00, while the lowest value is 13.2 g/kg at 06:00.

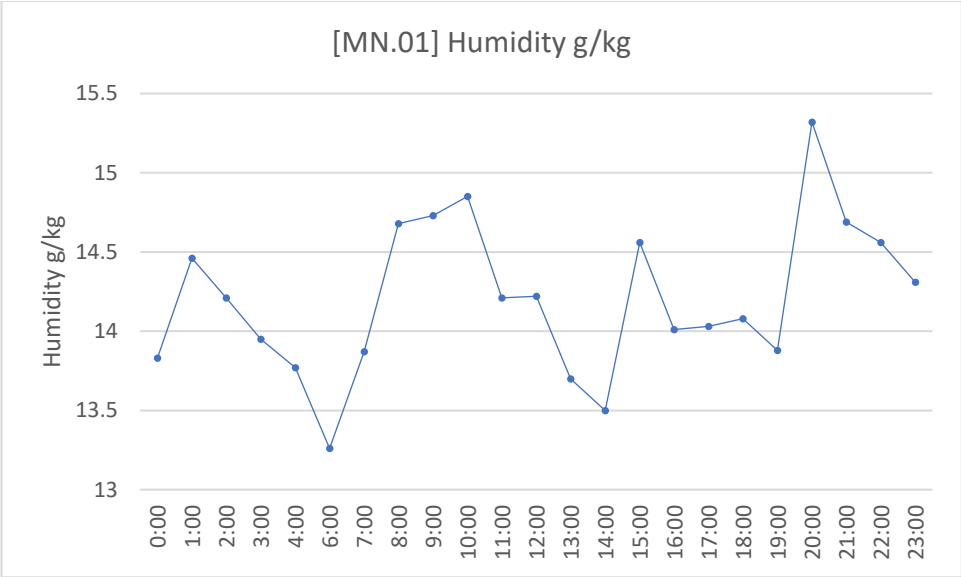

Figure 84. Microzone 1 [MN.01] humidity values.

5.1.2 Microzone 2 [MN.02]

The microzone 2 [MN.02] UTCI (C) graph is seen below. We can observe that the greatest temperature, 38.6 degrees Celsius, occurred at 14:00. Early in the morning, at 04:00, 18.2 has the lowest temperature. The graph indicates that the lowest temperatures occur at night while gradually rising during the day.

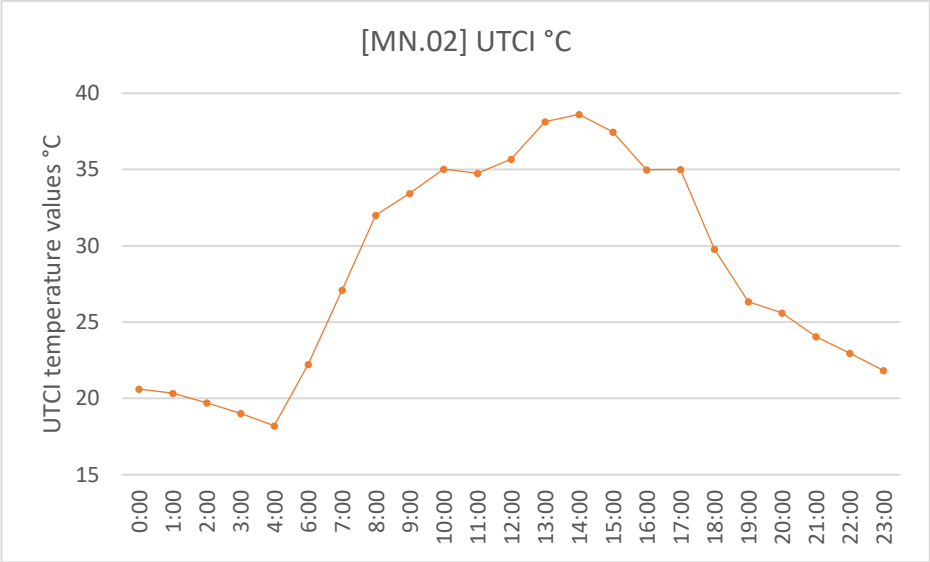

Figure 85. Microzone 2 [MN.02] UTCI values.

The readings for the air temperature for microzone 2 [MN.02] are displayed on the graph below. The temperature reaches a maximum of 32.3 degrees Celsius at 14:00, and a minimum of 18.9 degrees Celsius at 04:00.

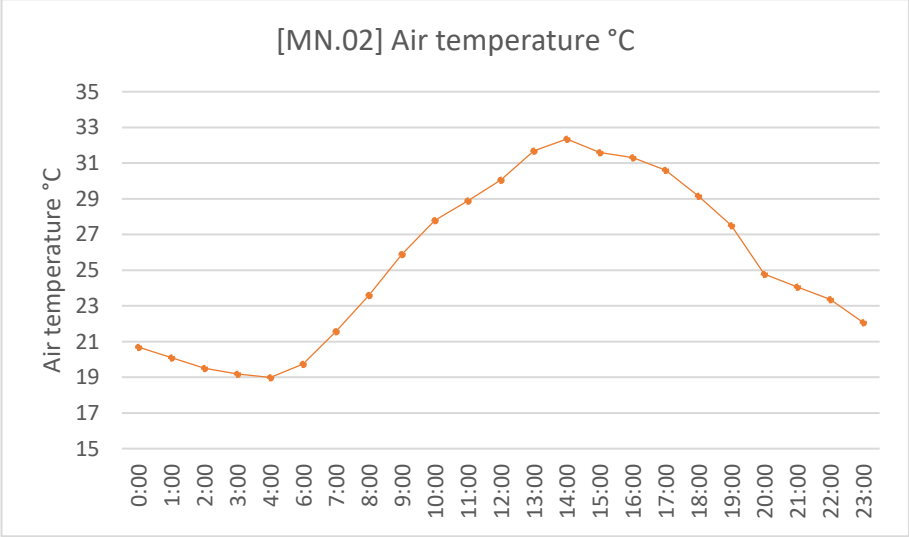

Figure 86. Microzone 2 [MN.02] air temperature values.

The mean radiant temperature data for microzone 2 [MN.02] are displayed on the graph below. The temperature reaches its peak at 14:00 with a reading of 55.4 degrees Celsius, and it reaches its lowest point at 05:00 with a reading of 11.4 degrees Celsius.

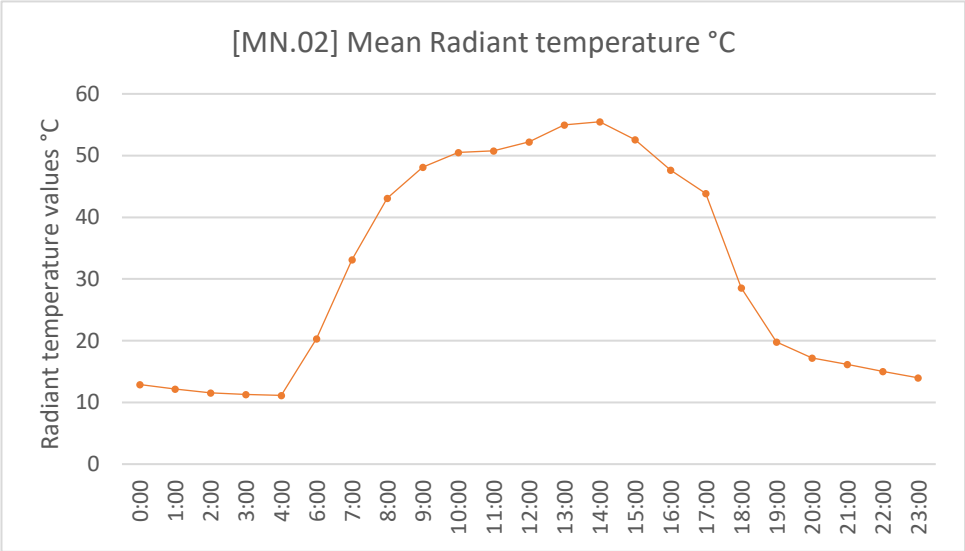

Figure 87. Microzone 2 [MN.02] mean radiant temperature values.

The values for the wind speed for Microzone 2 [MN.02] are displayed on the graph below. The lowest value is at 9:00 a.m. by 0.12 m/s, while the greatest value is at 18:00 a.m. at 1.47 m/s.

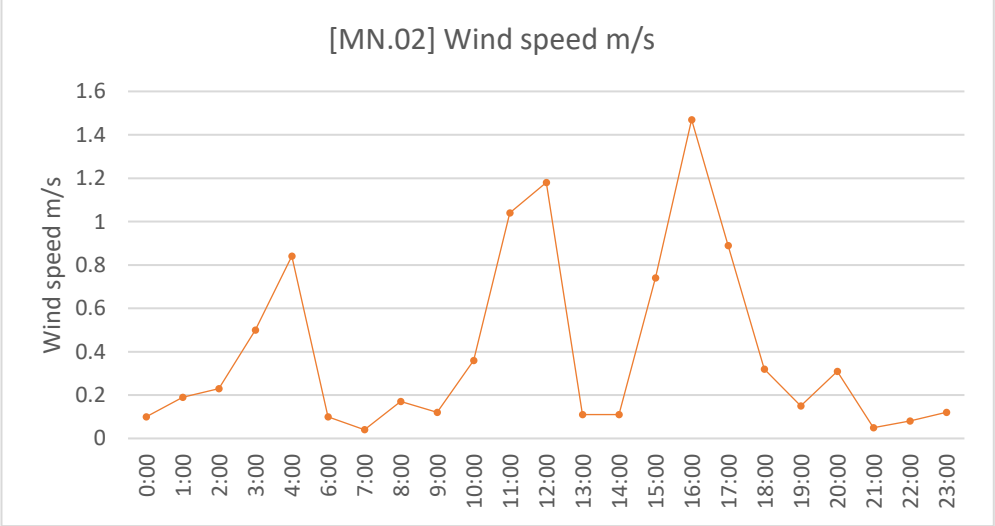

Figure 88. Microzone 2 [MN.02] wind speed values.

The Microzone 2 [MN.02] humidity levels can be seen on the graph below. The greatest value is 15.8 g/kg at 20:00, while the lowest value is 13.2 g/kg at 06:00.

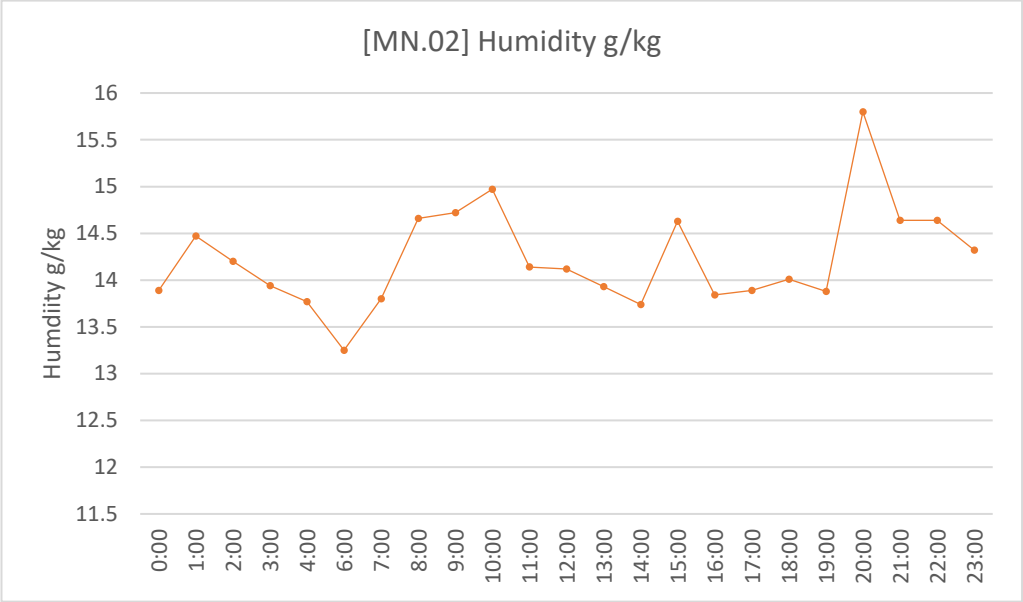

Figure 89. Microzone 2 [MN.02] humidity values.

5.1.3 Microzone 3 [MN.03]

The UTCI (C) graph for Microzone 3 [MN.03] is seen below. The greatest temperature, 37.6 degrees Celsius, was recorded at 14:00. The lowest temperature is recorded at 04:00 by 18.2 in the early morning. The graph demonstrates that temperatures are lowest at night and gradually rise during the day.

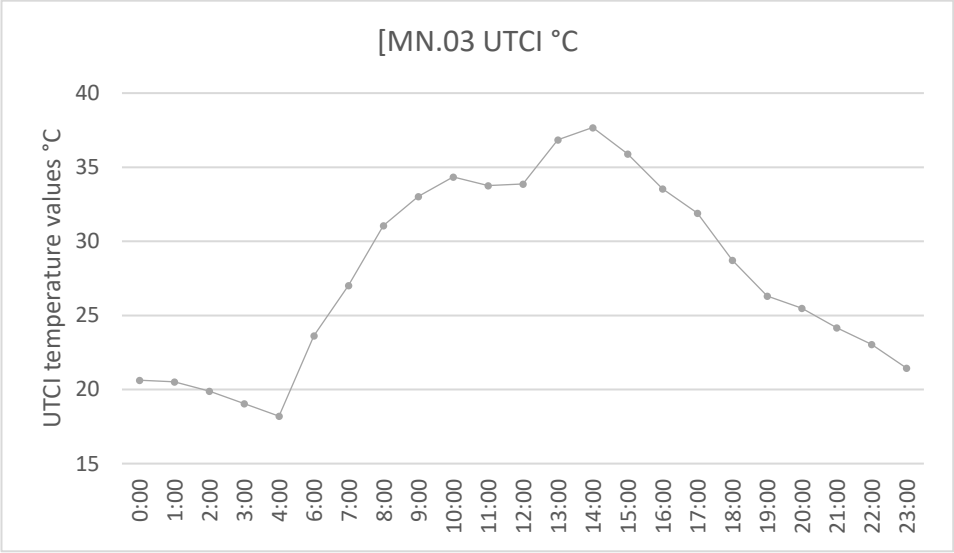

Figure 90. Microzone 3 [MN.03] UTCI values.

The readings for the air temperature for microzone 3 [MN.03] are displayed on the graph below. The maximum temperature is 32.7 degrees Celsius at 14:00, while the lowest temperature is 19.3 degrees Celsius at 05:00.

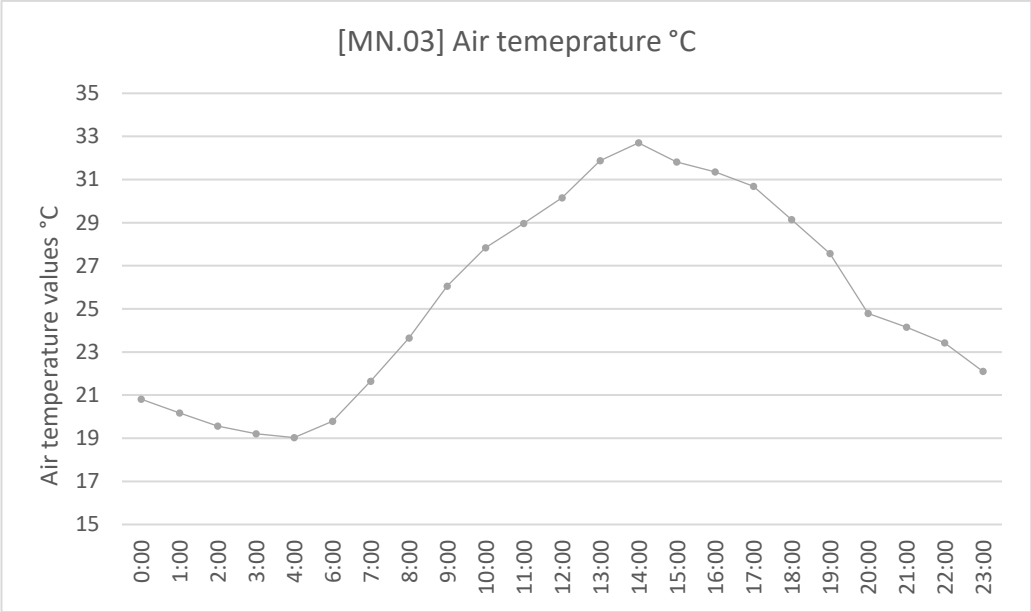

Figure 91. Microzone 3 [MN.03] air temperature values.

The mean radiant temperature data for microzone 3 [MN.03] are displayed on the graph below. The temperature reaches its peak at 14:00 with a value of 53.5 degrees Celsius, and it reaches its lowest point at 05:00 with a value of 11.5 degrees Celsius.

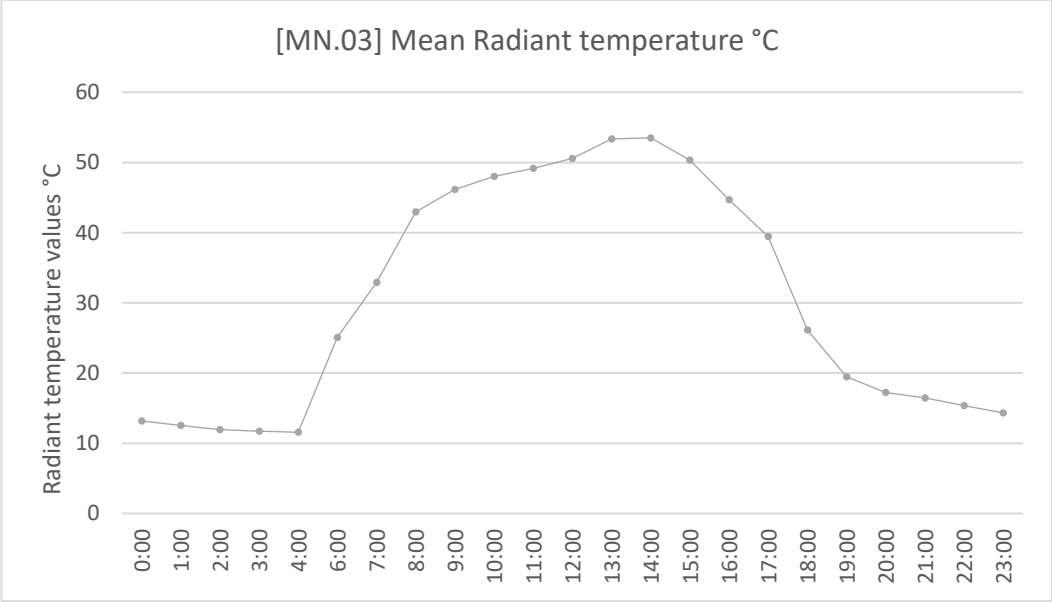

Figure 92. Microzone 3 [MN.03] mean radiant temperature values.

The values for the wind speed for Microzone 3 [MN.03] are displayed on the graph below. The lowest value is at 01:00 hours by 0.15 m/s, while the maximum value is at 18:00 hours with 2.14 m/s.

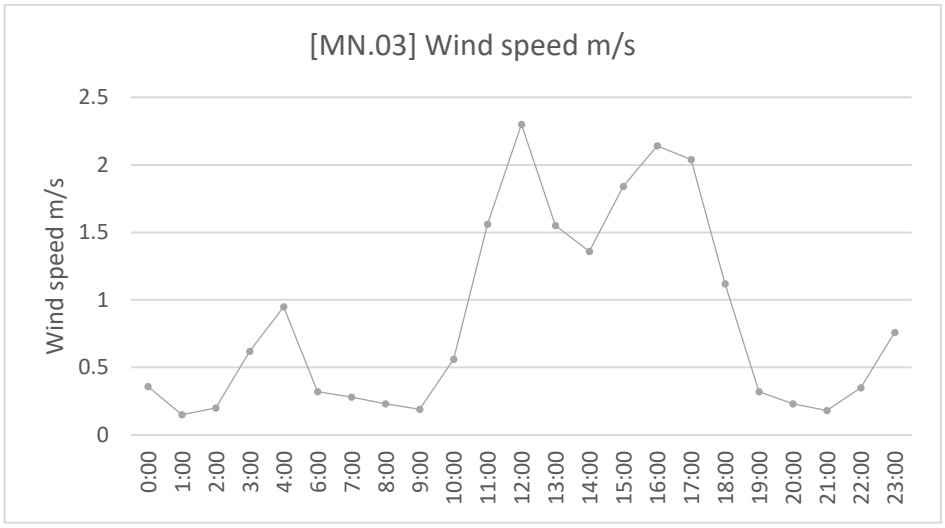

Figure 93. Microzone 3 [MN.03] wind speed values.

The Microzone 3 [MN.03] humidity levels are displayed on the graph below. The lowest value is at 06:00 hours, 13.2 g/kg, while the maximum value is at 20:00 hours, 15.5 g/kg.

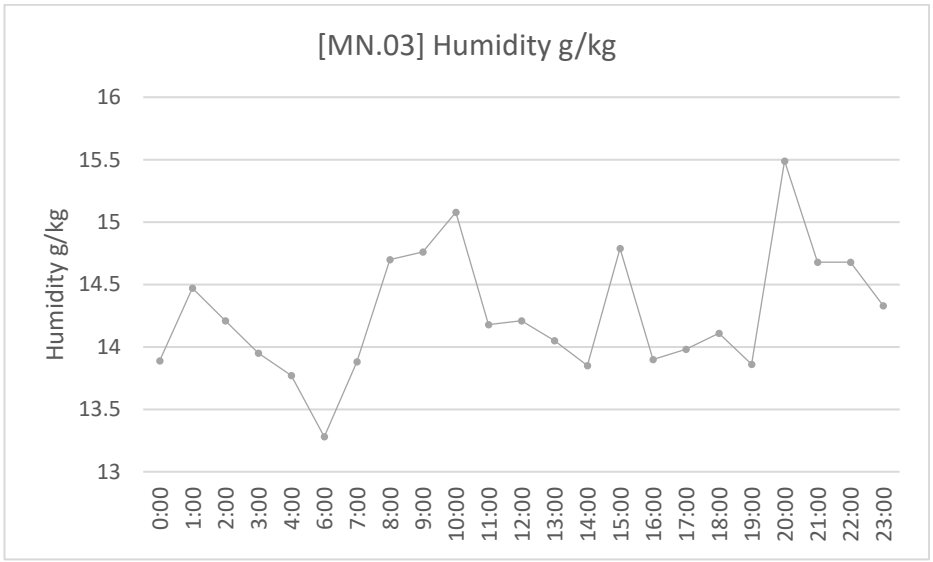

Figure 94. Microzone 3 [MN.03] humidity values.

5.1.4 Microzone 4 [MN.04]

The graph of Microzone 4 [MM.04] UTCI (C) is seen below. The greatest temperature, 38.5 degrees Celsius, was registered at 14:00. Early in the morning, at 04:00 by 18.5, the temperature is the lowest. The graph illustrates that temperatures are lowest at night and gradually rise during the day.

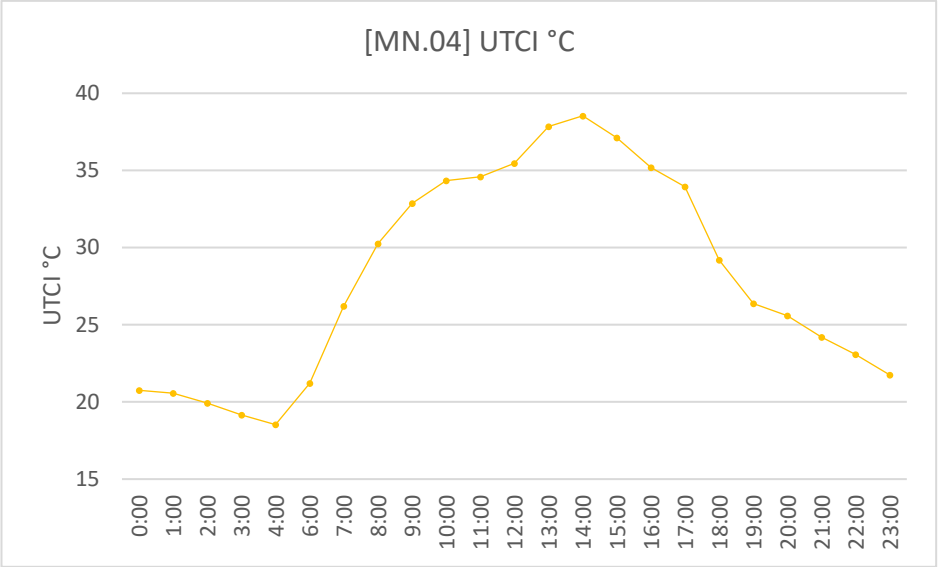

Figure 95. Microzone 4 [MN.04] UTCI values.

The air temperature data for the microzone 4 [MN.04] is presented on the graph below. The temperature reaches its highest value at 32.6 degrees Celsius at 14:00 and its lowest point at 19.01 degrees Celsius at 04:00.

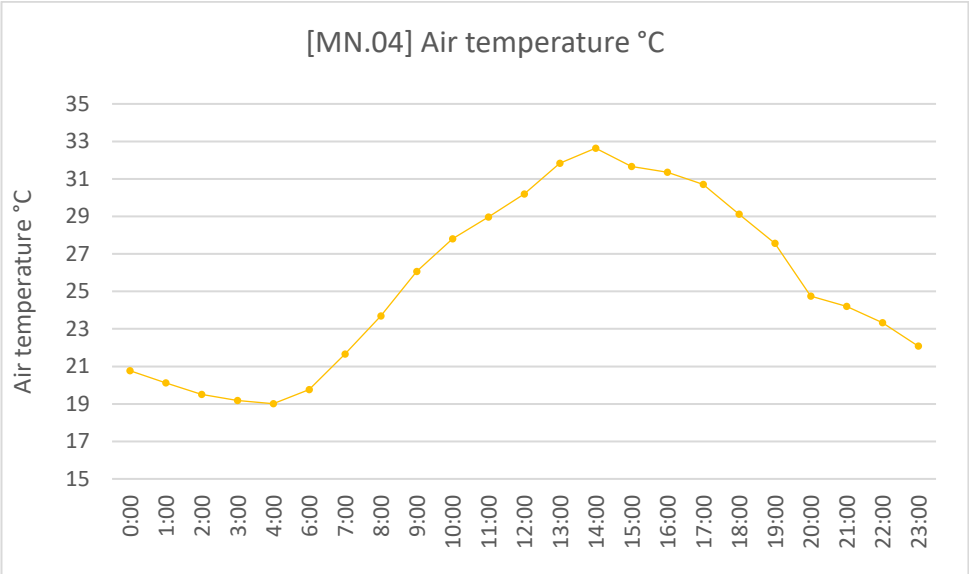

Figure 96. Microzone 4 [MN.04] air temperature values.

The mean radiant temperature data for the microzone 4 [MN.04] is presented on the graph below. The temperature reaches its peak at 14:00 with a measurement of 54.3 degrees Celsius, and it reaches its lowest point at 04:00 with a reading of 11.6 degrees Celsius.

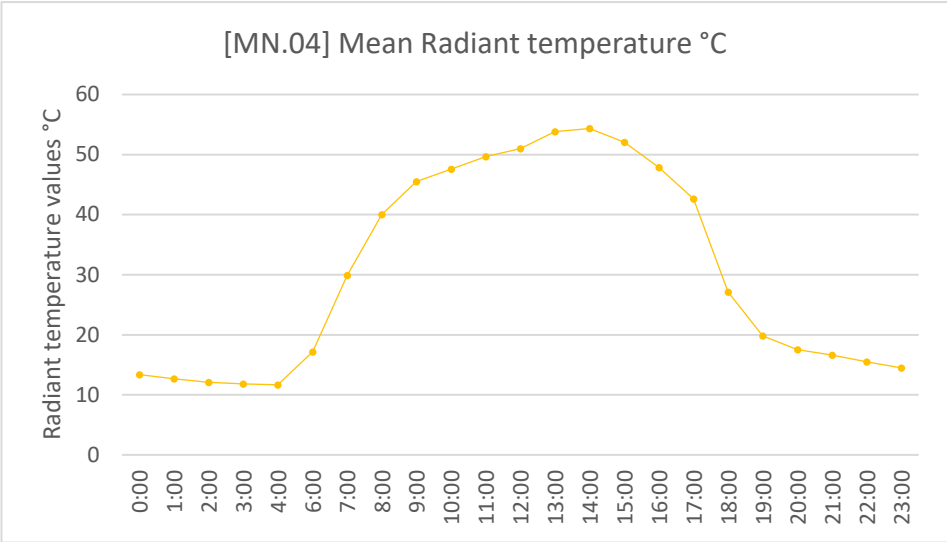

Figure 97. Microzone 4 [MN.04] mean radiant temperature values.

The wind speed values for the Microzone 4 [MN.04] are displayed on the graph below. The maximum value occurs at 18:00 hours with 1.42 m/s, while the minimum value occurs at 01:00 hours with 0.1 m/s.

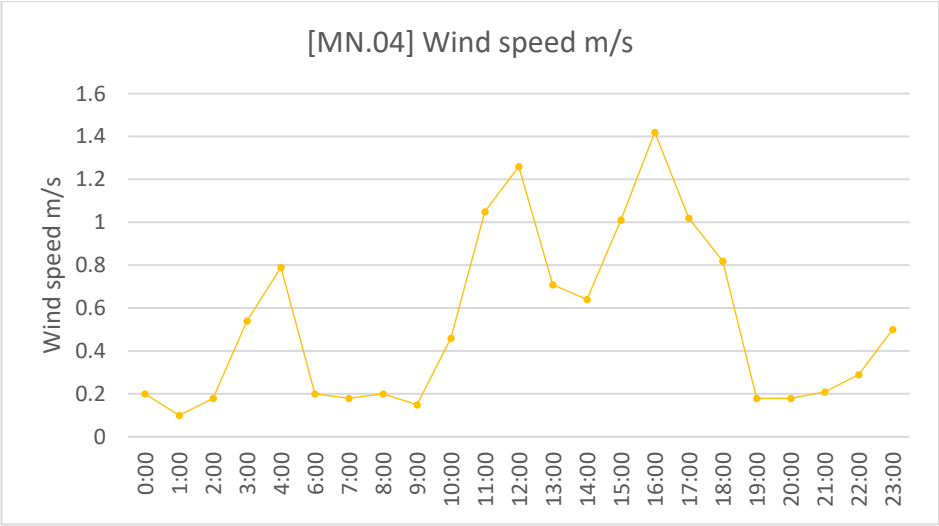

Figure 98. Microzone 4 [MN.04] wind speed values.

The Microzone 4 [MN.04] humidity levels are displayed on the graph below. The value is 15.5 g/kg at 20:00 hours, and 13.3 g/kg at 06:00 hours, when it is lowest.

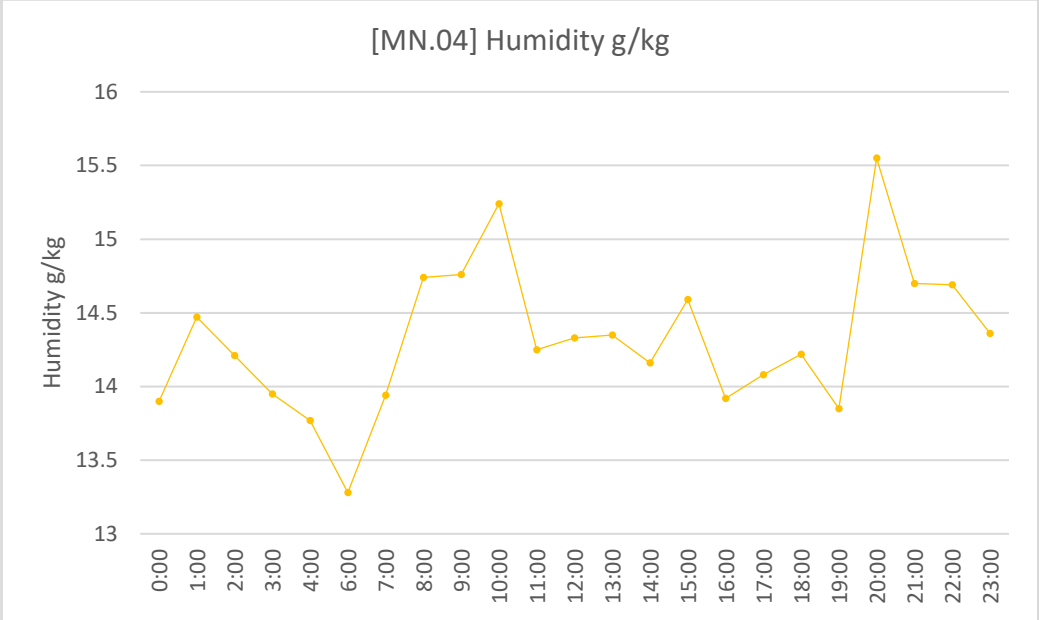

Figure 99. Microzone 4 [MN.04] humidity values.

5.2 Results and discussion [Skanderbeg square]

The graphs of UTCI, air temperature, mean radiant temperature, wind speed, and humidity below show the simulation results for the three microzones that we will investigate at Skanderbeg Square.

5.2.1Microzone 1 [MS.01]

The graph of UTCI (C) for microzone 1 [MS.01] is presented below. The greatest temperature, 39 degrees Celsius, was recorded at 14:00. The lowest temperature ever recorded was 16.9 degrees Celsius at 4:00 in the morning. The graph demonstrates that temperatures are lowest at night and gradually rise during the day.

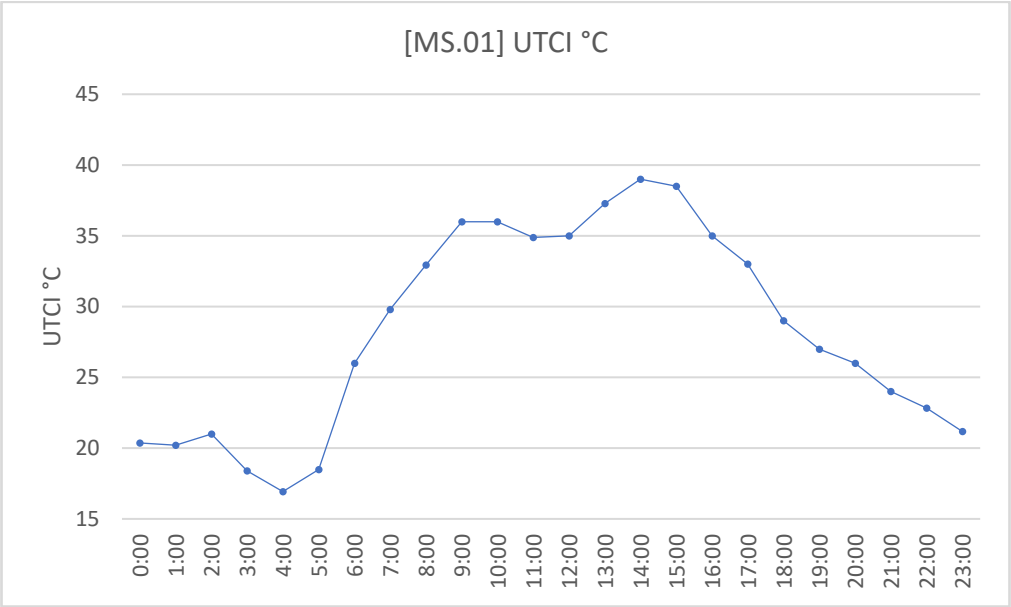

Figure 100. Microzone 1 [MS.01] UTCI values.

The air temperature data for the Microzone 1 [MS.01] are displayed on the graph below. The temperature reaches its peak at 31.9 degrees Celsius at 14:00, and it reaches its lowest point at 19.14 degrees Celsius at 04:00.

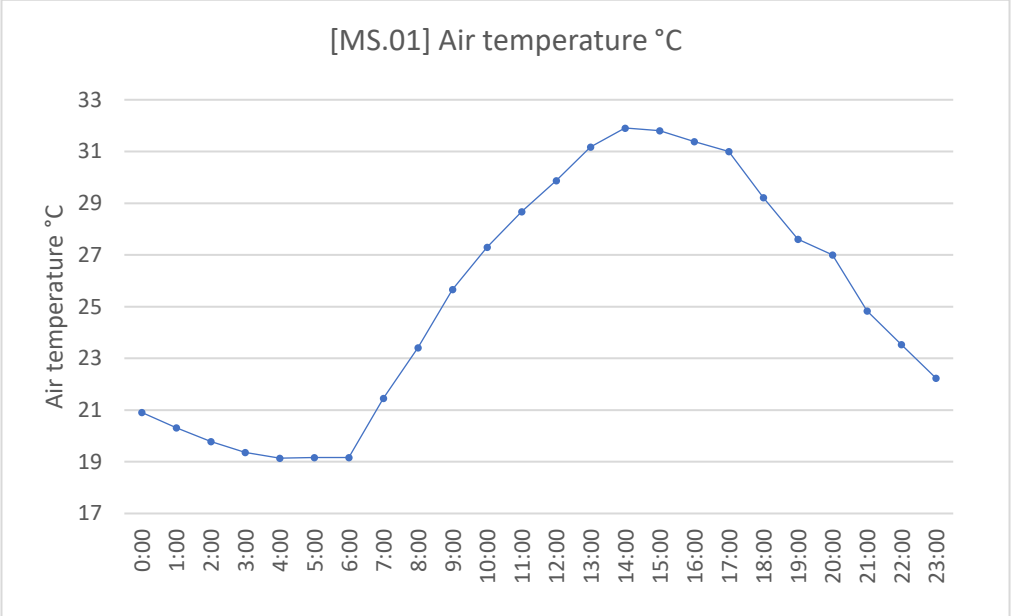

Figure 101. Microzone 1 [MS.01] air temperature values.

The mean radiant temperature data for Microzone 1 [MS.01] are displayed on the graph below. The temperature reaches a maximum of 58.2 degrees Celsius at 14:00 and a minimum of 11.2 degrees Celsius at 04:00.

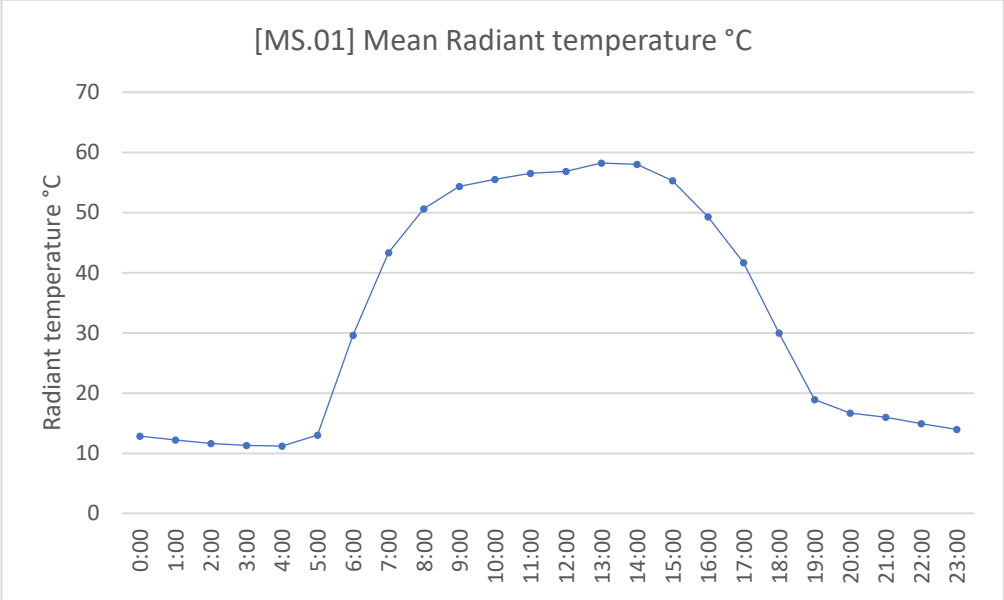

Figure 102. Microzone 1 [MS.01] mean radiant temperature values.

The values for the Microzone 1 [MS.01] wind speed is shown on the graph below. The maximum value, 2.61 m/s, occurs at 18:00 hours, while the lowest value, 0.22 m/s, occurs at 0900 hours.

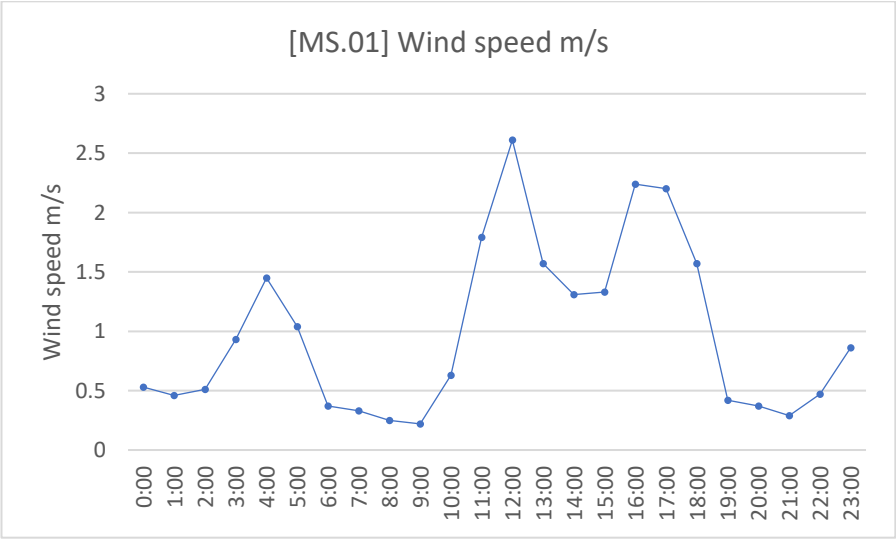

Figure 103. Microzone 1 [MS.01] wind speed values.

The Microzone 1 [MS.01] humidity levels are displayed on the graph below. The lowest value is at 06:00 hours, 13.2 m/s, while the greatest value is at 20:00 hours, 15.6 m/s.

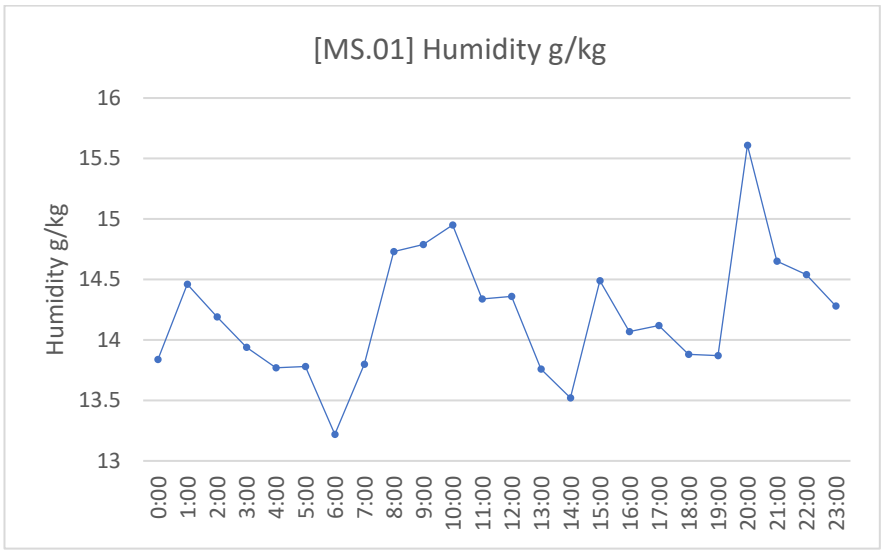

Figure 104. Microzone 1 [MS.01] humidity values.

5.2.2 Microzone 2 [MS.02]

The graph of UTCI (C) for microzone 2 [MS.02] is shown below. The greatest temperature, 38.1 degrees Celsius, was recorded at 14:00. The lowest temperature ever recorded was 17.5 degrees Celsius at 4:00 in the morning. The graph demonstrates that temperatures are lowest at night and gradually rise during the day.

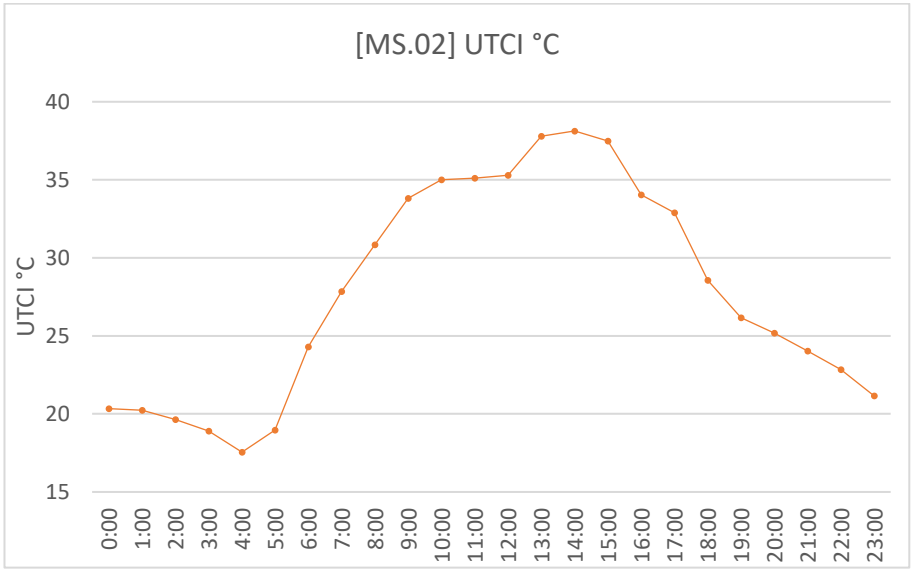

Figure 105.Microzone 2 [MS.02] UTCI values.

The air temperature data for the Microzone 2 [MS.02] can be seen on the graph below. The temperature reaches its peak at 31.5 degrees Celsius at 14:00 and its lowest point at 19.01 degrees Celsius at 04:00.

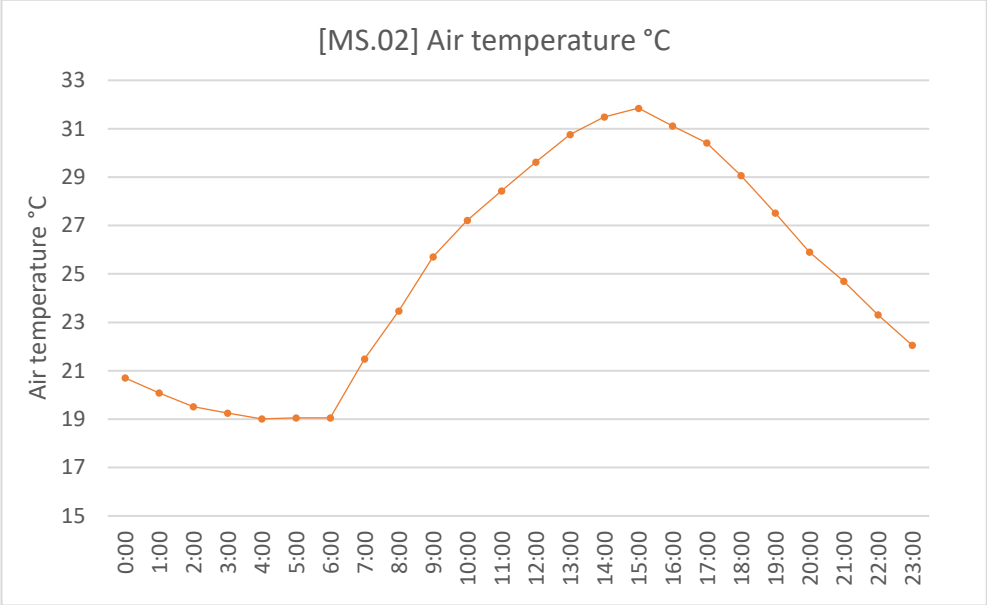

Figure 106.Microzone 2 [MS.02] air temperature values.

The mean radiant temperature data for Microzone 2 [MS.02] are displayed on the graph below. The temperature reaches its peak at 15:00 and reaches its lowest point at 05:00, both measured in degrees Celsius.

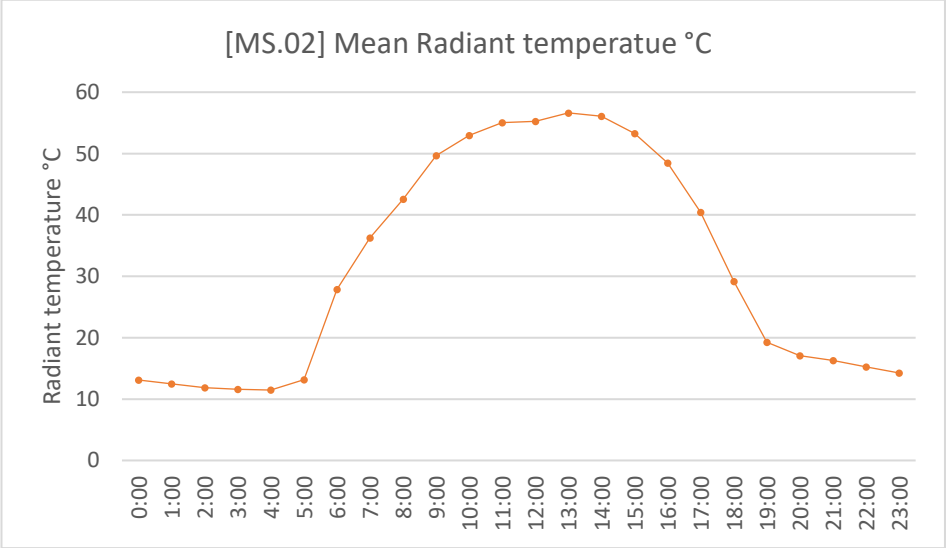

Figure 107. Microzone 2 [MS.02] mean radiant temperature values.

The values for the Microzone 2 [MS.02] wind speed is displayed on the graph below. The lowest value is at 09:00 hours with 0.16 m/s, while the maximum value is at 18:00 hours with 1.71 m/s.

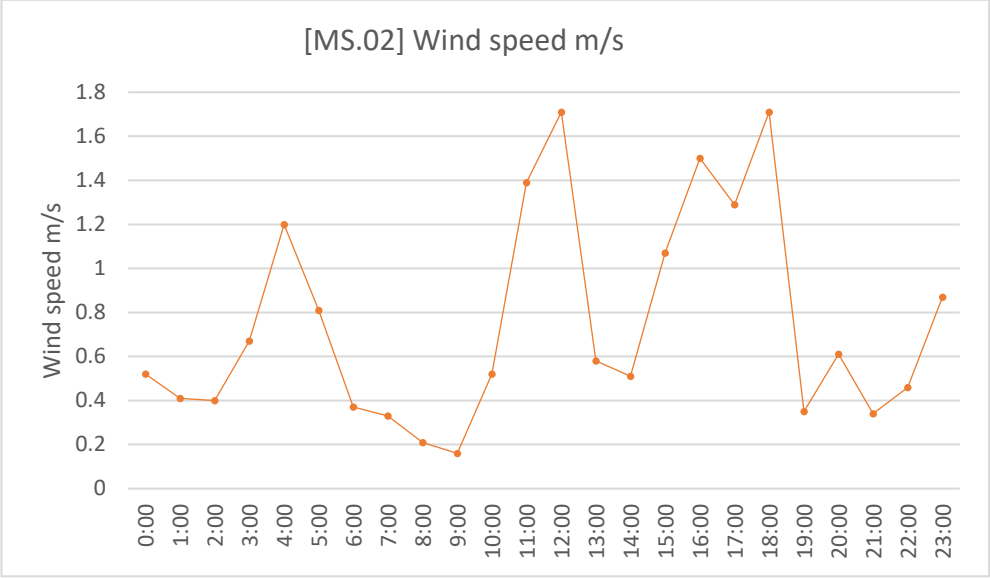

Figure 108. Microzone 2 [MS.02] wind speed values.

The Microzone 2 [MS.02] humidity levels are displayed on the graph below. The lowest value is at 06:00 hours with 13.2 m/s, while the maximum value is at 20:00 with 15.5 m/s.

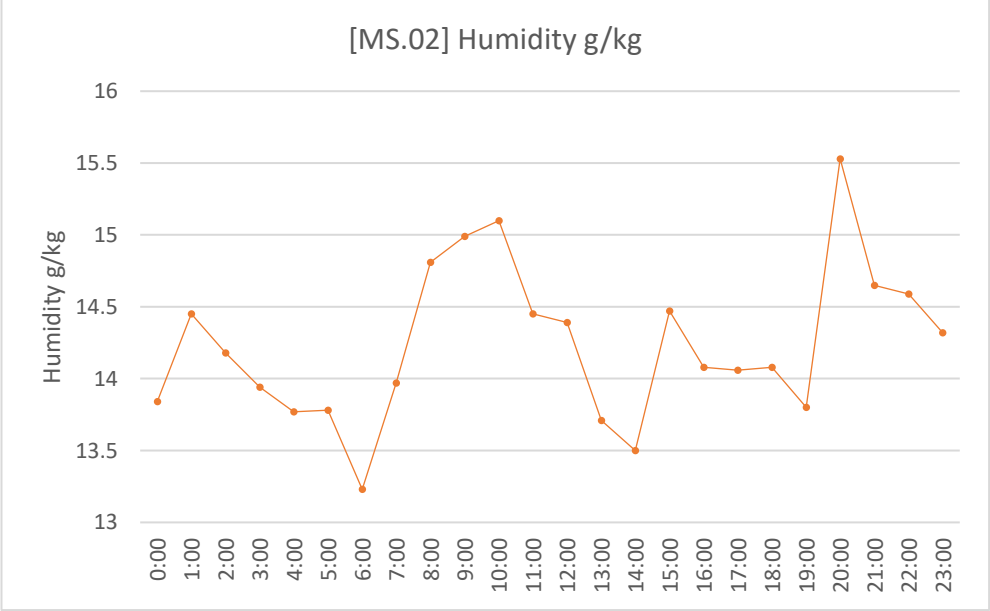

Figure 109. Microzone 2 [MS.02] humidity values.

5.2.3 Microzone 3 [MS.03]

The graph of UTCI (C) for microzone 3 [MS.03] is seen below. The highest temperature, 37.9 degrees Celsius, was recorded at 14:00. The lowest temperature ever recorded was 18.7 degrees Celsius at 04:00 in the morning. The graph demonstrates that temperatures are lowest at night and gradually increase during the day.

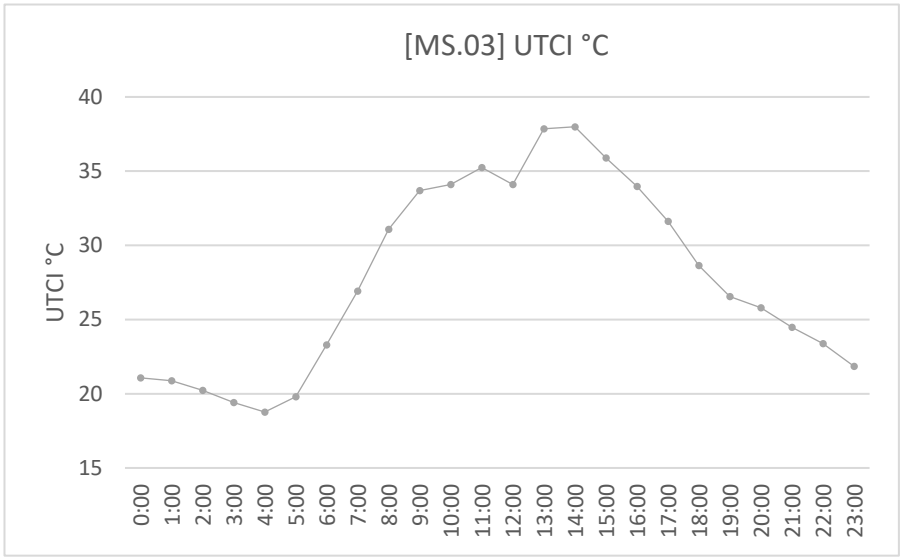

Figure 110. Microzone 3 [MS.03] UTCI values.

The air temperature data for the Microzone 3[MS.03] are displayed on the graph below. The temperature reaches its peak at 32.2 degrees Celsius at 14:00 and its lowest point at 19.9 degrees Celsius at 04:00.

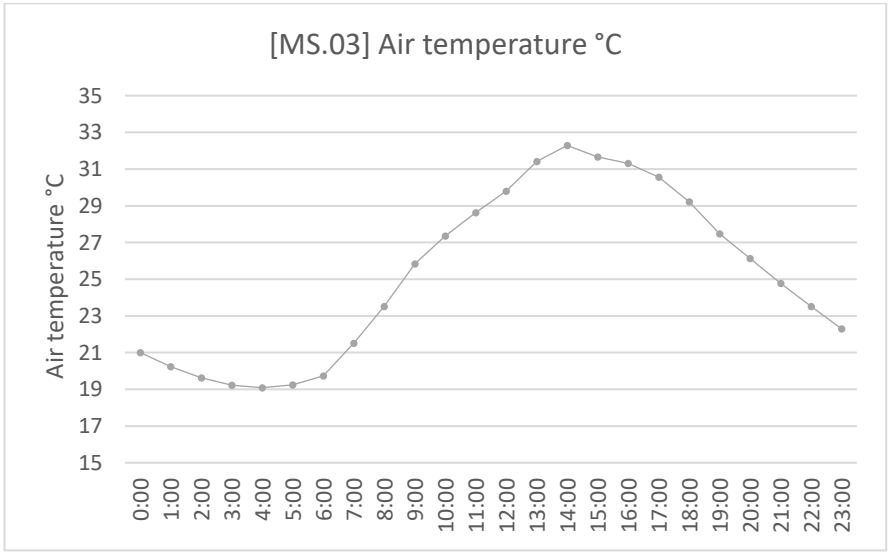

Figure 111. Microzone 3 [MS.03] air temperature values.

The values for the Microzone 3[MS.03] mean radiant temperature are displayed on the graph below. The temperature reaches its highest value at 14:00 and reaches its lowest point at 05:00, both expressed in degrees Celsius.

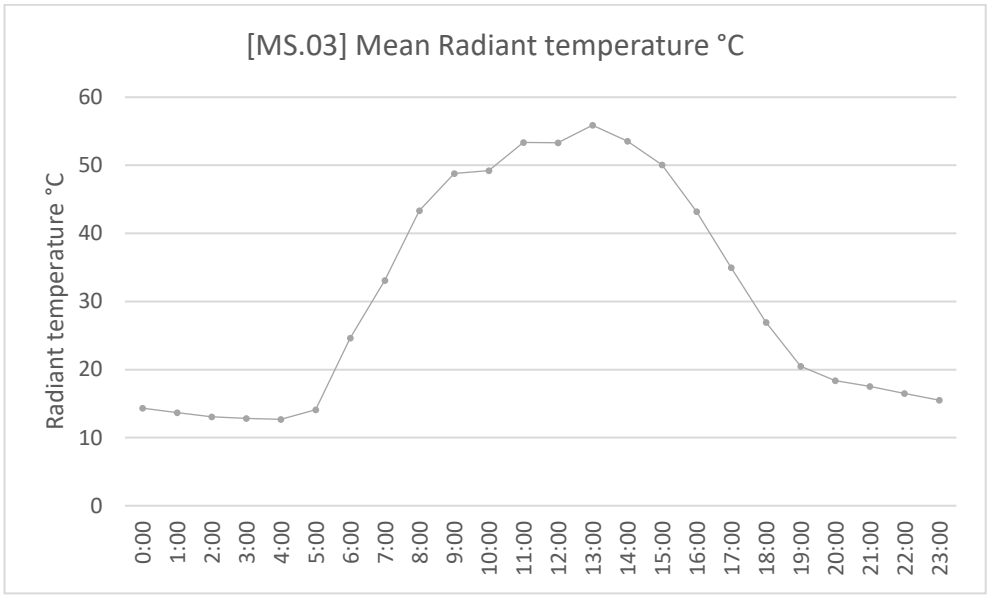

Figure 112. Microzone 3 [MS.03] mean radiant temperature values.

The values for the Microzone 3 [MS.03] wind speed is displayed on the graph below. The lowest value is at 08:00 hours by 0.2 m/s, while the maximum value is at 15:00 hours by 1.64 m/s.

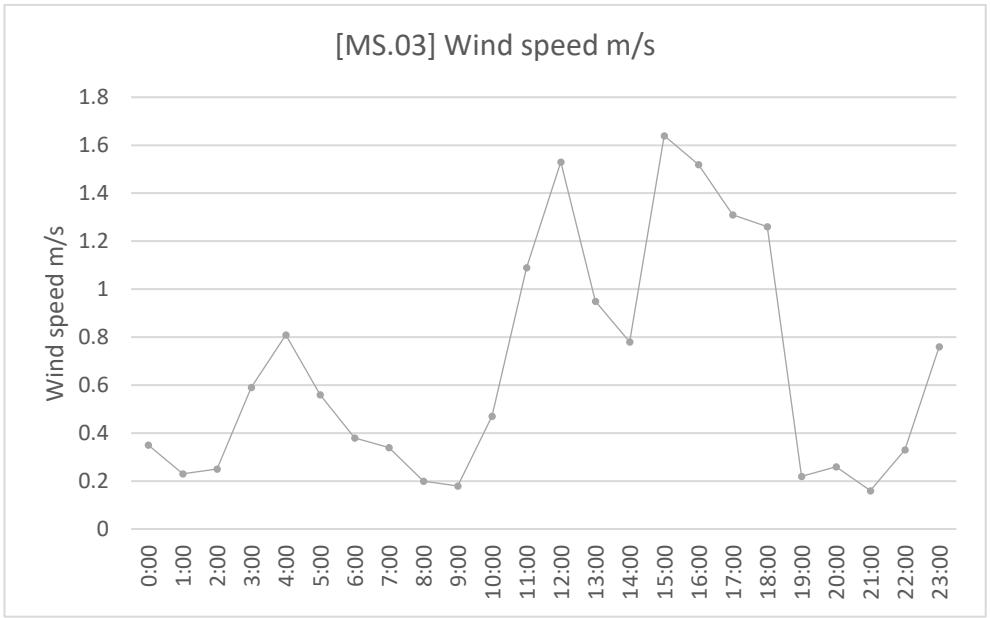

Figure 113. Microzone 3 [MS.03] wind speed values.

The Microzone 3 [MS.03] humidity levels are displayed on the graph below. The lowest value is at 06:00 hours with 13.2 m/s, while the maximum value is at 20:00 with 15.4 m/s.

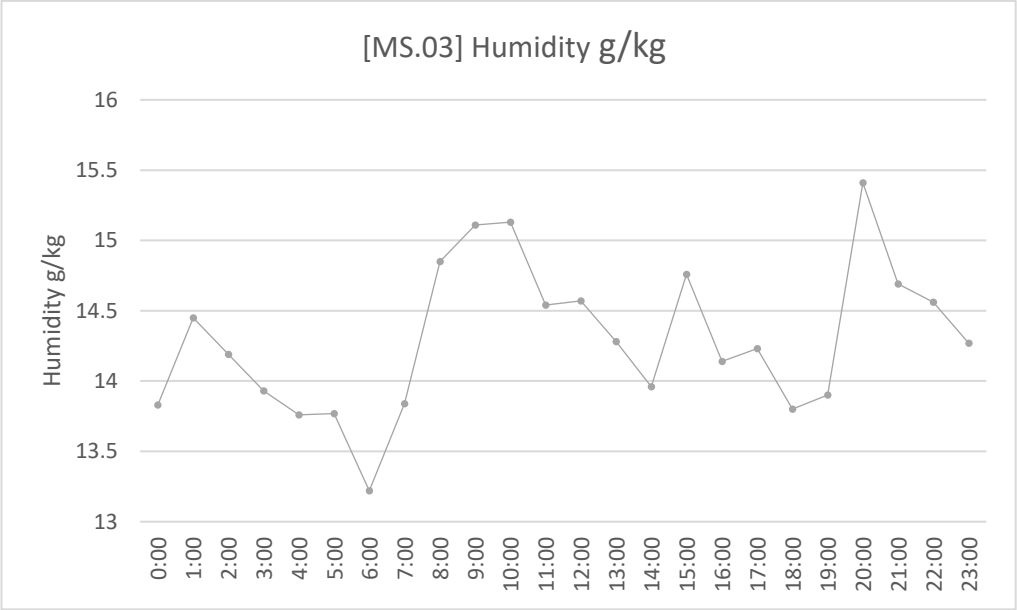

Figure 114. Microzone 3 [MS.03] humidity values.

5.3 Results and discussion/Comparison [Skanderbeg square]

5.3.1 UTCI [Skanderbeg square]

The graphs for the three microzones of Skanderbeg Square, [MS.01], [MS.02], and [MS.03], are displayed below. The graph shows that [MS.01] values are greater than those of the other two microzones. By 39 degrees Celsius, or around 0.5 degrees higher than the other two microzones, the microzone 1 has the greatest value at 14:00. The lowest reading of 16.9 degrees Celsius is recorded also in [MS.01] at 4:00 am. By having

fairly comparable temperature readings around 35 degrees Celsius, it can be observed that the graphs meet around 11:00 AM.

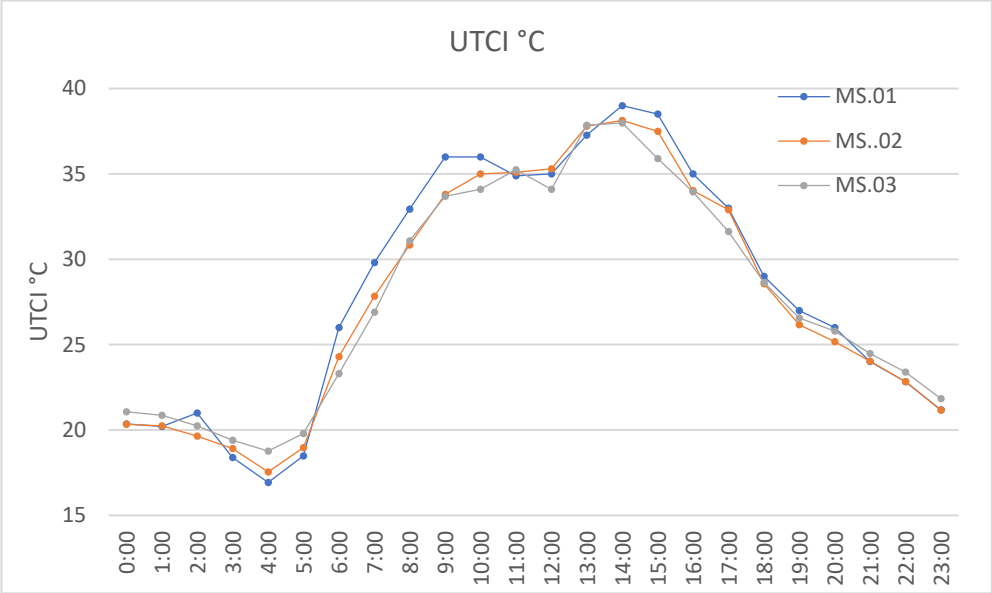

Figure 115. UTCI values for [MS.01], [MS.02] and [MS.03].

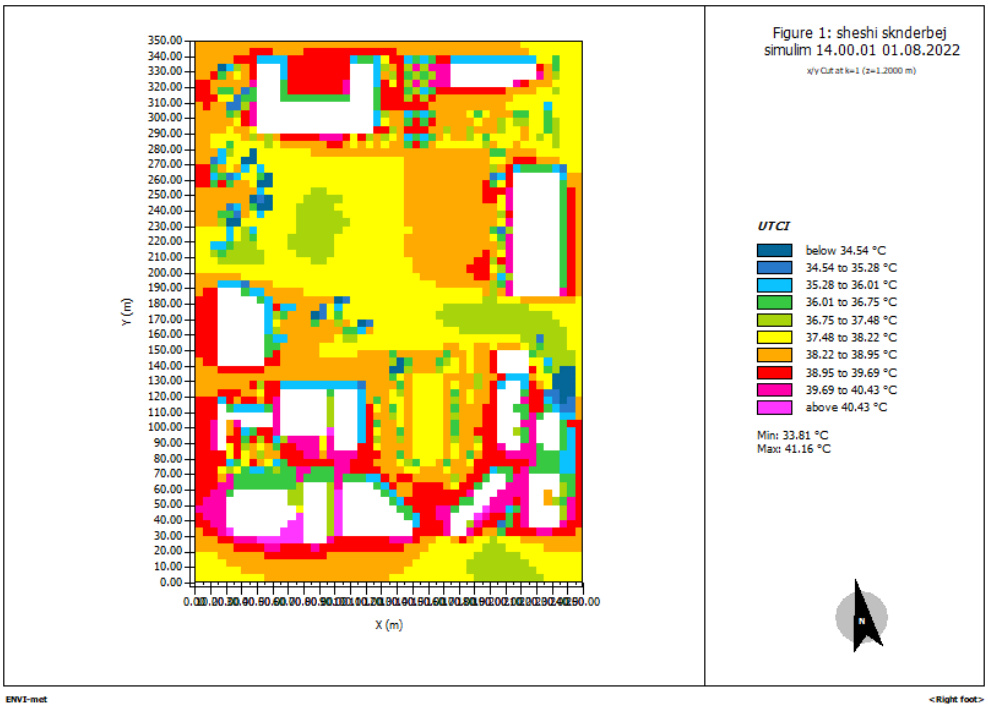

Figure 116. Figure 107. UTCI values in 14:00 hours for [MS.01], [MS.02] and [MS.03] shown in Envimet map with different color per value.

The three microzones' average and maximum values are displayed below. From the chart, it can be observed that [MS.01] has the highest average temperature readings by 28.3 degrees Celsius, while [MS.02] has the lowest by 27.8 degrees.

On the chart of maximum values, [MS.01] has the highest maximum value by 39 degrees, while [MS.03] has the lowest.

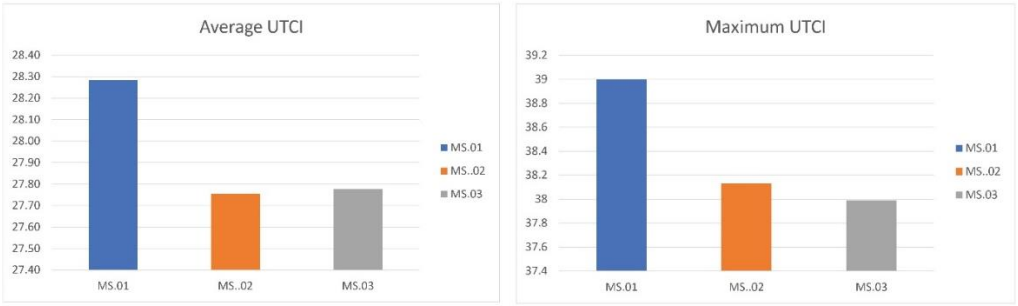

Figure 117.Average and maximum UTCI values for [MS.01], [MS.02] and [MS.03].

5.3.2 Air temperature [Skanderbeg square]

The graphs for the three microzones of Skanderbeg Square, [MS.01], [MS.02], and [MS.03], are displayed below. The graph shows that [MS.03] values are greater than those of the other two microzones. By 32.2 degrees Celsius, or around 0.2 degrees higher than the other two microzones, the microzone 3 has the greatest value at 14:00. The lowest reading of 19 degrees Celsius is recorded also in [MS.01] at 4:00 am. By having fairly comparable temperature readings around 35 degrees Celsius, it can be observed that the graphs meet around 11:00 AM.

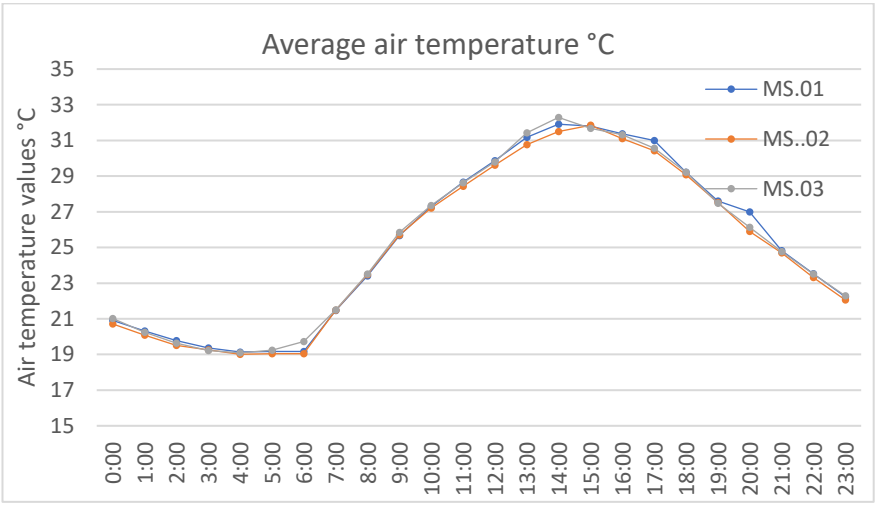

Figure 118. Air temperature values for [MS.01], [MS.02] and [MS.03].

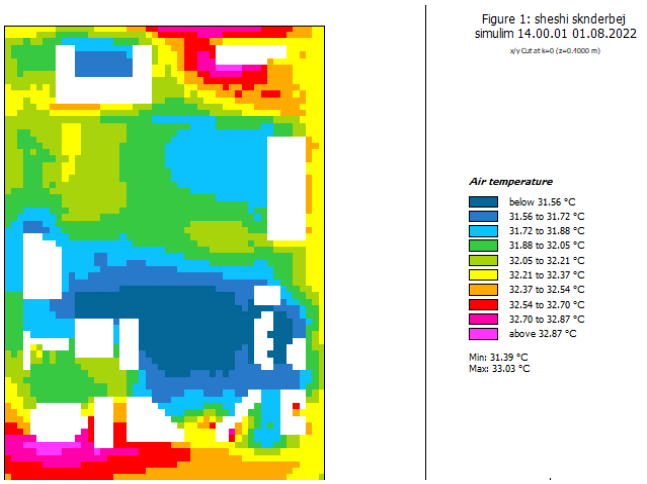

Figure 119. Air temperature values in 14:00 hours of [MS.01], [MS.02] and [MS.03] shown in Envimet map with different color per value.

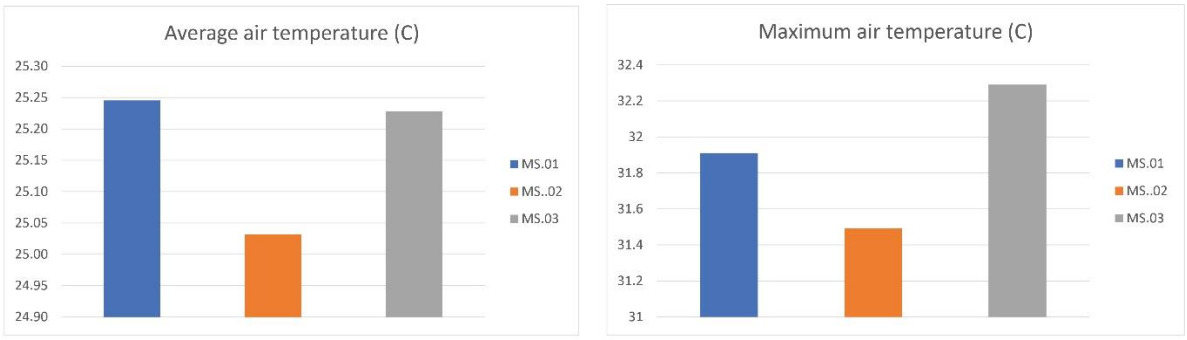

Figure 120. Average and maximum air temperature values for [MS.01], [MS.02] and [MS.03].

5.3.3 Mean radiant temperature [Skanderbeg square]

The graphs for the three microzones of Skanderbeg Square, [MS.01], [MS.02], and [MS.03], are displayed below. The graph shows that [MS.01] values are greater than those of the other two microzones. By 58.2 degrees Celsius, or around 2 degrees higher than the other two microzones, the microzone 1 has the greatest value at 14:00. The lowest reading of 19 degrees Celsius is recorded also in [MS.01] at 4:00 am. By having

fairly comparable temperature readings around 35 degrees Celsius, it can be observed that the graphs meet around 05:00 AM.

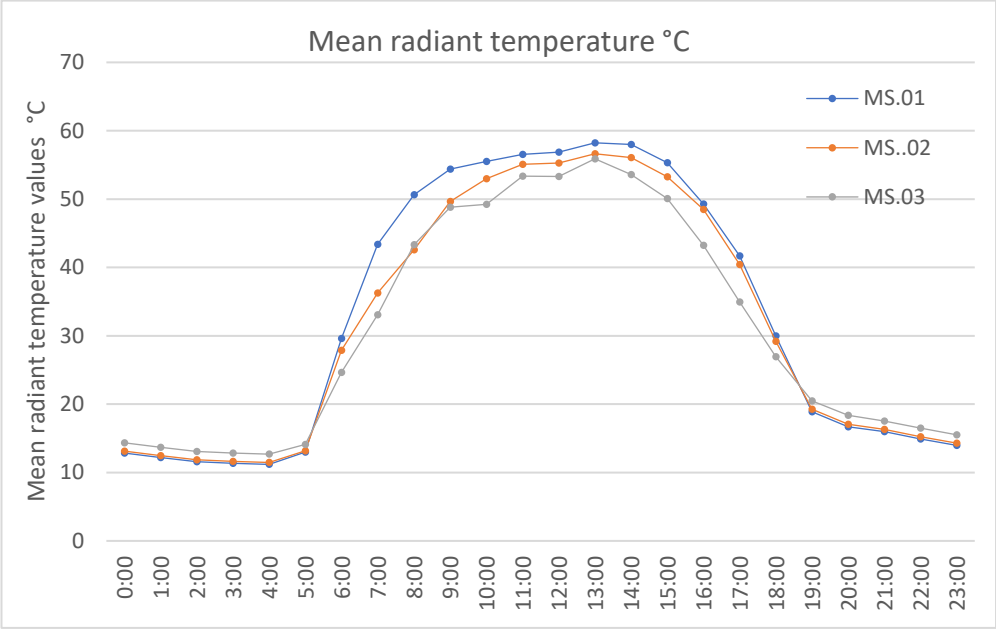

Figure 121. Mean radiant temperature values for [MS.01], [MS.02] and [MS.03].

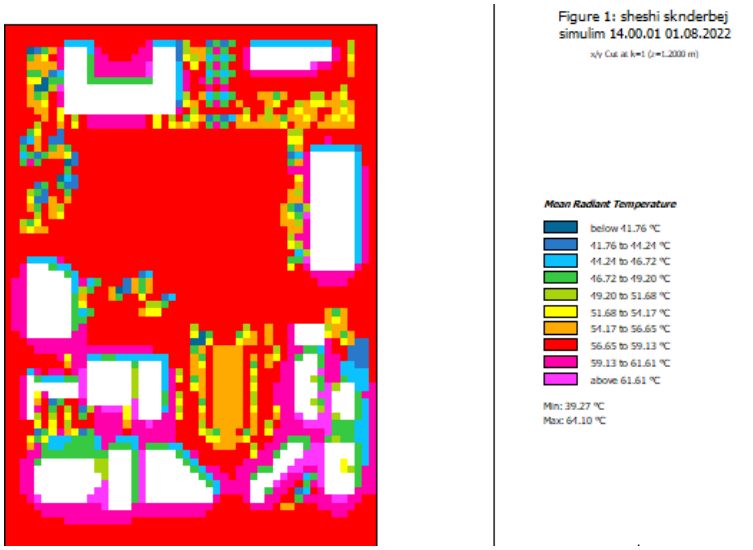

Figure 122. Mean radiant temperature values in 14:00 hours of [MS.01], [MS.02] and [MS.03] shown in Envimet map with different color per value.

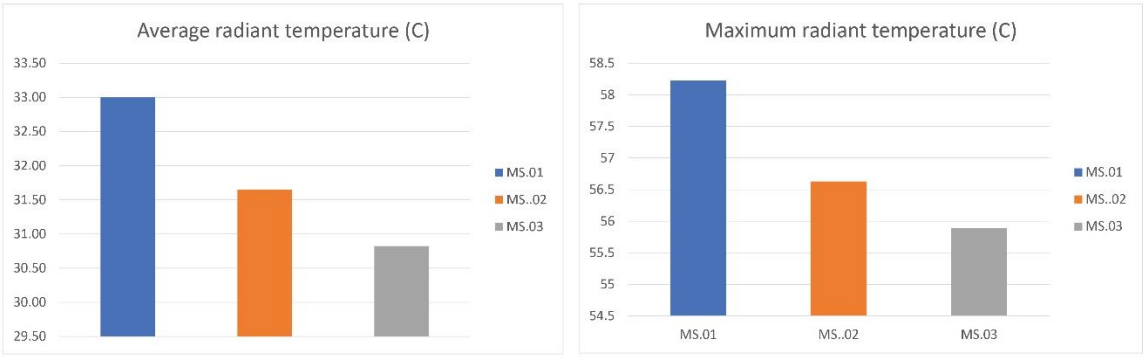

Figure 123. Average and maximum mean radiant temperature values for [MS.01], [MS.02] and [MS.03].

5.3.4 Wind speed [Skanderbeg square]

The graphs for the three microzones of Skanderbeg Square, [MS.01], [MS.02], and [MS.03], are displayed below. The graph shows that [MS.01] values are greater than those of the other two microzones. By 2.61m/s, or around 0.2 m/s faster than the other two microzones, the microzone 1 has the greatest value at 14:00. The lowest reading of 0.2 m/s is recorded also in [MS.03] at 8:00 am. By having fairly comparable temperature readings around 0.2 m/s, it can be observed that the graphs meet around 06:00 AM.

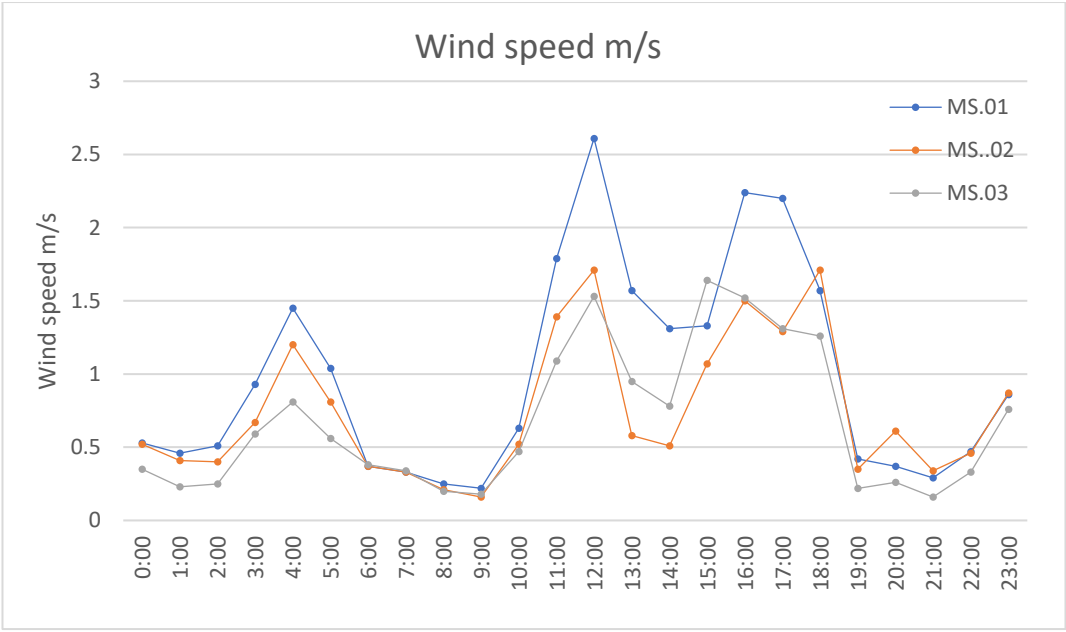

Figure 124. Wind speed values for [MS.01], [MS.02] and [MS.03].

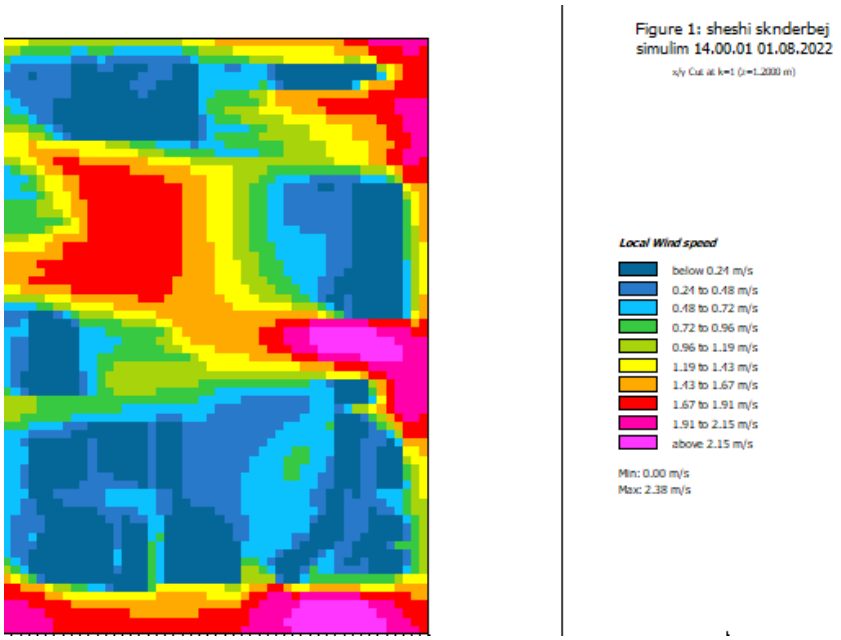

Figure 125. Wind speed values in 14:00 hours of [MS.01], [MS.02] and [MS.03] shown in Envimet map with different color per value.

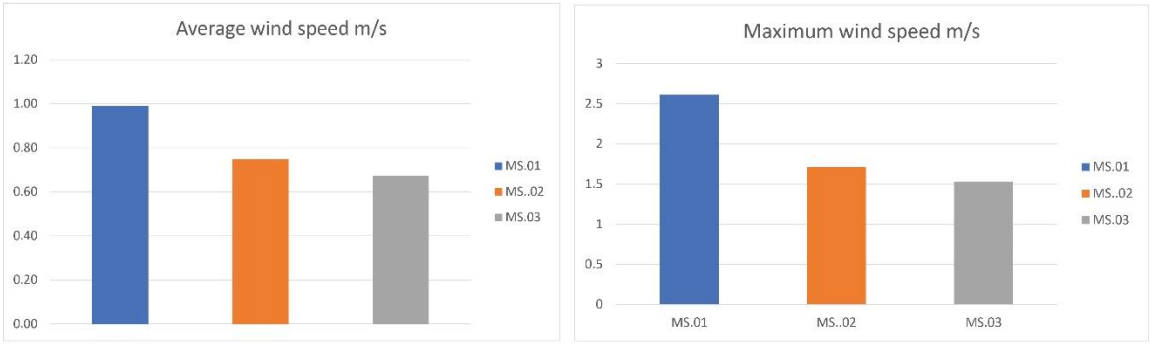

Figure 126. Average and maximum wind speed values for [MS.01], [MS.02] and [MS.03].

5.3.5 Humidity [Skanderbeg square]

The graphs for the three microzones of Skanderbeg Square, [MS.01], [MS.02], and [MS.03], are displayed below. The graph shows that [MS.01] values are greater than those of the other two microzones. By 15.6 g/kg, or around 0.1 m/s denser than the other two microzones, the microzone 1 has the greatest value at 20:00. The lowest reading of

13.2 g/kg is recorded also in [MS.01] and [MS.03] at 6:00 am where the graphs meet each other.

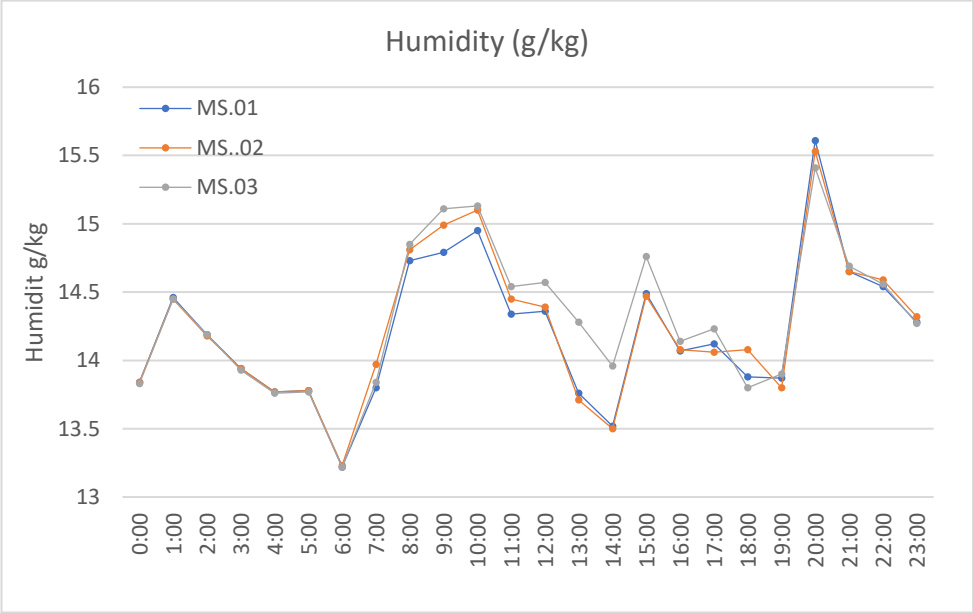

Figure 127. Humidity values for [MS.01], [MS.02] and [MS.03].

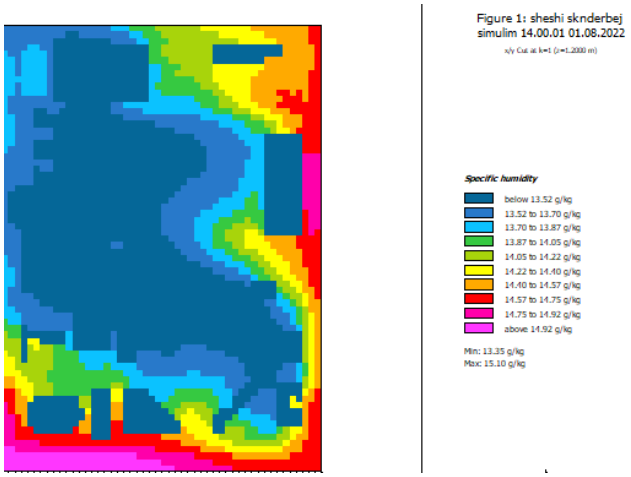

Figure 128. Humidity values in 14:00 hours of [MS.01], [MS.02] and [MS.03] shown in Envimet map with different color per value.

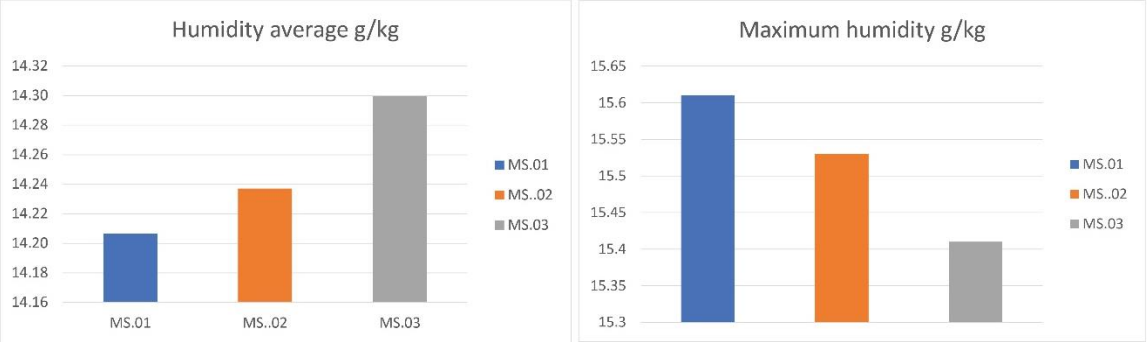

Figure 129. Average and maximum humidity values for [MS.01], [MS.02] and [MS.03].

5.4 Results and discussion/Comparison [Mother Teresa Square]

5.4.1 UTCI [Mother Teresa Square]

The graphs for the three microzones of Mother Teresa square, [MN.01], [MN.02], and [MN.03], [MN.04] are displayed below. The graph shows that [MN.02] values are greater than those of the other two microzones. By 38.6 degrees Celsius, or around 0.6 degrees higher than the other three microzones, the microzone 2 has the greatest value at 14:00. The lowest reading of 18.2 degrees Celsius is recorded also in [MS.03] at 4:00 am. By having fairly comparable temperature readings around 18.2 degrees Celsius, it can be observed that the graphs meet around 04:00 AM.

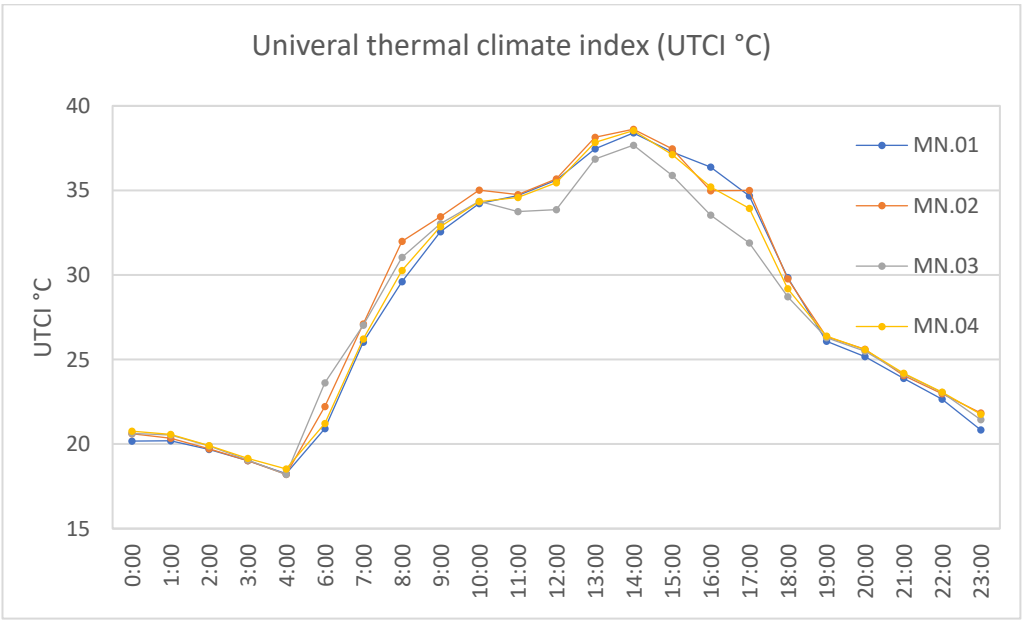

Figure 130. UTCI values for [MN.01], [MN.02], [MN.03] and [MN.04].

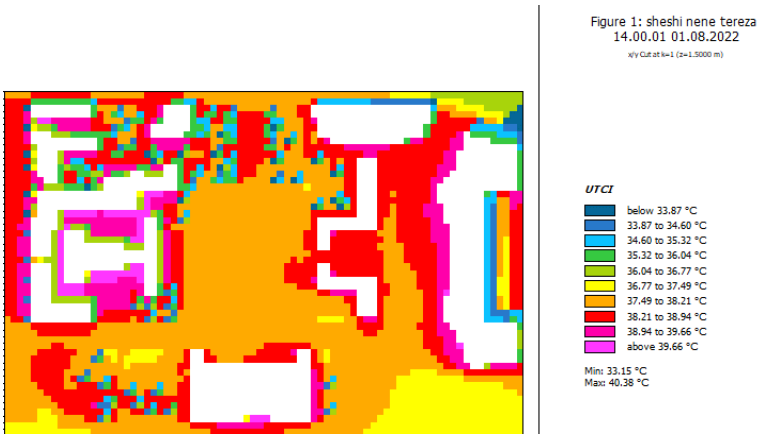

Figure 131. UTCI values in 14:00 hours for [MN.01], [MN.02], [MN.03] and [MN.04] shown in Envimet map with different color per value.

Figure 132. Average and maximum UTCI values for [MN.01], [MN.02], [MN.03] and [MN.04].

5.4.2 Air temperature [Mother Teresa Square]

The graphs for the three microzones of Mother Teresa square, [MN.01], [MN.02], and [MN.03], [MN.04] are displayed below. The graph shows that [MN.03] values are greater than those of the other two microzones. By 32.7 degrees Celsius, or around 0.1 degrees higher than the other two microzones, the microzone 3 has the greatest value at 14:00. The lowest reading of 18.9 degrees Celsius is recorded in [MN.02] at 4:00 am. By having fairly comparable temperature readings around 19 degrees Celsius, it can be observed that the graphs meet around 04:00 AM.

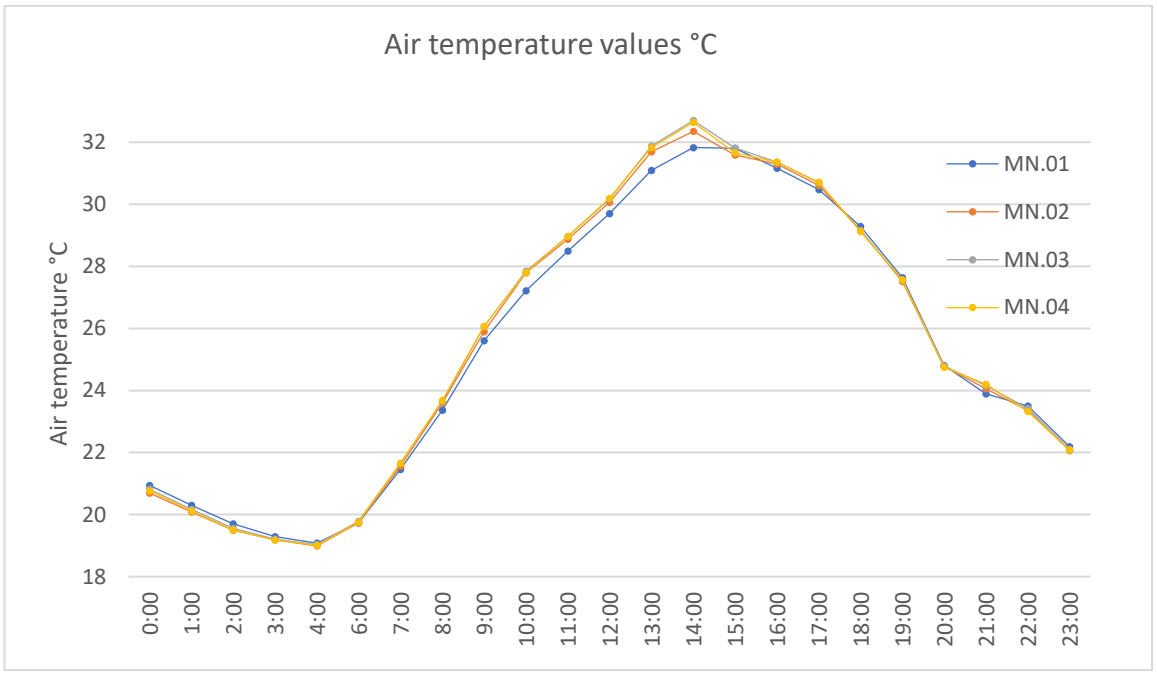

Figure 133. Air temperature values for [MN.01], [MN.02], [MN.03] and [MN.04].

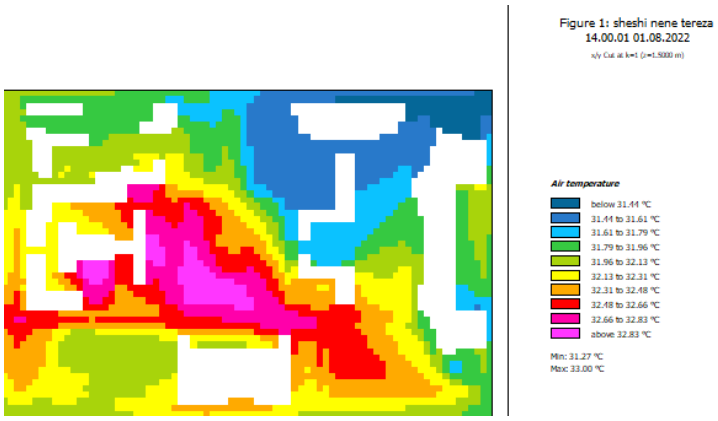

Figure 134. Air temperature values in 14:00 hours for [MN.01], [MN.02], [MN.03] and [MN.04] shown in Envimet map with different color per value.

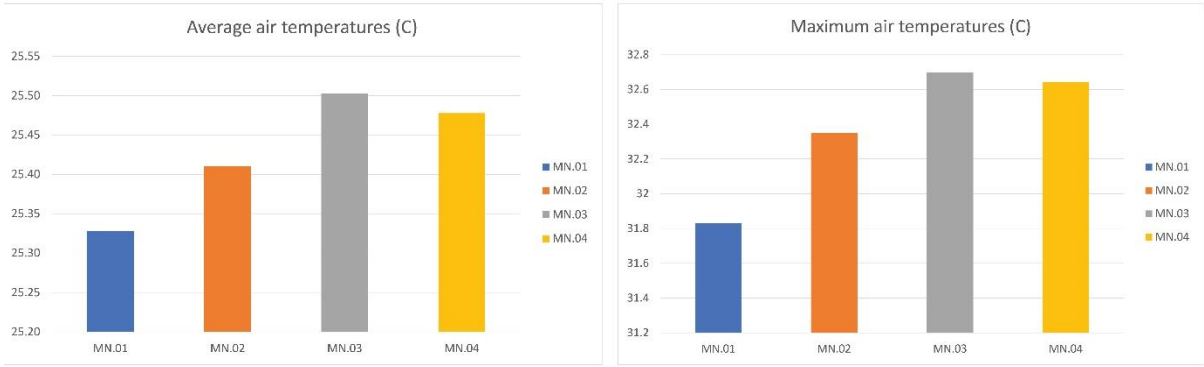

Figure 135. Average and maximum air temperature values for [MN.01], [MN.02], [MN.03] and [MN.04].

5.4.3 Mean radiant temperature [Mother Teresa Square]

The graphs for the three microzones of Mother Teresa square, [MN.01], [MN.02], and [MN.03], [MN.04] are displayed below. The graph shows that [MS.01] values are greater than those of the other two microzones. By 57.4 degrees Celsius, or around 0.5degrees higher than the other two microzones, the microzone 1 has the greatest value at 14:00. The lowest reading of 10.9 degrees Celsius is recorded also in [MS.01] at 4:00 am. By having fairly comparable temperature readings around 11 degrees Celsius, it can be observed that the graphs meet around 04:00 AM.

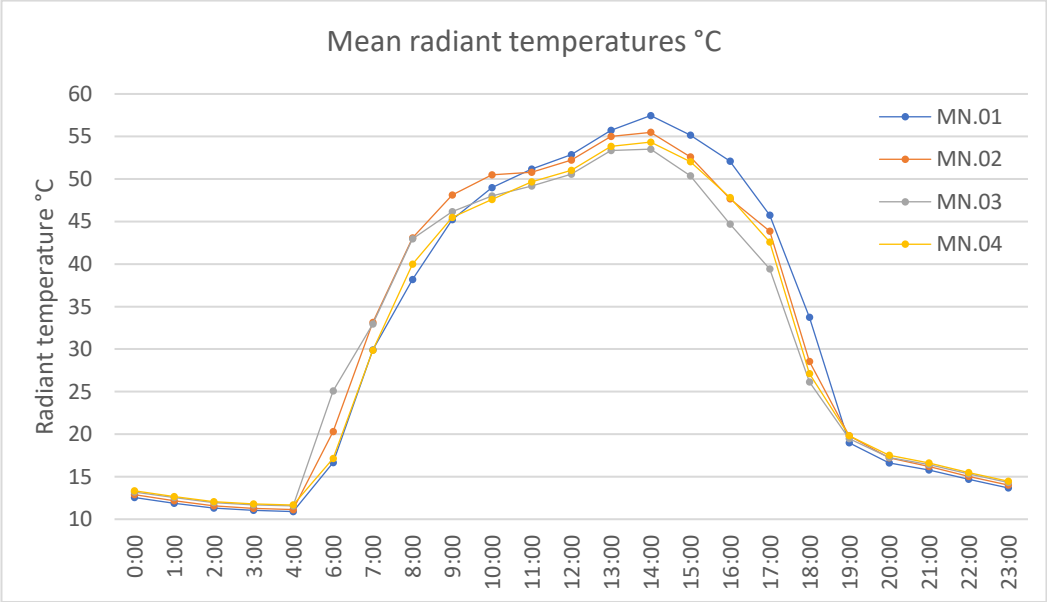

Figure 136.Mean radiant temperature values for [MN.01], [MN.02], [MN.03] and [MN.04].

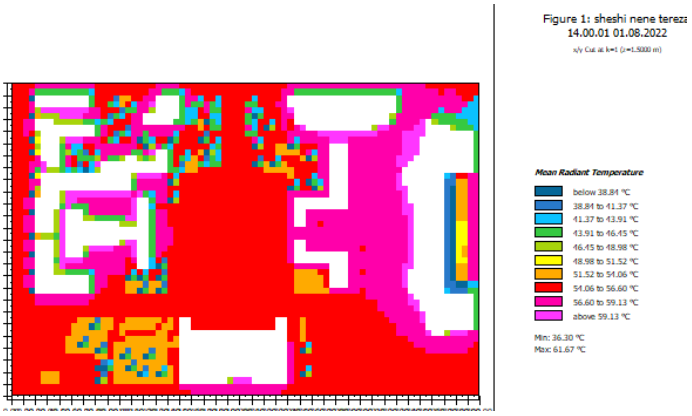

Figure 137. Mean radiant temperature values in 14:00 hours for [MN.01], [MN.02], [MN.03] and [MN.04] shown in Envimet map with different color per value.

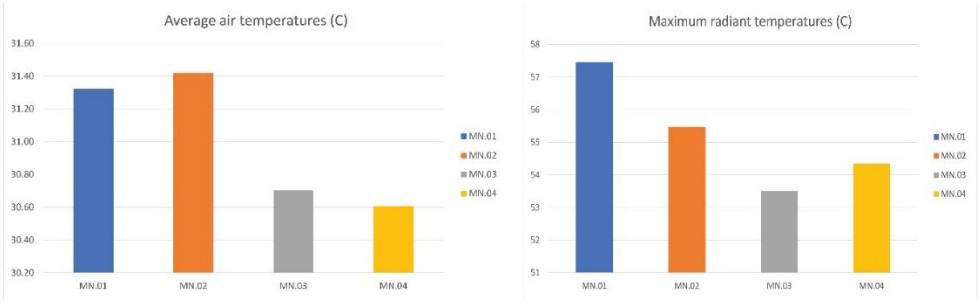

Figure 138. Average and maximum mean radiant temperature values for [MN.01], [MN.02], [MN.03] and [MN.04].

5.4.4 Wind speed [Mother Teresa Square]

The graphs for the three microzones of Mother Teresa square, [MN.01], [MN.02], and [MN.03], [MN.04] are displayed below. The graph shows that [MN.03] values are greater than those of the other two microzones. By 2.14m/s, or around 0.4 m/s faster than the other two microzones, the microzone 1 has the greatest value at 14:00. The lowest reading of 0.18 m/s is recorded also in [MS.04] at 8:00 am. By having fairly comparable temperature readings around 0.5 m/s and 0.2, it can be observed that the graphs meet around 03:00 AM and 08:00 AM.

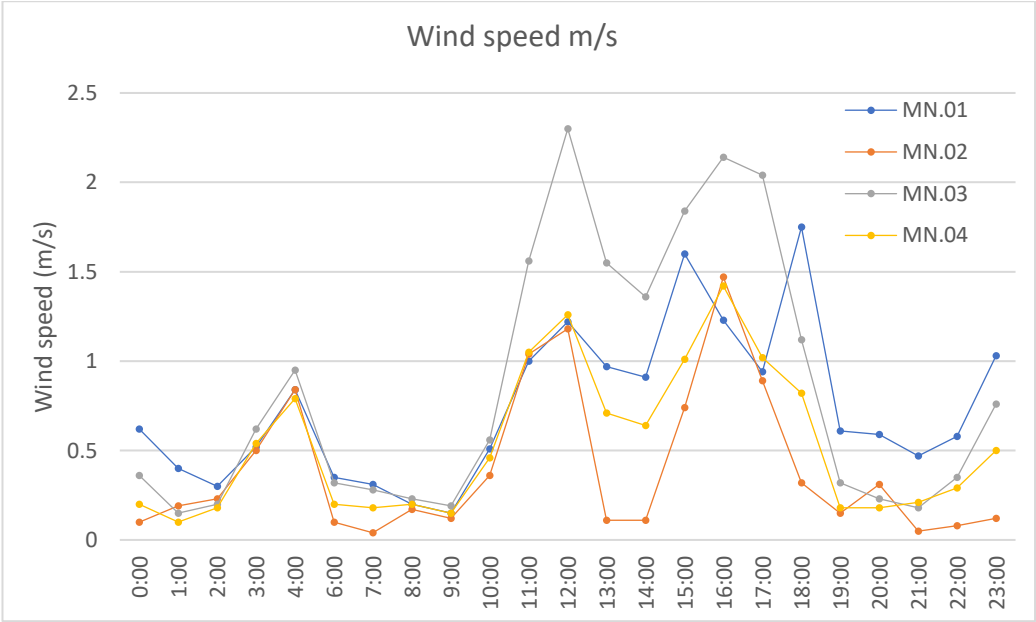

Figure 139. Wind speed values for [MN.01], [MN.02], [MN.03] and [MN.04].

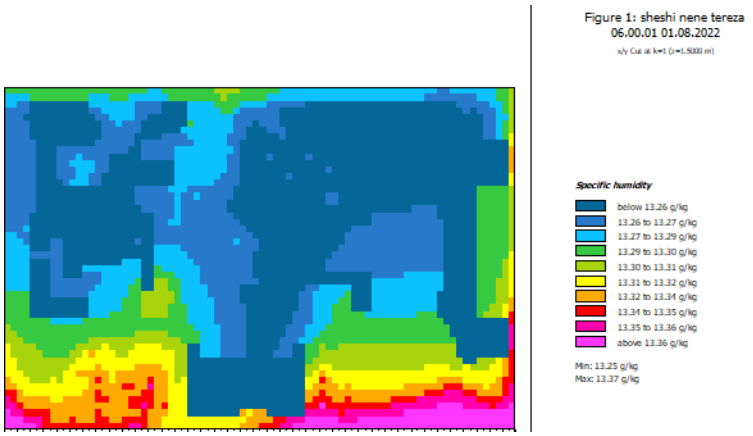

Figure 140. Wind speed values in 14:00 hours for [MN.01], [MN.02], [MN.03] and [MN.04] shown in Envimet map with different color per value.

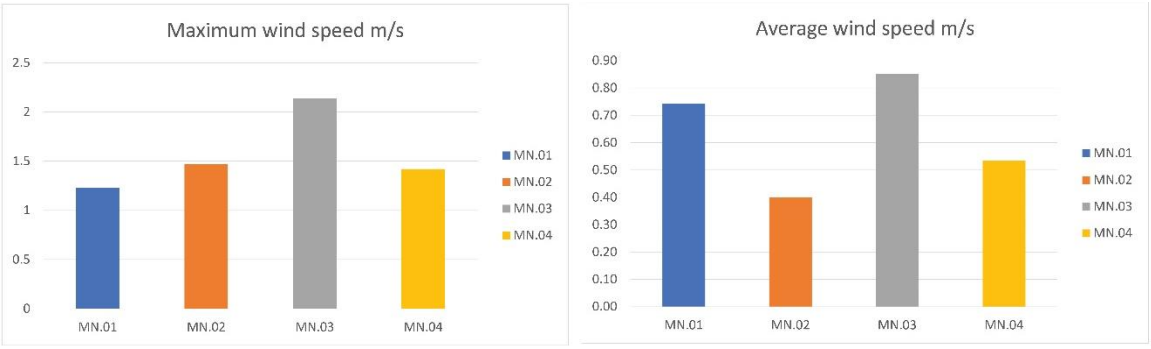

Figure 141. Average and maximum wind speed values for [MN.01], [MN.02], [MN.03] and [MN.04].

5.4.5 Humidity [Mother Teresa Square]

The graphs for the three microzones of Mother Teresa square [MN.01], [MN.02], and [MN.03], [MN.04] are displayed below. The graph shows that [MN.04] values are greater than those of the other two microzones. By 15.8g/kg, or around 0.1 m/s denser than the other two microzones, the microzone 2 has the greatest value at 20:00. The

lowest reading of 13.2 g/kg is recorded also in [MN.01] and [MN.02] at 6:00 am where the graphs meet each other by 0.2 m/s.

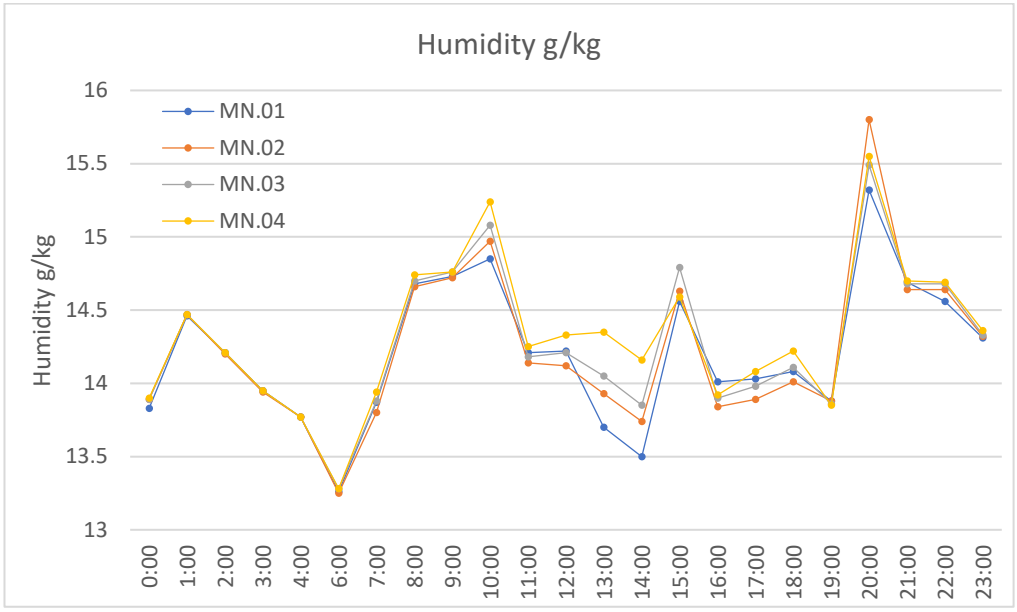

Figure 142. Wind speed values for [MN.01], [MN.02], [MN.03] and [MN.04].

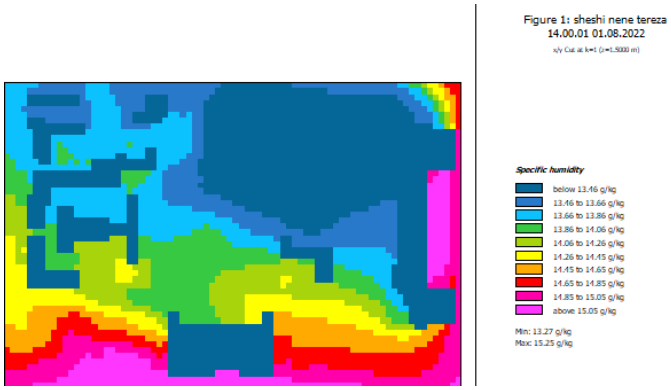

Figure 143. Humidity values in 14:00 hours for [MN.01], [MN.02], [MN.03] and [MN.04] shown in Envimet map with different color per value.

Figure 144. Average and maximum humidity values for [MN.01], [MN.02], [MN.03] and [MN.04]

CHAPTER 6

DESIGN BASED OPTIMIZATION STRATEGIES

6.1 Design based optimization strategies

For a number of reasons, it is crucial to lower the temperature in public areas. First of all, it improves people's comfort and wellbeing, making the atmosphere more enjoyable for everyone. Cooler temperatures can lessen the discomfort caused by the heat, minimizing dehydration and heat exhaustion. Second, it encourages productivity and attention, especially in professional environments and educational settings where individuals tend to be more concentrated. Additionally, as certain organisms prefer warmer climates, reducing temperatures can slow the spread of infectious illnesses. Additionally, correctly maintained cooling systems increase energy efficiency, resulting in lower energy use and a smaller environmental effect. Overall, keeping public areas cooler promotes everyone's comfort and a sustainable environment. It also benefits people's physical and emotional health. To address the many issues related to urbanization and climate change, it is crucial to mitigate the UHI impact. The UHI impact may be considerably reduced by using environmentally friendly structures such as urban parks, rooftops with vegetation, and tree canopies. To direct and encourage the development of sustainable communities, the U.S. Green Building Council (USGBC) developed the LEED-ND certification system (USGBC, 2022).

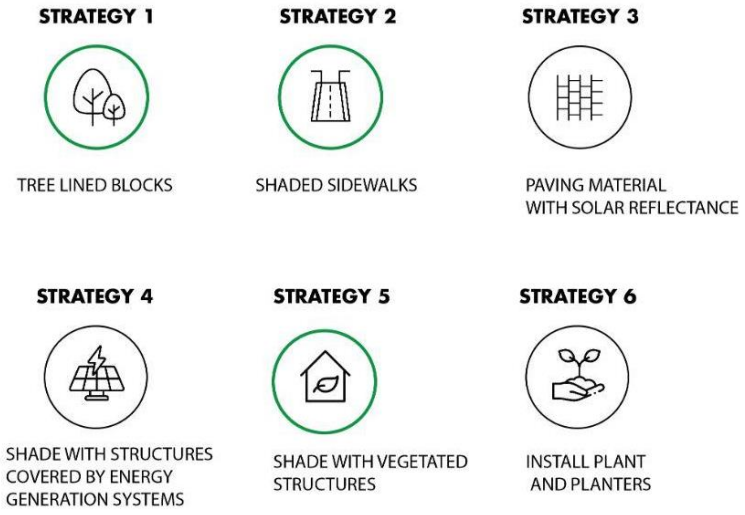

Figure 145. Design based optimization strategies

A number of strategies to mitigate temperatures and the urban heat island are listed below, which will enhance the thermal comfort of pedestrians:

Strategy 1

Tree lined blocks

Integrating trees between the road travel way and sidewalk at distances of no more than 12 meters throughout at least 60% of the length of all existing and proposed blocks within the project as well as on the project side of blocks surrounding the project. Alleys may not be included in estimates for block length.

Strategy 2

Shaded sidewalks

Trees must provide shade for 40% of the sidewalk's length. Each tree implemented may provide 6 linear meters of shade.

Strategy 3

Paving materials with solar reflectance

High solar reflectance paving materials are frequently referred to as “cool surfaces”. In order to reduce the UHI effect and raise the average temperature in urban areas, these materials are made to reflect greater amounts of light and absorb a smaller amount of heat. High solar reflectance pavement materials include some of the following: light colored concrete, coatings with reflective pigments, permeable pavers or other porous pavement materials. (Governatori et al., 2022)

Strategy 4

Shaded structures covered by energy generation systems

Creating shade with buildings covered with energy-producing technologies, such as solar thermal collectors, solar energy systems, and turbines for wind power, in order to partially offset the usage of non-renewable resources.

Strategy 5

Shaded vegetated structures

Those structures combine the evaporative cooling supplied by plants with the cooling benefits of shade to generate more pleasant microclimates and lessen the negative effects of the urban heat island. (Iaria & Susca, 2022) Here are a few instances of typical

shaded vegetation structures: green roofs, pergolas, living walls or green walls, shade sails etc.

Strategy 6

Installing plants and planters

The quantity of direct sunlight that penetrates the earth's surface and nearby surfaces can be diminished by trees, bushes, and tall plants in pots. Transpiration is the term for the process through which plants naturally discharge moisture. They chill the surrounding air by absorbing water from the earth and releasing it via their leaves. Evapotranspiration is the term for this process, which lowers the local temperature.

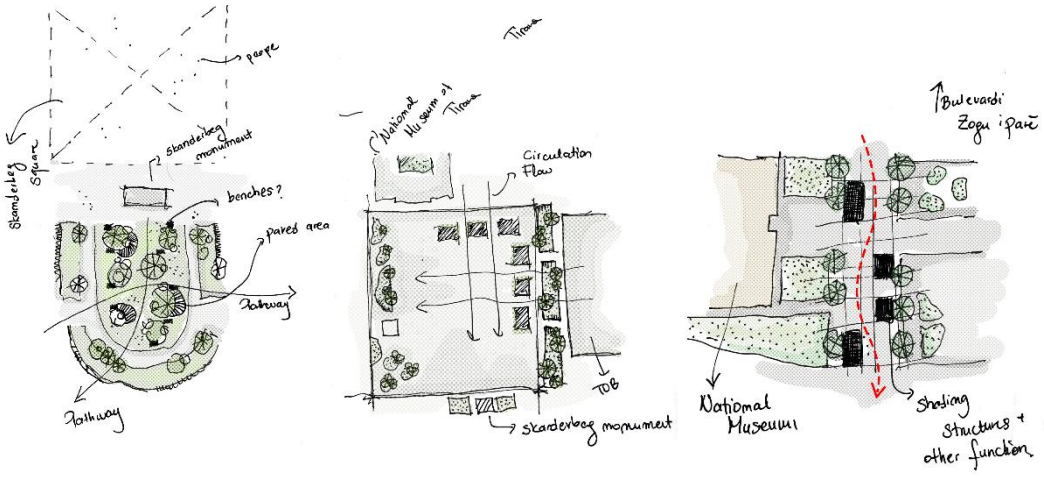

Figure 146. Conceptual sketches of deisgn based optimization ideas

6.2 Microzone design-based optimization strategies

Microzone 1 [MS.01] optimization tactics include a variety of cutting-edge methods designed to maximize effectiveness and sustainability in small urban areas. Integrating shade structures with solar panels or reflecting materials is a major strategy. In addition to offering sun protection, this also captures solar energy to power the Microzone [MS.01]. Additionally, using modular systems offers adaptability and flexibility in setups, allowing for fast alterations to meet various demands and functions within the constrained space. Incorporating vegetated structures, such as green walls or roof top

gardens, is another essential component. These features not only improve aesthetics but also boost air quality, lessen the impact of heat islands, and promote biodiversity.

Figure 147. Design based strategy for the optimization of Microzone 1 [MS.01]

The two main components of the optimization techniques for Microzone 3 [MS.03] are modular systems and shade structures made of reflecting materials or solar panels. The Microzone can regulate solar radiation and harvest renewable energy by including shade structures made of reflecting materials or solar panels. These buildings offer shade, which lowers heat absorption and improves the environment. Additionally, the use of solar panels enables the creation of clean energy, enhancing the sustainability of the Microzone. Modular systems are also used in Microzone 2 to provide flexibility and adaptability. These solutions make it simple to reconfigure and personalize the area, effectively meeting a range of purposes. Overall, the employment of these optimization techniques in Microzone 2 [MS.02] provides increased customer satisfaction, environmental responsibility, and energy efficiency.

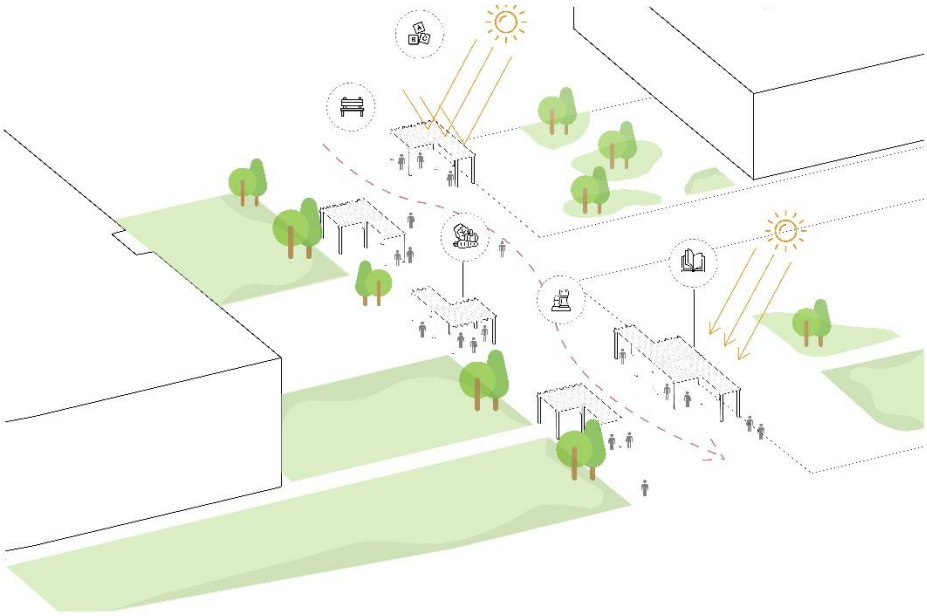

Figure 148.Design based strategy for the optimization of Microzone 3 [MS.03]

Three key components that support a peaceful and sustainable urban environment are the focus of Microzone 2 [MS.02] optimization methodologies. First off, strategically placing trees within a Microzone helps to provide shade, lessen the impact of the heat island effect, and improve aesthetics. These trees contribute to increased biodiversity and air quality in addition to providing a comfortable environment for guests. Second, the addition of new seats built from recyclable materials demonstrates the Microzone's dedication to environmental responsibility. In addition to providing comfortable seating, these seats encourage resource reuse, minimizing their negative environmental effects. Last but not least, the inclusion of additional narrow routes improves pedestrian circulation inside the Microzone and encourages greater exploration and interaction with the area.

Figure 149.Design based strategy for the optimization of Microzone 2 [MS.02]

To build a thriving urban paradise, Microzone 2 [MN.02] optimization tactics give priority to sustainability and green technologies. Green facades, which are vegetal structures gracing the exteriors of buildings, are one important strategy. These facades provide the Microzone with several ecological advantages in addition to a touch of aesthetic appeal. They serve as living filters that clean the air, lower the amount of carbon dioxide levels, and enhance air quality in general. Additionally, the Microzone's eco-friendliness is further improved by the placement of trees in well chosen locations. These trees give much-needed shade, reducing the impact of the heat island and giving tourists a break.

Figure 150. Design based strategy for the optimization of Microzone 2 [MN.02]

6.3 Results and comparison

The graphs below compare the Microzones UTCI temperature readings before and after the optimization process was performed. It is clear from the first Microzone [MS.01] that temperatures are reduced, with the highest temperature reaching 37.7 °C at 14:00 as opposed to 39 °C before. This indicates a 1.3 °C increase in temperature values. After design-based optimization, the temperatures are displayed on the graph of [MS.01 O]. The two plots intersect at 16:00 and 17:00 in the afternoon with comparable measurements of temperature. The temperatures are lowered by 3 °C around 9:00, creating the biggest impact.

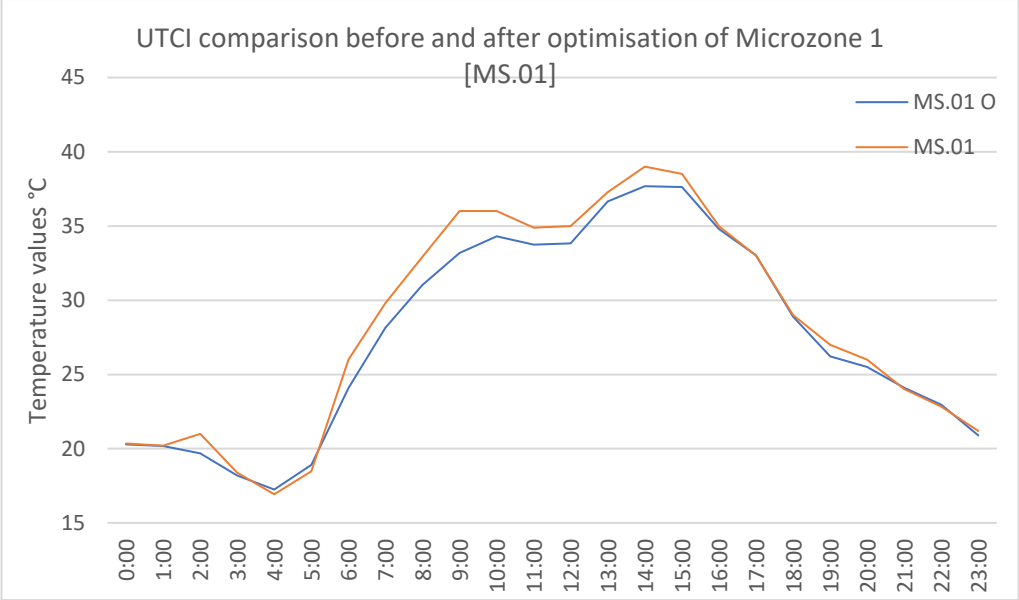

Figure 151.UTCI comparison graph of Microzone 1 [MS.01]

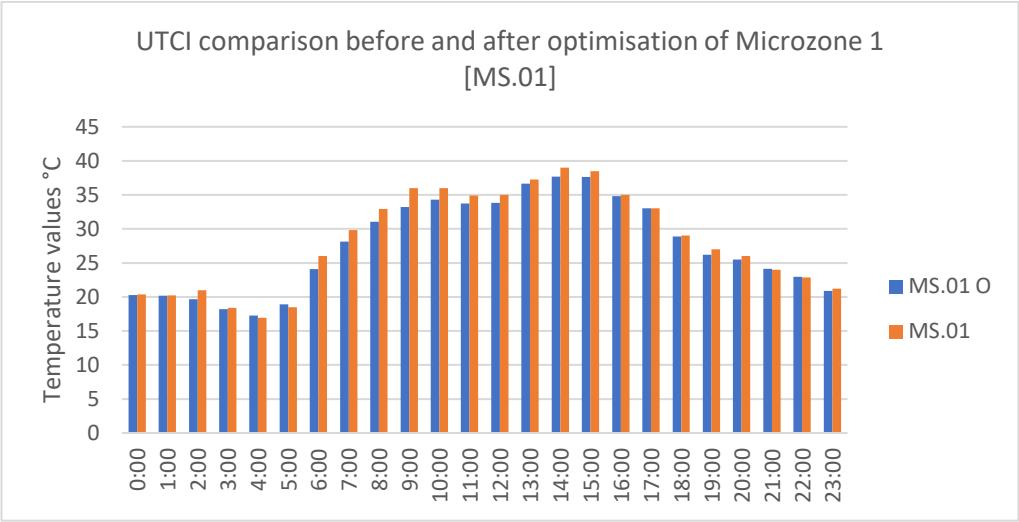

Figure 152.UTCI comparison chart of Microzone 1 temperature values before and after optimization [MS.01]

The graphs below show a comparison between the Microzones UTCI temperature readings prior to and during the optimization procedure. Temperatures are dropping, as seen by the first Microzone [MS.02], where the greatest temperature was 37.3 °C at 14:00 as compared to 38.1 °C earlier. This denotes a rise in temperature readings of 0.8 °C. Following design-based optimization, the temperatures are shown on the [MS.02 O] graph. At 16:00 and for the whole evening, the two charts overlap with similar temperature readings. The strongest effect occurs about 11:00, when temperatures drop by 1.2 °C.

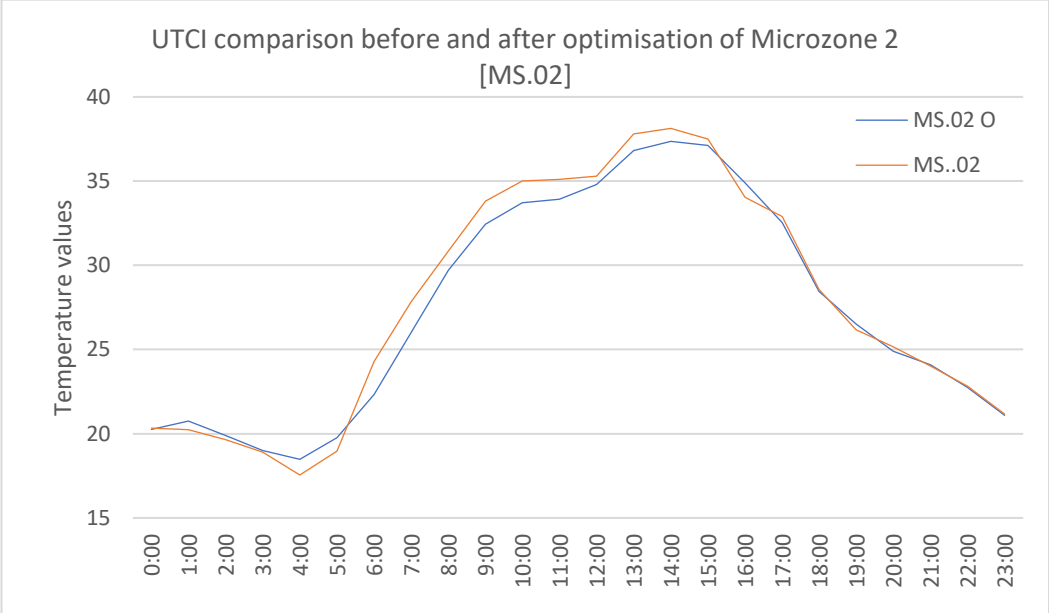

Figure 153.UTCI comparison graph of Microzone 2 [MS.02]

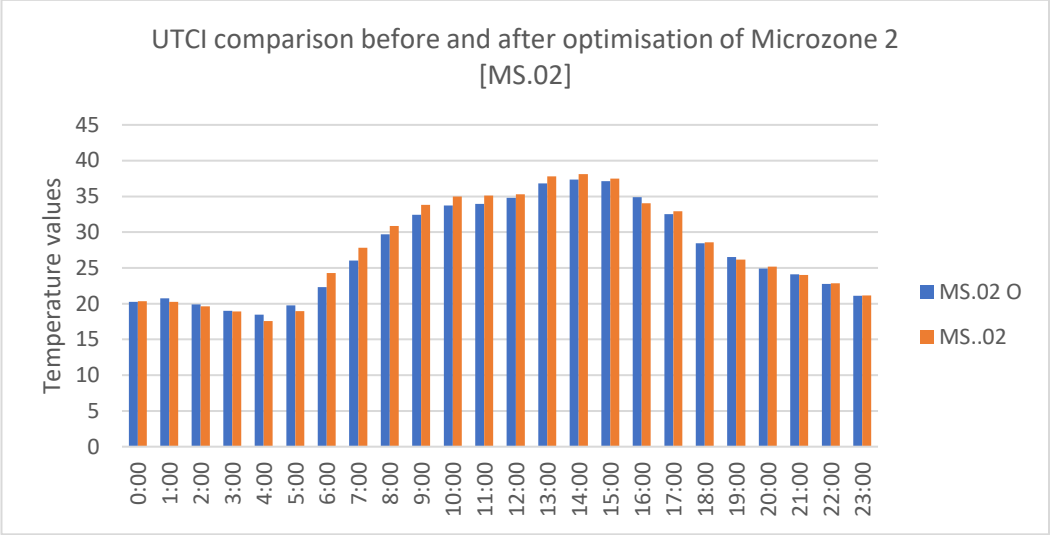

Figure 154. UTCI comparison chart of Microzone 2 temperature values before and after optimization [MS.02]

The graphs below compare the temperature readings from the Microzones UTCI taken before and after the optimization process. The first Microzone [MS.03], where the highest temperature was 37.3 °C at 14:00 as opposed to 37.9 °C earlier, shows that temperatures are declining. This indicates a 0.7 °C increase in temperature measurements. The [MS.03 O] graph displays the temperatures after design-based optimization. The two plots overlap at 16:00 and throughout the entire evening with

comparable temperature values. When temperatures fall by 1.8 °C about 8:00, the impact is highest.

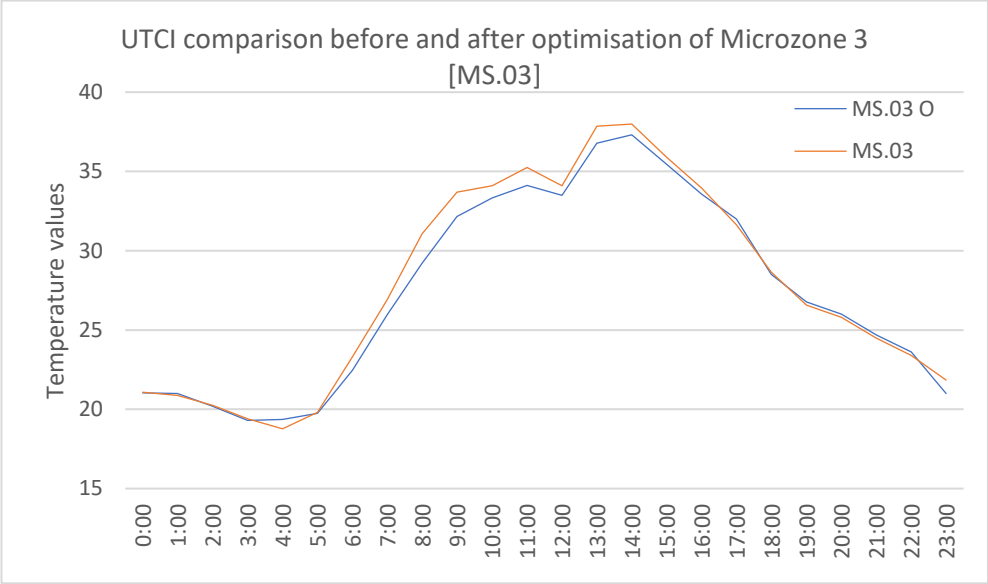

Figure 155.UTCI comparison graph of Microzone 3 [MS.03]

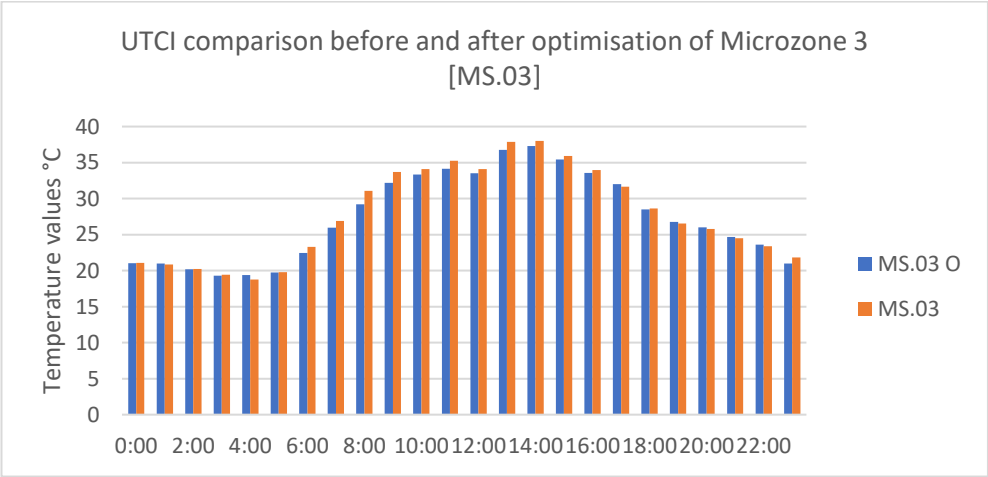

Figure 156.UTCI comparison chart of Microzone 3 temperature values before and after optimization [MS.03].

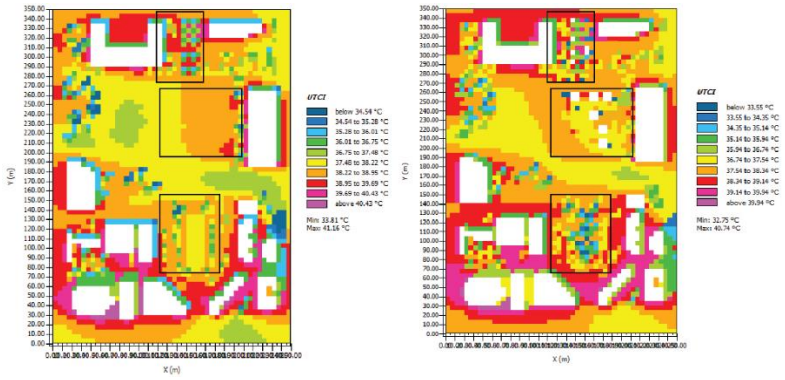

Figure 157. Data visualization showing microzones of Skanderbeg square before and after optimization.

The temperature data from the Microzones UTCI obtained before and after the optimization procedure are compared in the graphs below. Temperatures are decreasing as seen by the first Microzone [MS.03], where the peak temperature decreased to 37.4 °C at 14:00 from 38.6 °C earlier. It indicates an increase in temperature measurements of 1.2 °C. After design-based optimization, the temperatures are shown on the [MS.03 O] graph. At 18:00 and for the rest of the evening, the two graphs cross over while maintaining similar temperature readings. The impact is greatest at approximately 4:00 when temperatures drop by 1.8 °C.

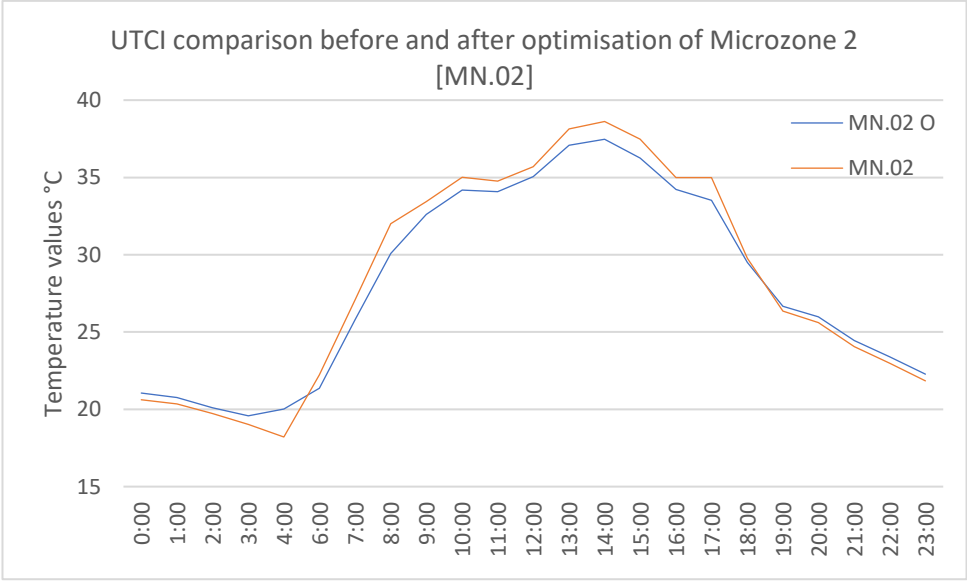

Figure 158.UTCI comparison graph of Microzone 2 [MN.02]

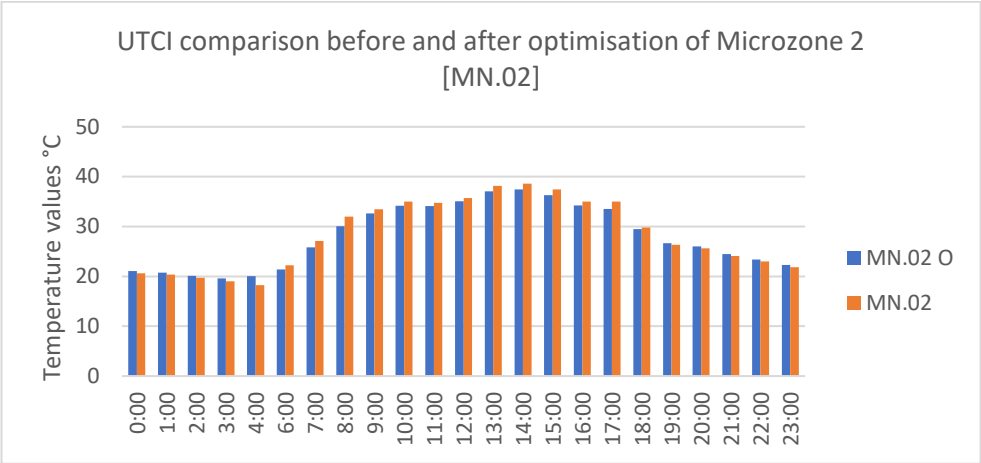

Figure 159.UTCI comparison chart of Microzone 2 temperature values before and after optimization [MN.02].

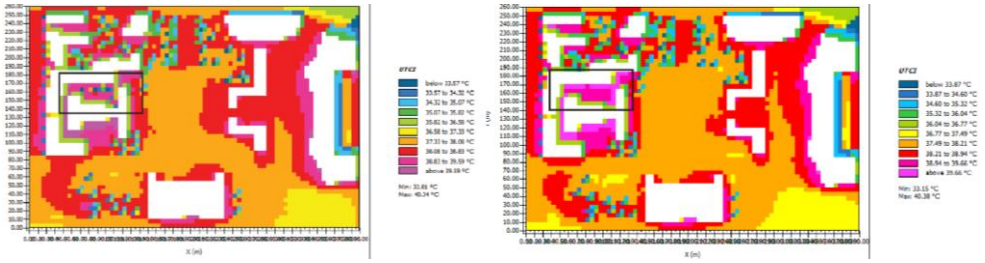

Figure 160.Data visualization showing Microzone 2 [MN.02] of Mother Teresa square before and after optimization.

Below are some illustrative collages of the optimization designs that demonstrate how they may seem when applied to the actual microzone.

Figure 161. Collage of Microzone 1 [MS.01] after optimization.

Figure 162.Collage of Microzone 3 [MS.03] after optimization.

Figure 163. Collage of Microzone 2 [MS.02] after optimization.

Figure 164.Residential complex in Shanghai using green facade Shang Kai Steel's SKA.

CHAPTER 7

CONCLUSION

7.1 Conclusions

This thesis examined how urban public spaces' microclimates transform as well as design-based methods for regulating and enhancing those squares. By additionally developing recreational and user-friendly places, the goal was to improve the thermal comfort conditions for those who used these areas. To determine how future urban weather would affect pedestrian thermal comfort, its functioning, and the factors that affect it, such as air temperature, mean radiant temperature, wind speed, and humidity, a theoretical analysis was conducted. Envi-met, a software used by urban planners and architects to particularly build certain regions, was used to simulate and evaluate the outdoor microclimate in those metropolitan areas. The importance of this study can be seen in its focus on sites, which in this case are public plazas. These areas are crucial for public space in Tirana since they are not only used often by residents but also are considered city symbols.

According to the study's findings, it can be concluded that:

The presence of vegetation significantly lowers the temperatures. The highest tree height in the research is 10 meters. The microzones with observable vegetation have temperatures that are 1°C lower than those of other microzones. Temperature readings decreased during the hottest parts of the day after implementing trees using design-based solutions. More precisely, they are lower at 14:00, but the analysis reveals that certain locations appear to have greater temperatures than others by night and early in the morning.

According to the analysis, internal courtyards without vegetation appear to function poorly and have higher temperature values than other microzones or areas that are broader and have trees on at least one side of them. This results from higher mean radiant temperatures from the buildings' facades, which either retain heat or, if made of

reflecting materials, reflect it at this inner courtyard with its tiny openings. As a result of the absence of openings, which favors the high temperatures, the wind speed appears to be lower.

The use of vegetated buildings and green facades has been found to help reduce temperatures. Temperatures in the study microzones were lowered by 0.5 to 1 °C as a result of the adaption of these structures. The reduction in temperature is the result of evapotranspiration, which occurs when plants release water vapor through their leaves and causes a cooling effect, improved air circulation (vegetation encourages air movement and ventilation, which can dissipate heat and enhance cooling), and other factors like heat absorption and reflection of heat. The findings of the optimization of the vegetation structures for the Microzons [MS.01] and [MN.02] reveal a reduction in temperature for Microzone 1 to 1.3°C for the first Microzone and 1.2°C for the second one.

In two of the Microzones where they have been constructed, shading structures have efficiently lowered temperatures while also improving pedestrian thermal comfort. After those areas were optimized, the temperature values decreased by 0.8 °C to 1.3 °C, reducing the urban island effect (UHI). Shading structures can aid in lowering the UTCI by minimizing the quantity of sunlight that enters the human body. In comparison with standing in direct sunlight, those exposed to shaded regions feel more comfortable and experience less heat stress, especially during hot, bright weather conditions.

The study of the Universal Thermal Climate Index (UTCI) is crucial for comprehending and addressing the problems brought on by changes in the climate. I believe that the findings of the study assist in the planning of public areas in the future. This thesis will serve as a guideline for improving such areas' efficiency but also it will enhance the pedestrian experience there.

Design-based optimization is essential to the aim of this thesis because it offers a methodical and effective way to solve issues. By concentrating on the design factors that have a big influence on the targeted outcomes, it helps researchers get the best findings possible. Design-based optimization aids researchers in finding the ideal set of parameters that optimize performance, reduce costs, or satisfy certain requirements by utilizing a variety of optimization tools, such as computational modeling, simulation,

and data analysis. This method not only improves the research's quality but also cuts down on the time and money needed for experimenting.

Researchers can examine and improve different design factors by using these techniques to find the best treatments, designs, or solutions. This makes it possible for decision-makers to decide on a course of action based on empirical facts and data-driven insights, improving performance and results. By enabling the investigation of alternative tactics and expanding the parameters of what is thought to be practical, design-based optimization strategies also encourage creativity.

Additionally, by ensuring that suggestions are solid, trustworthy, and repeatable, these tactics raise their credibility and broaden their usefulness. It can increase productivity, efficacy, and the general effect generated by given suggestions by using design-based optimization methodologies. This will enable to make significant progress in a variety of domains and disciplines.

REFERENCES

Al-Kodmany, K. (2018). Skyscrapers in the Twenty-First Century City: A Global Snapshot. *Buildings*. doi:https://doi.org/10.3390/buildings8120175

Al-Kodmany, K., & Ali, M. (2013). *The Future of the City.* Southampton; Billerica: Wit press.

Al-Kodmany, K., & Ali, M. (2018). *The Vertical City: A Sustainable Development Model.* Southam; Billerica: WIT Press; Computational Mechanics.

Al-Tamim, N. A. (2011, October 23). *Impact of Building Envelope Modifications on The Thermal Performance of Glazed High-Rise Residential Buildings in The Tropics.* Retrieved from Repository@UMS: http://eprints.usm.my/45708/

Besnik, A., Lulo, K., Myftiu, G., Pone, S., Shqarri, E., & Kenuti, P. (2004). *Tirana: The Challenge of Urban Development*. Sloalba.

Breheny, M. (1996). Centrists, Decentrists and Compromisers: Views on the. In E. Burton, M. Jenks, & K. Williams, *The compact city : a sustainable urban form?* (pp. 10-29). London: E&FN Spon.

Capolino, P. (2011). Tirana: A Capital City transformed by the Italians. *Planning Perspectives*, *26*(4), 591–615. https://doi.org/10.1080/02665433.2011.601610

C.K.Cheung, R.J.Fuller, & M.B.Luther. (2005). Energy-efficient envelope design for high-rise apartments. *Energy and Buildings*, 37-48. doi:https://doi.org/10.1016/j.enbuild.2004.05.002

Etheridge, D. (2011). *Natural Ventilation of Buildings: Theory, Measurement and Design.* Chichester, West Sussex, UK: John Wiley & Sons.

Governatori, M., Cedillo-González, E. I., Manfredini, T., & Siligardi, C. (2022). Solar reflective properties of porcelain tiles for UHI mitigation: Effect of highly reflective frits in the ENGOBE's formulation. *Materials Today Sustainability*, *20*, 100255. https://doi.org/10.1016/j.mtsust.2022.100255

Hassan, A. S., & Al-Ashwal, N. T. (2015). Impact of Building Envelope Modification on Energy Performance of High-Rise Apartments in Kuala Lumpur, Malaysia. *researchgate*. doi:DOI:10.14456/itjemast.2015.11

Hultgren, J. (2014). The nature of American immigration restrictionism. *New Political Science*, 52-75.

J, Z., L, X., V, S., S, T., H, S., S, L., & T, R. (2019). Impact of urban block typology on building solar potential and energy use efficiency in tropical high-density

city. *Applied Energy, 240*, 513-533. doi:https://doi.org/10.1016/j.apenergy.2019.02.033

Javanroodi, K., Mahdavinejad, M., & M.Nik, V. (2018). Impacts of urban morphology on reducing cooling load and increasing ventilation potential in hot-arid climate. *Applied Energy*, 714-746. doi:https://doi.org/10.1016/j.apenergy.2018.09.116

Johnson, M. P. (2001). Environmental Impacts of Urban Sprawl: A Survey of the Literature and Proposed Research Agenda. *Environment and Planning A: Economy and Space*. doi:https://doi.org/10.1068/a3327

Juan, Y.-H., Wen, C.-Y., Li, Z., & Yang, A.-S. (2021). Impacts of urban morphology on improving urban wind energy potential for generic high-rise building arrays. *Applied Energy*. doi:https://doi.org/10.1016/j.apenergy.2021.117304

Kuo, C.-Y., Wang, R.-J., Lin, Y.-P., & Lai, C.-M. (2020). Urban Design with the Wind: Pedestrian-Level Wind Field in the Street Canyons Downstream of Parallel High-Rise Buildings. *Energies 13(11)*. doi:https://doi.org/10.3390/en13112827

Li, Y., & Chen, L. (2020). Study on the influence of voids on high-rise building on the wind environment. *BUILD SIMUL 13*, 419–438. doi:https://doi.org/10.1007/s12273-019-0584-7

Liua, K., Lian, Z., Dai, X., & Lai, D. (2022). Comparing the effects of sun and wind on outdoor thermal comfort: A case study based on longitudinal subject tests in cold climate region. *Science of The Total Environment*. doi:https://doi.org/10.1016/j.scitotenv.2022.154009

M, A.-D., A, R., J, N., O, O., J, Y., M, B., . . . A, K. (2020). Impacts of the morphology of new neighborhoods on microclimate and building energy. *Renewable and Sustainable Energy Reviews*, 133. doi:https://doi.org/10.1016/j.rser.2020.110030

Margolin, V. (2015). The Good City: Design for Sustainability. *She Ji*, 1(1) 34-43. doi:https://doi.org/10.1016/j.sheji.2015.07.001

Mirrahimi, S., Mohamed, M. F., Haw, L. C., Ibrahim, N. L., Yusoff, W. F., & & Aflaki, A. (2016). The effect of building envelope on the thermal comfort and energy saving for high-rise buildings in hot-humid climate. *Renewable and Sustainable Energy Reviews*, https://doi.org/10.1016/j.rser.2015.09.055.

Nechyba, T. J., & Walsh, R. P. (2004). Urban Sprawl. *Journal of Economic Perspectives*, 177–200.

Okeil, A. (2010). A holostic approach to energy efficient building forms. *Energy and Buildings*. doi:10.1016/j.enbuild.2010.03.013

Pantavou, K., Theoharatos, G., Santamouris, M., & Asimakopoulos, D. (2013). Outdoor thermal sensation of pedestrians in a Mediterranean climate and a

comparison with UTCI. *Building and Environment*, 82-95. doi:http://dx.doi.org/10.1016/j.buildenv.2013.02.014

Park, S., Tuller, S. E., & Jo, M. (2014). Application of Universal Thermal Climate Index (UTCI) for microclimatic analysis in urban thermal environments. *Landscape and Urban Planning*, 146-155.

Raji, B., Tenpierik, M. J., Bokel, R., & Dobbelsteen, A. v. (2019). Natural summer ventilation strategies for energysaving in high-rise buildings: a case study in the. *International Journal of Ventilation*. doi:https://doi.org/10.1080/14733315.2018.1524210

Rubiera-Morollón, F., & Garrido-Yserte, R. (2020). Recent Literature about Urban Sprawl: A Renewed Relevance of the Phenomenon from the Perspective of Environmental Sustainability. *Sustainability 12(16)*. doi:https://doi.org/10.3390/su12166551

S, M., G, K. O., I, E. K., & I, S. (2021). The impact of urban form on building energy and cost efficiency in temperate-humid zones. *Journal of Building Engineering*, 33. doi:https://doi.org/10.1016/j.jobe.2020.101626

Safee, F. A., M.*, Y. M., Ismail, S., Ariffin, N. F., & Isa, N. K. (2015). ESTABLISHING ELEMENTS OF A GOOD CITY PLANNING: AN ANALYSIS OF CITY PLANNING THEORIES. *Jurnal*, 101-105. doi:https://doi.org/10.11113/jt.v75.5242

Saroglou, T., Meir, I. A., Theodosiou, T., & Givoni, B. (2017). Towards Energy Efficient Skyscrapers. *ENB 7638*. doi: http://dx.doi.org/doi:10.1016/j.enbuild.2017.05.057

Simmonds, P. (2015). *The ASHRAE Design Guide for Tall, Supertall and Megatall Building Systems.* American Society of Heating, Refrigerating, and Air-Conditioning Engineer.

T.Sarogloua, *. I. (2017). Quantifying Energy Consumption in Skyscrapers |of Various Heights. *Procedia Environmental Sciences 38*, 314 – 321. doi:https://doi.org/10.1016/j.proenv.2017.03.085

Tong, S., Wong, N. H., Tan, C. L., Jusuf, S. K., Ignatius, M., & Tan, E. (2017). Impact of urban morphology on microclimate and thermal comfort in northern China. *Solar Energy*, 212-223. doi:https://doi.org/10.1016/j.solener.2017.06.027

Wood, A., & Salib, R. (2013). *Natural ventilation in high-rise office buildings.* New York: Routledge.

Y, T., W, Z., Y, Q., Z, Z., & J, Y. (2019). The effect of urban 2D and 3D morphology on air temperature in residential neighborhoods. *Landscape Ecology*, 1161-1178. doi:https://doi.org/10.1007/s10980-019-00834-7

Yang, J., Shi, B., Shi, Y., Marvin, S., Zheng, Y., & Xia, G. (2019). Air pollution dispersal in high density urban areas: Research on the triadic relation of wind,

air pollution, and urban form. *Sustainable Cities and Society*. doi:https://doi.org/10.1016/j.scs.2019.101941

Yuan, M., Yin, C., Sun, Y., & Chen, W. (2019). Examining the associations between urban built environment and noise pollution in high-density high-rise urban areas: A case study in Wuhan, China. *Sustainable Cities and Society*. doi:https://doi.org/10.1016/j.scs.2019.101678

Zhou, L., Yuan, B., Hu, F., Wei, C., Dang, X., & Sun, D. (2022). Understanding the effects of 2D/3D urban morphology on land surface temperature based on local climate zones. *Building and Environment*. doi:https://doi.org/10.1016/j.buildenv.2021.108578

APPENDIX

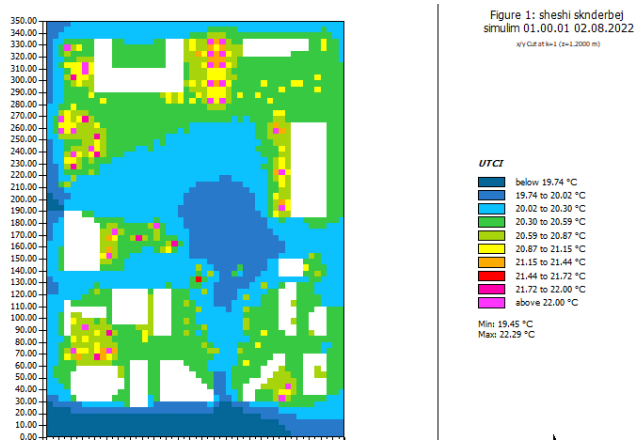

Figure 165.UTCI map for Skanderbeg square at 01:00

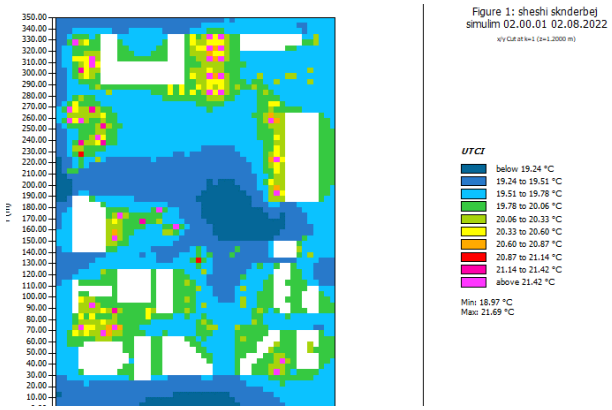

Figure 166.UTCI map for Skanderbeg square at 02:00

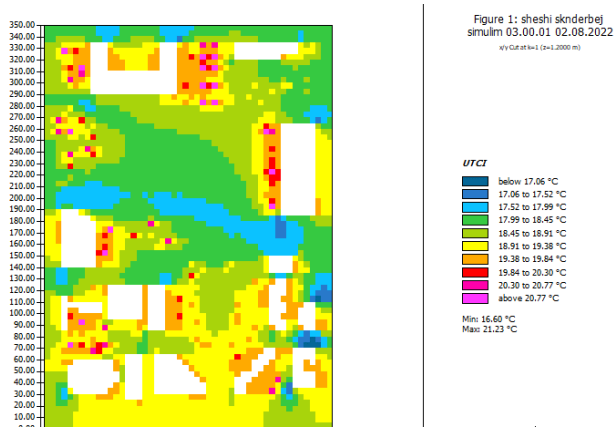

Figure 167.UTCI map for Skanderbeg square at 03:00

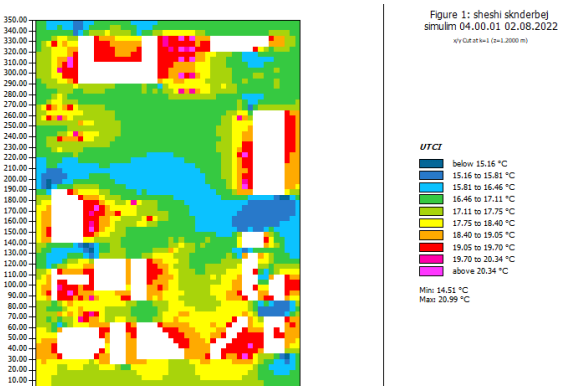

Figure 168.UTCI map for Skanderbeg square at 04:00

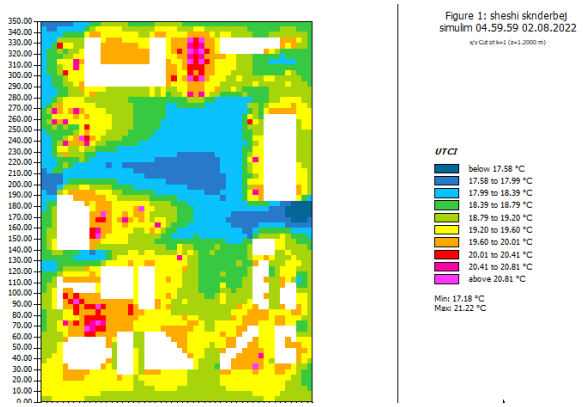

Figure 169.UTCI map for Skanderbeg square at 05:00

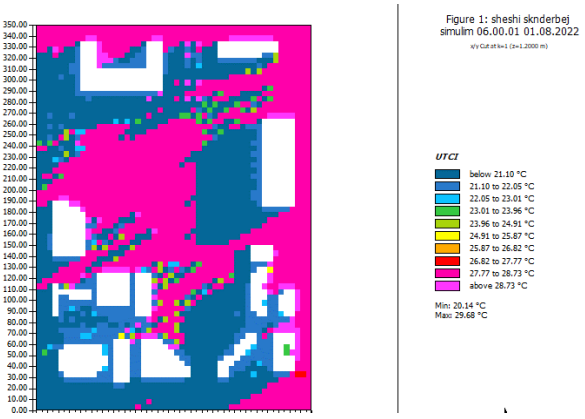

Figure 170.UTCI map for Skanderbeg square at 06:00

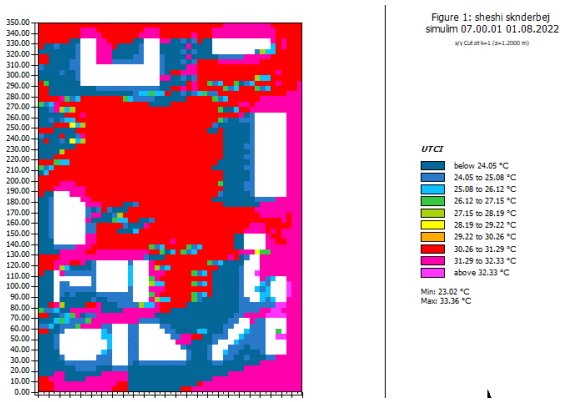

Figure 171.UTCI map for Skanderbeg square at 07:00

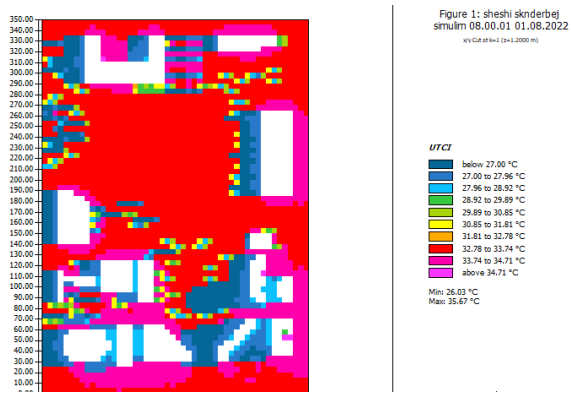

Figure 172.UTCI map for Skanderbeg square at 08:00

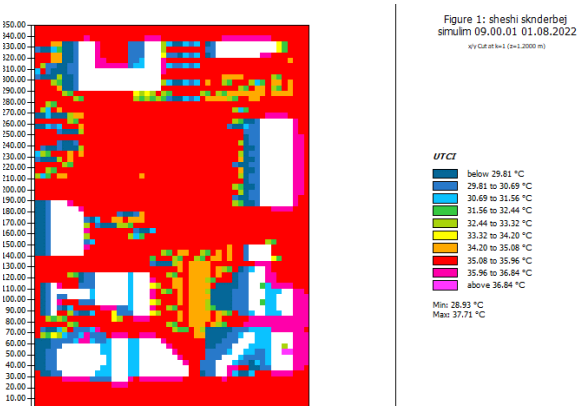

Figure 173.UTCI map for Skanderbeg square at 09:00

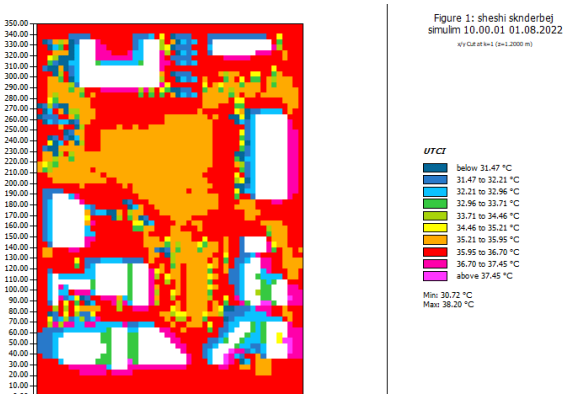

Figure 174.UTCI map for Skanderbeg square at 10:00

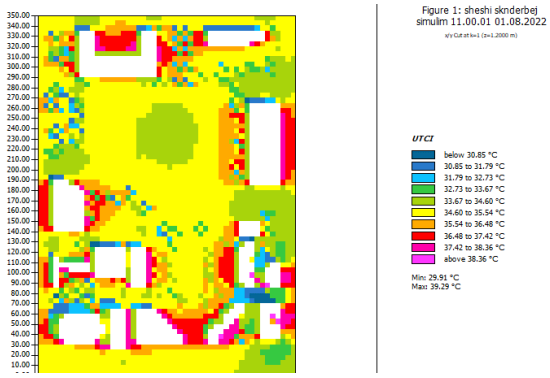

Figure 175.UTCI map for Skanderbeg square at 11:00

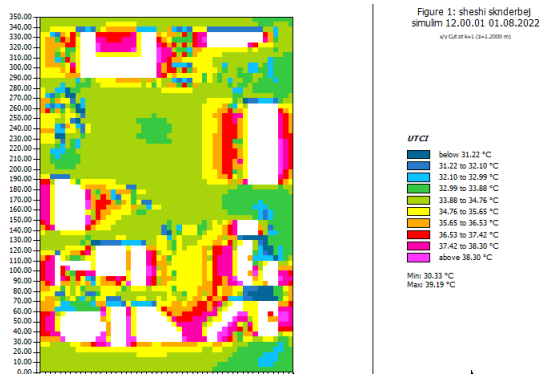

Figure 176.UTCI map for Skanderbeg square at 12:00

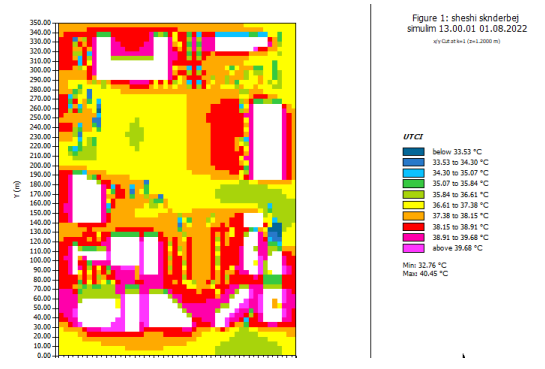

Figure 177.UTCI map for Skanderbeg square at 13:00

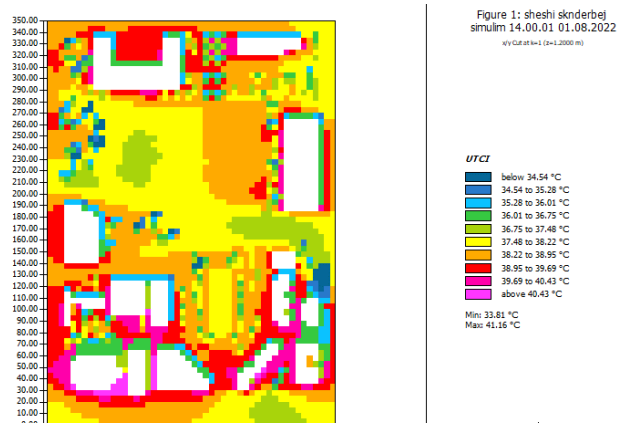

Figure 178.UTCI map for Skanderbeg square at 14:00

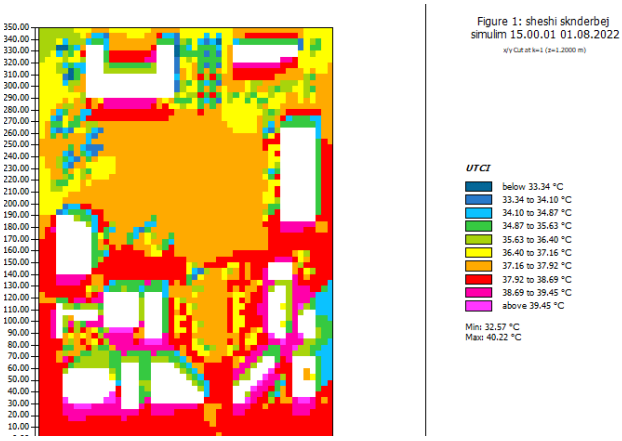

Figure 179.UTCI map for Skanderbeg square at 16:00

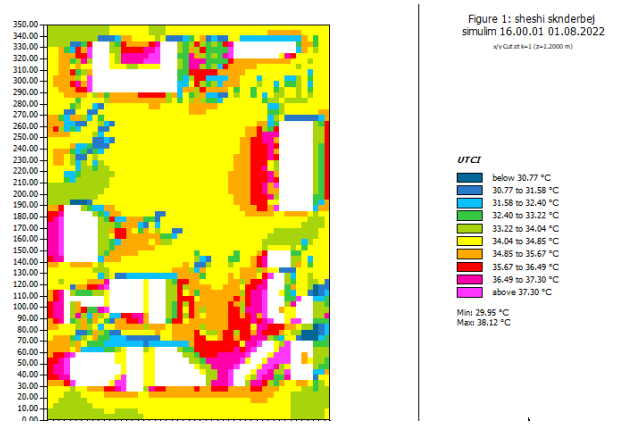

Figure 180.UTCI map for Skanderbeg square at 16:00

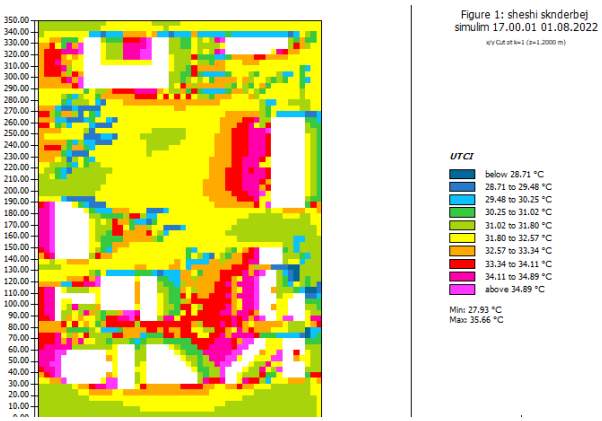

Figure 181.UTCI map for Skanderbeg square at 01:00

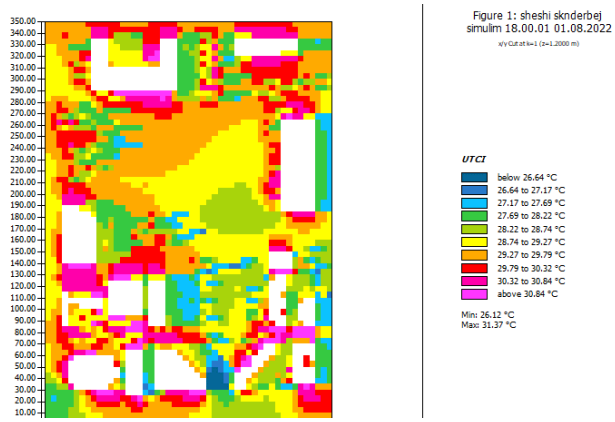

Figure 182.UTCI map for Skanderbeg square at 18:00

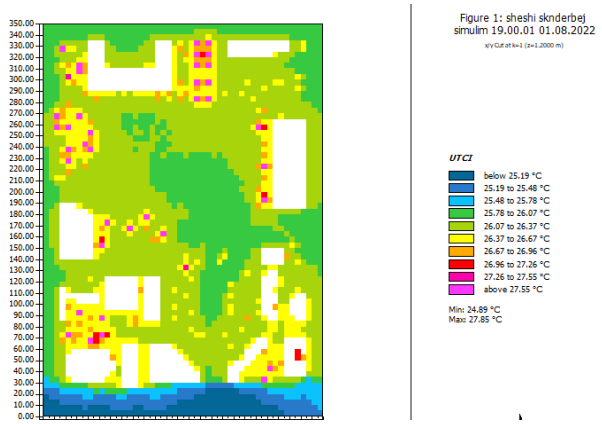

Figure 183.UTCI map for Skanderbeg square at 19:00

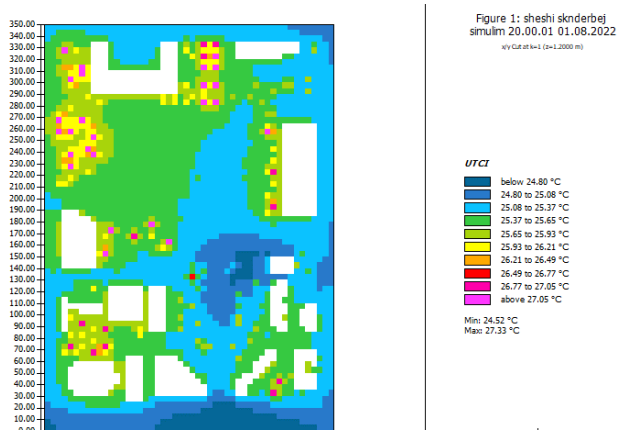

Figure 184.UTCI map for Skanderbeg square at 20:00

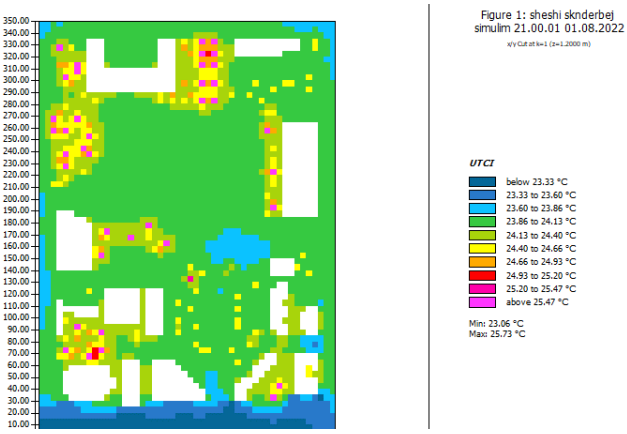

Figure 185.UTCI map for Skanderbeg square at 21:00

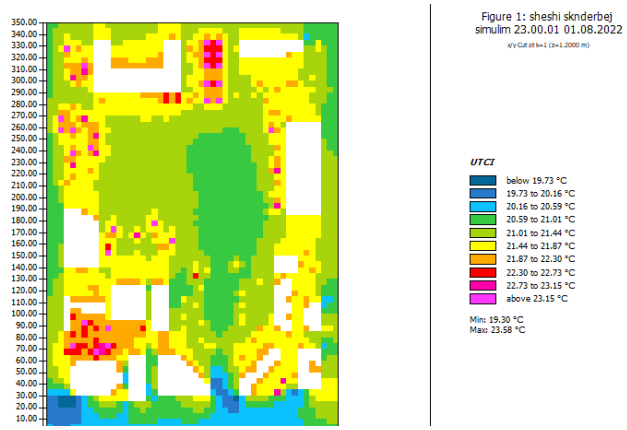

Figure 186.UTCI map for Skanderbeg square at 22:00

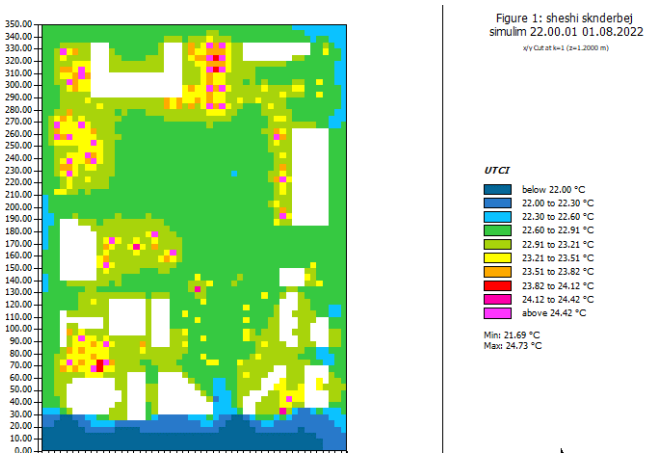

Figure 187.UTCI map for Skanderbeg square at 23:00

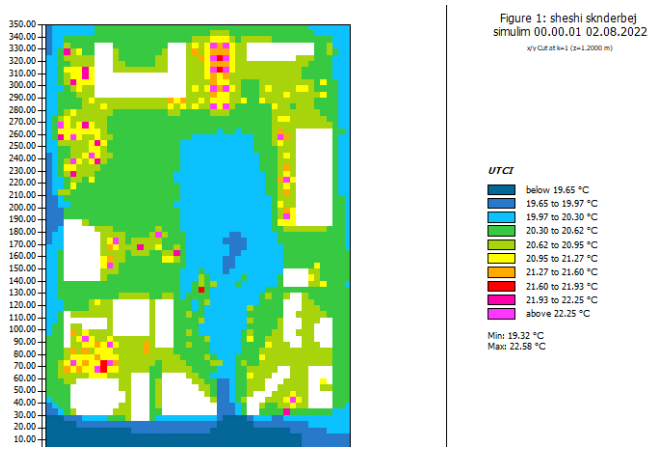

Figure 188.UTCI map for Skanderbeg square at 00:00

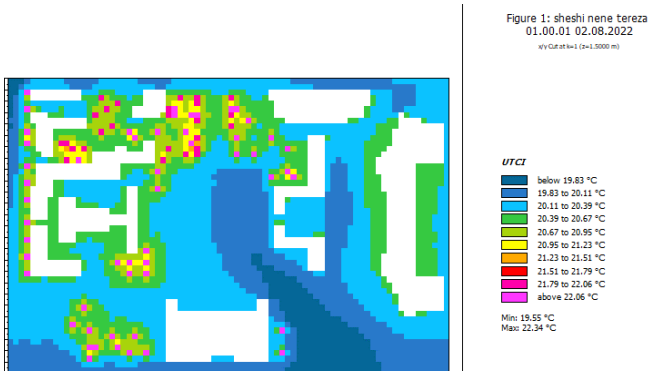

Figure 189.UTCI map for Mother Teresa square at 01:00

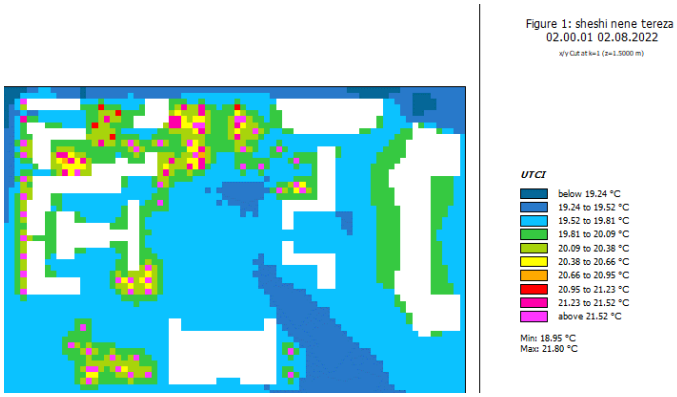

Figure 190.UTCI map for Mother Teresa square at 02:00

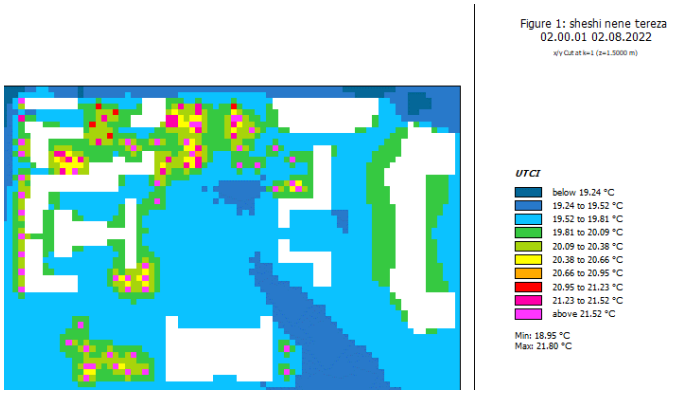

Figure 191.UTCI map for Mother Teresa square at 03:00

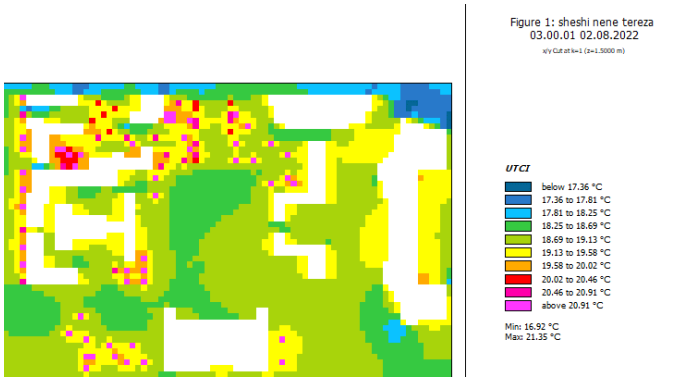

Figure 192.UTCI map for Mother Teresa square at 04:00

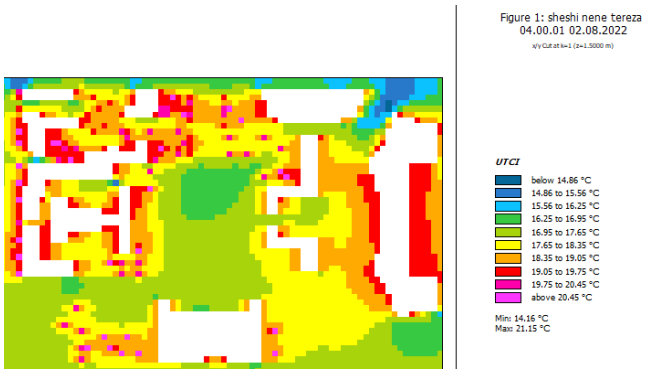

Figure 193.UTCI map for Mother Teresa square at 05:00

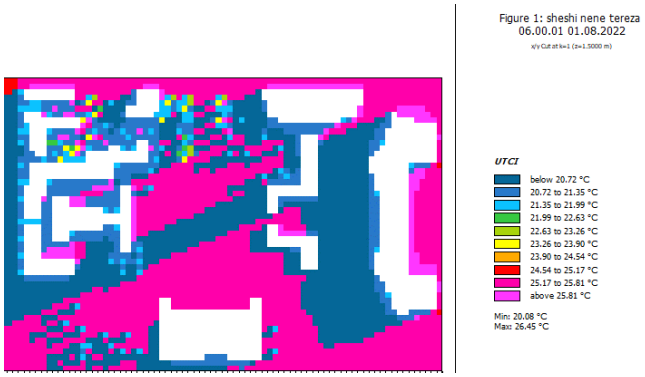

Figure 194.UTCI map for Mother Teresa square at 06:00

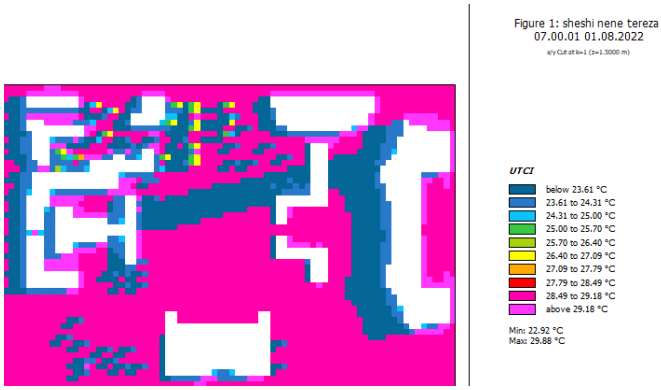

Figure 195.UTCI map for Mother Teresa square at 07:00

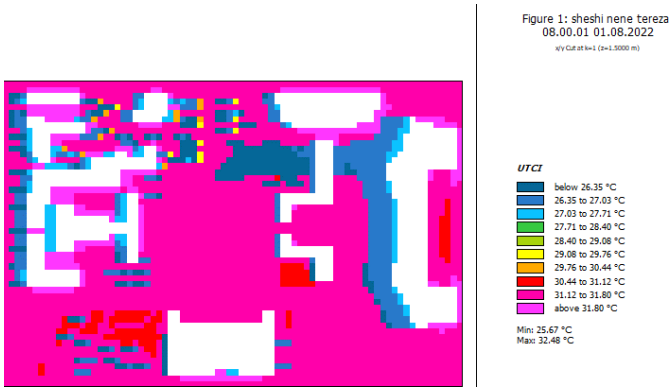

Figure 196.UTCI map for Mother Teresa square at 08:00

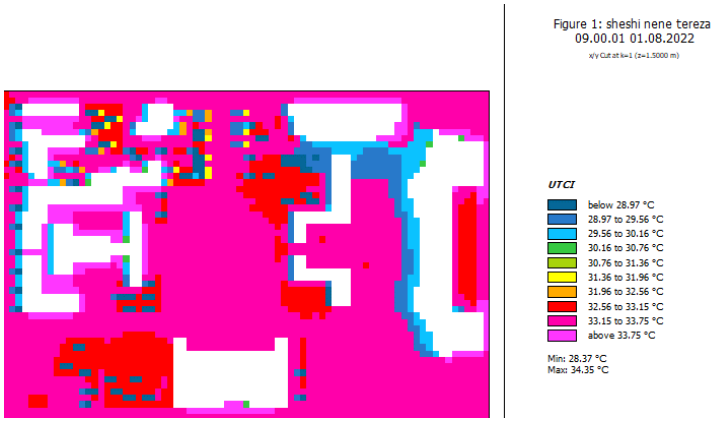

Figure 197.UTCI map for Mother Teresa square at 09:00

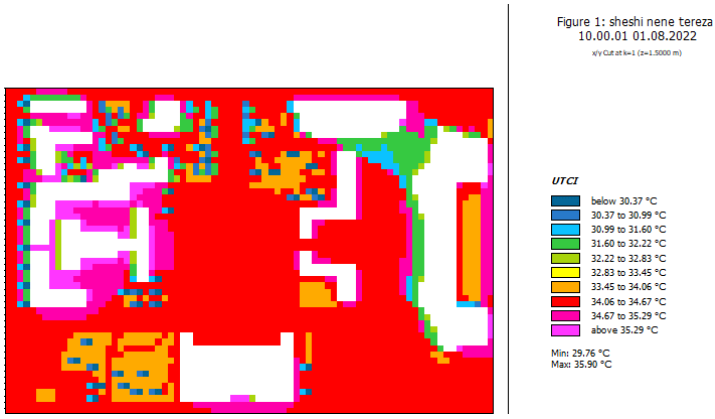

Figure 198.UTCI map for Mother Teresa square at 10:00

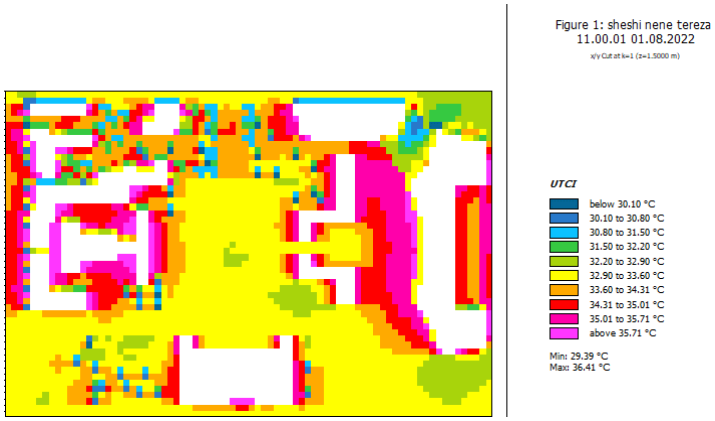

Figure 199.UTCI map for Mother Teresa square at 11:00

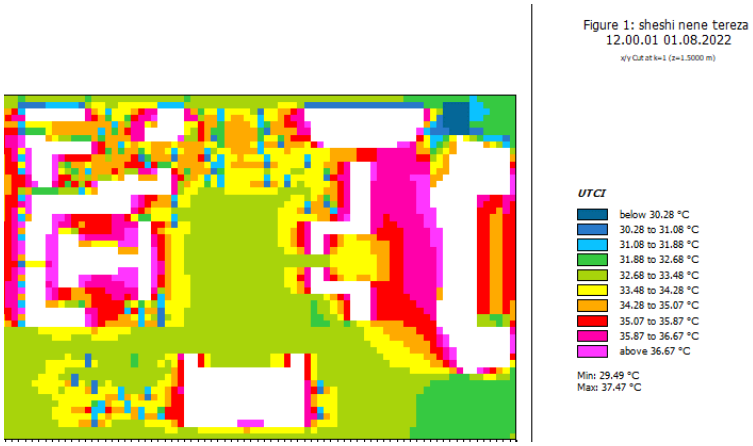

Figure 200.UTCI map for Mother Teresa square at 12:00

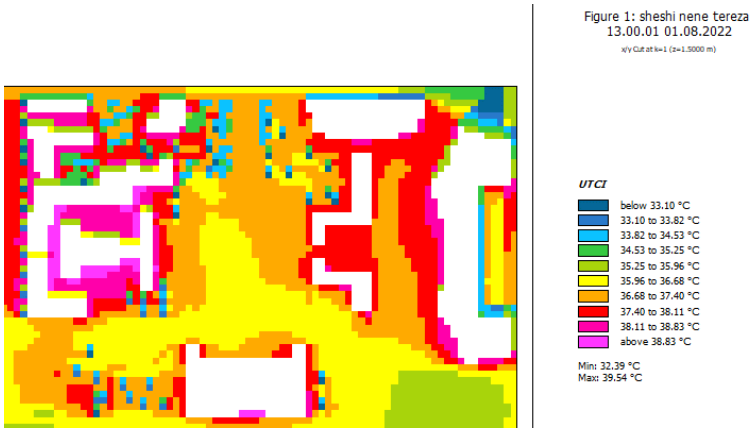

Figure 201.UTCI map for Mother Teresa square at 13:00

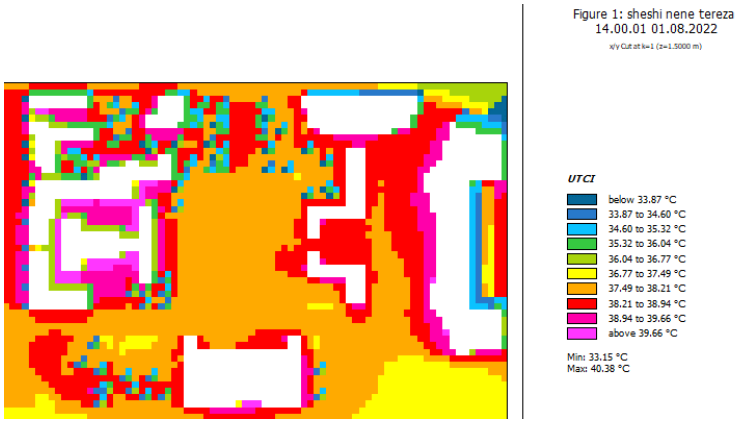

Figure 202.UTCI map for Mother Teresa square at 14:00

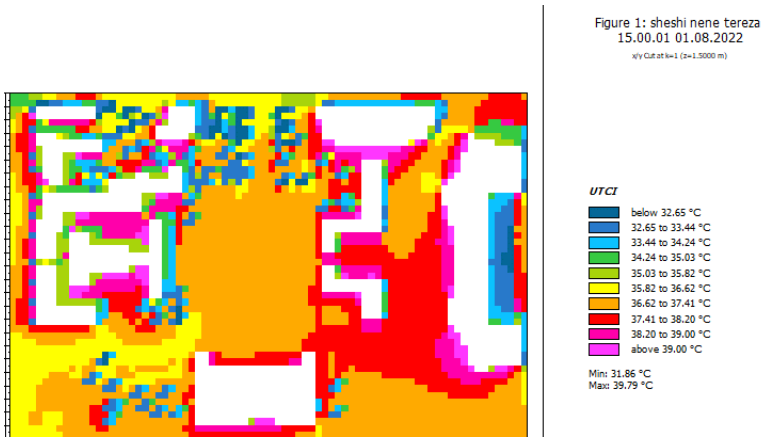

Figure 203.UTCI map for Mother Teresa square at 15:00

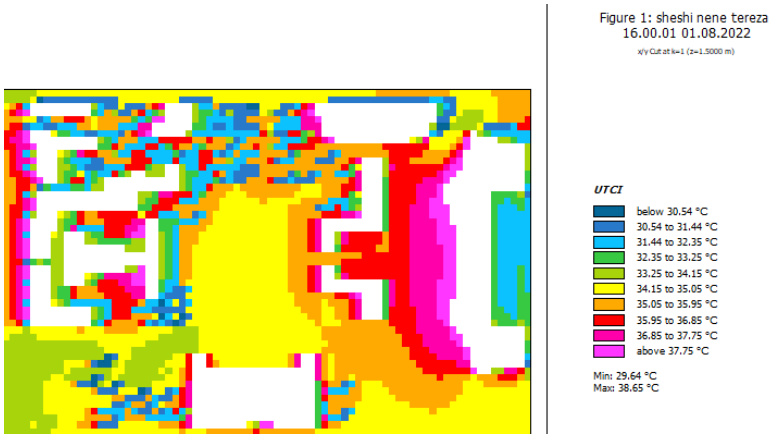

Figure 204.UTCI map for Mother Teresa square at 16:00

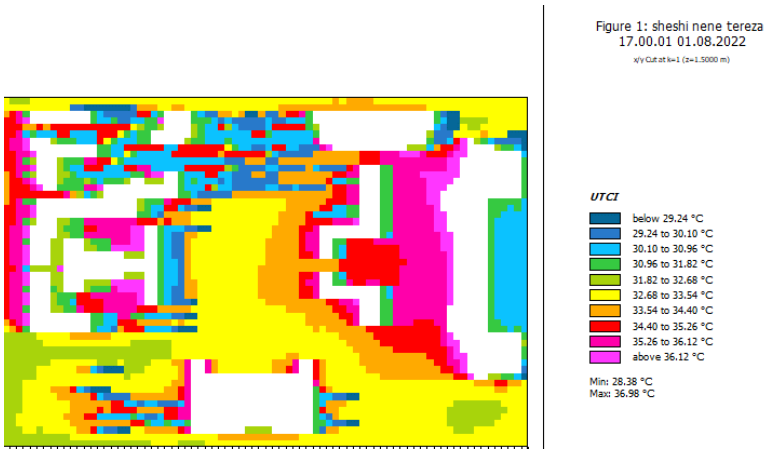

Figure 205.UTCI map for Mother Teresa square at 17:00

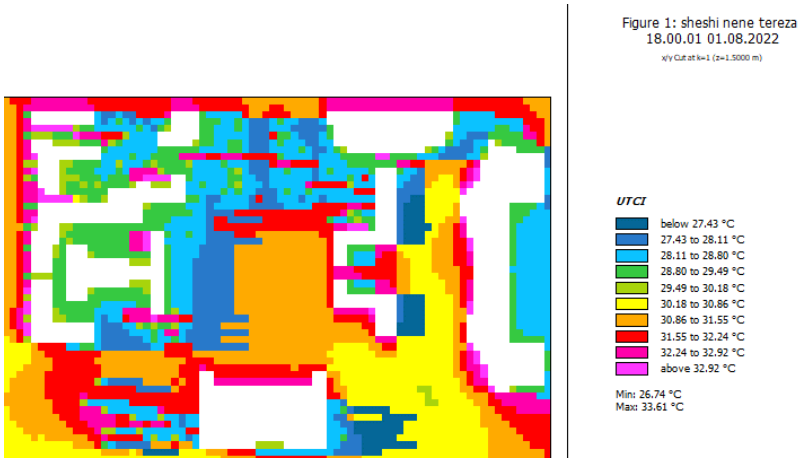

Figure 206.UTCI map for Mother Teresa square at 18:00

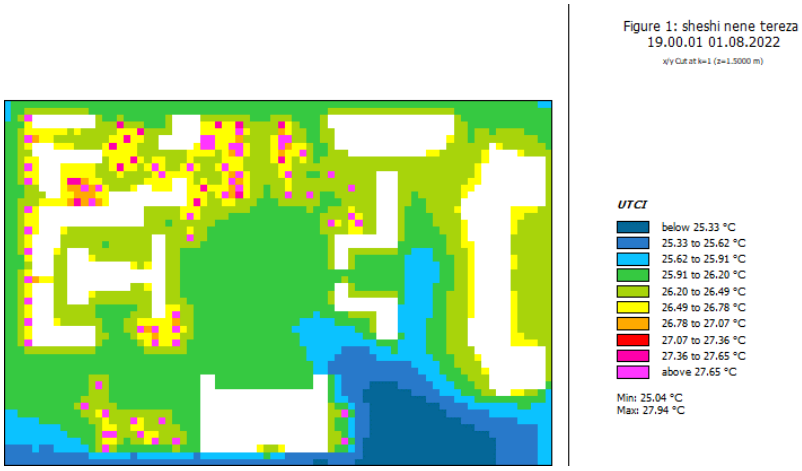

Figure 207.UTCI map for Mother Teresa square at 19:00

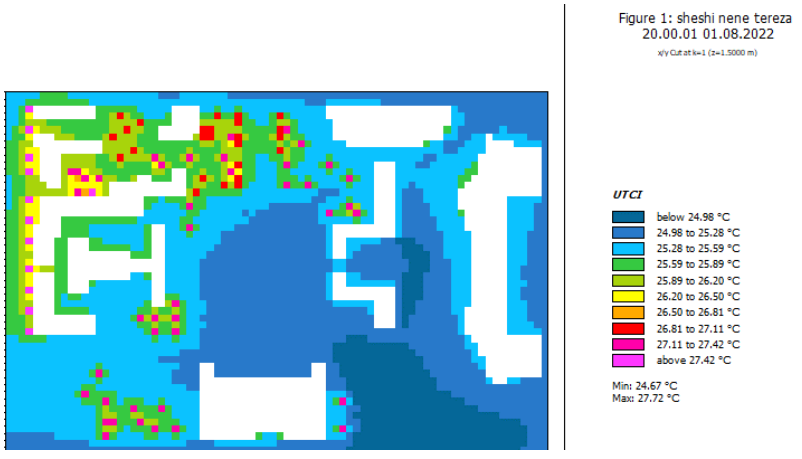

Figure 208.UTCI map for Mother Teresa square at 20:00

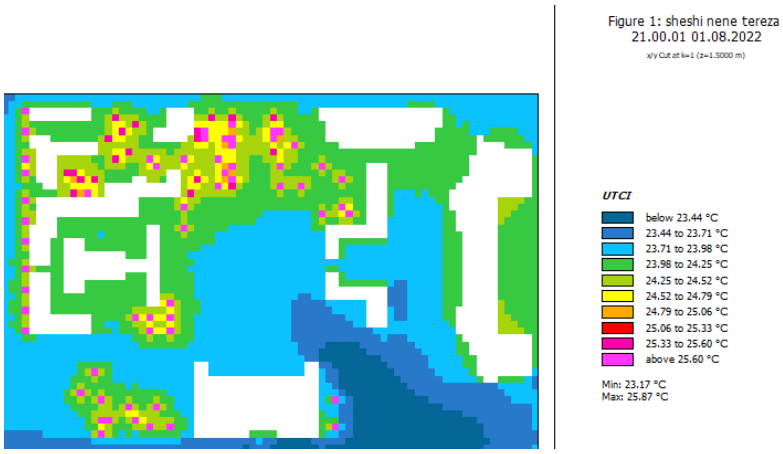

Figure 209.UTCI map for Mother Teresa square at 21:00

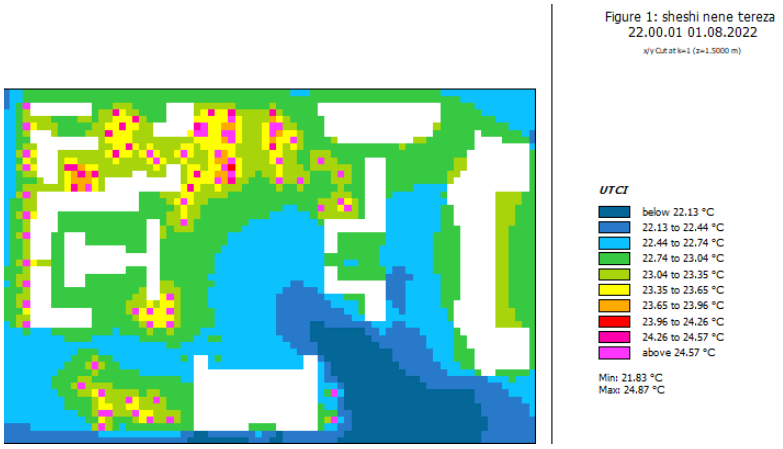

Figure 210.UTCI map for Mother Teresa square at 23:00

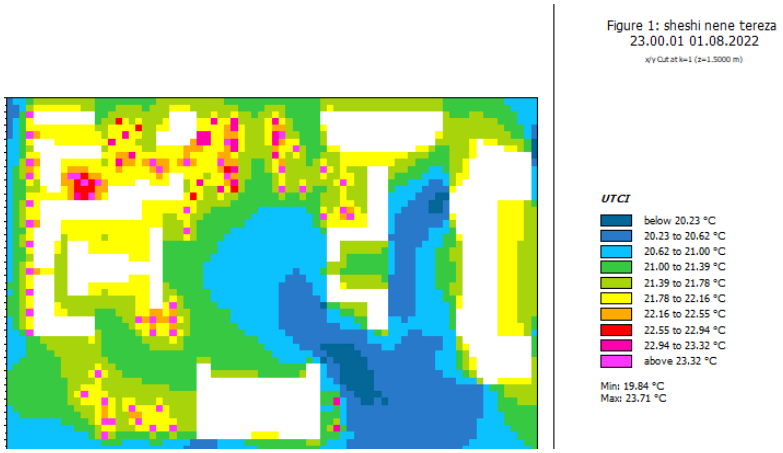

Figure 211.UTCI map for Mother Teresa square at 23:00

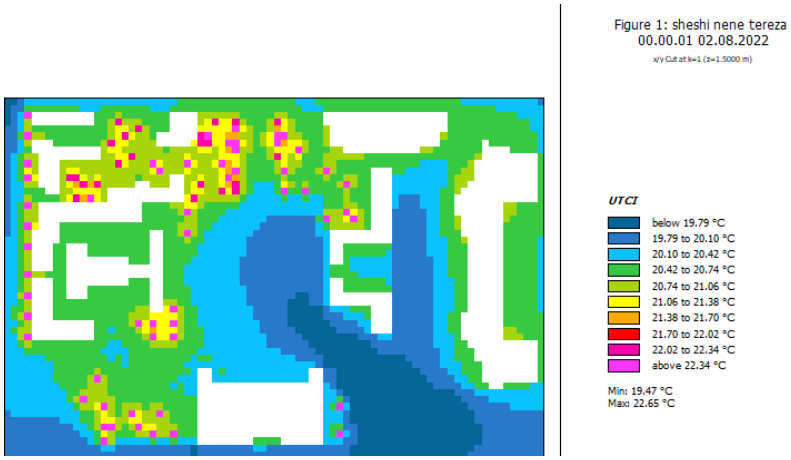

Figure 212.UTCI map for Mother Teresa square at 00:00